Dynamic control of deep-level mine cooling systems using artificial intelligence

MC Furumele

orcid.org/ 0000-0001-9649-8808

Dissertation accepted in fulfilment of the requirements for the degree *Master of Engineering in Electrical and Electronic Engineering* at the North-West University

Supervisor: Dr JH Marais

Graduation: S April 2024

ABSTRACT

Title: Dynamic control of deep-level mine cooling systems using artificial intelligence

Author: Musa Charles Furumele

Supervisor: Dr JH Marais

Keywords: mining; energy saving, cooling, dynamic control, time series forecasting, machine learning, artificial intelligence

Deep-level mines face high electricity costs, posing a challenge as it significantly impacts production costs, consequently decreasing overall profitability. Complex energy-intensive cooling systems, including ventilation and refrigeration, contribute to approximately 28% of the mine's total energy consumption. Hence, implementing energy savings initiatives for cooling systems in deep-level mining can mitigate production costs in the industry.

The existing approaches to reducing electricity consumption on mine cooling systems rely on static control strategies and fail to adapt to the dynamic conditions prevalent in deep-level mines. The mining industry has rarely embraced time series forecasting models using artificial intelligence (AI) to develop control strategies for cooling systems. This study introduces AI-based temperature forecasting to address these limitations to enable the development of a dynamic control strategy for cooling systems in deep-level mines. By leveraging AI, the proposed approach aims to overcome the shortcomings of the existing methods and improve energy efficiency in the mining industry.

The proposed dynamic control strategy focused on the surface bulk air cooling (BAC) plants and fans of a deep-level gold mine, considering system parameters closely related to the underground conditions and the operating characteristics of the system components. Long short-term memory recurrent neural network (LSTM-RNN) models were employed with five different forecasting horizons to forecast the surface and underground air temperatures. The accuracy of the temperature forecasting model was validated against real data and previous literature. The best-performing model (30-minute forecast) yielded a coefficient of variation for the root mean square error

(CV(RMSE)) of 1.66% and 1.55%, a root mean square error (RMSE) of 0.40°C and 0.37°C and a mean absolute percentage error (MAPE) of 2.29% and 1.01% for the surface air wet bulb temperatures and underground wet bulb temperatures. These findings confirm that the model accurately forecasts surface and underground air temperatures. Subsequently, the model was used to identify a dynamic control strategy for the surface BAC system components, further enhancing the system's energy efficiency. A possible electricity cost savings of ZAR 1.5 million per annum were realised based on the proposed strategy.

The models used to determine the control strategies only required significant maintenance when an unforeseen event occurred, such as adding or removing a fridge plant. Implementing such models aids the mine in achieving electricity cost savings without any additional changes to the current infrastructure. However, implementing an automated system will supplement the existing savings by making factors such as human error inconsequential.

ACKNOWLEDEGMENTS

As the author, I would like to express my sincere gratitude to the following contributors who were critical to the success of this study:

- ETA Operations (Pty) Ltd and IPGIP for the opportunity to further my studies, for funding the research project, and for providing all the data required to complete this dissertation.
- Dr Johan Marais and Dr Jean van Laar for their academic input and guidance throughout the study.
- My co-workers Righardt Marais and Claudio Caromba for their continuous support and motivation to complete this dissertation.
- My Friends, especially Fortunate Olifant, Daniel Phiri, Wanga Mudau, and Dzulani Tshinetise, for their patience, support, and laughter to keep me motivated during the hard times throughout the study.
- My Parents, Dr Musa S Furumele and Dr Khanyakude Mashao, for their inspiration to further pursue my academic career and endless support to keep me on my toes.
- My brother, Nyiko Furumele, for being the pillar I could lean on during the good and difficult days.
- To the Heavenly Father for the opportunity and ability to complete this study. I am forever grateful.

All information portrayed in this dissertation acknowledged sources and referenced published work.

TABLE OF CONTENTS

LIST OF FIGURES

NOMENCLATURE

Symbol	Description
ε_t	Error
σ	Sigmoid function
C	Hidden cell state
c_t	Cell state
$E_{i,j}$	Energy consumption
f	Objective function
f_t	Forget gate
h	Hidden state vector
h_t	Output vector/New state
$\mathrm{i_t}$	Input gate
m_n	Regression coefficient or weight
N	total number of observations
o_t	Output gate
p	Number of previous values considered
q	Number of error terms that are considered
T	Temperature (°C)
U_z	Weighted matrix for the hidden state
W_z	Weighted matrix for the input state
x	Input vector
$\|x\|_2$	Euclidean norm
Y_t	True output
Y_o	Model output
z	Update gate

ABBREVIATIONS

AI	Artificial intelligence
ANN	Artificial neural network
AP	Ammonia plant
AR	Auto-regressive
ARIMA	Auto-regressive integrated moving average
ARMA	Auto-regressive moving average
BAC	Bulk Air Cooler
CNN	Convolutional Neural Networks
CV(RMSE)	Coefficient of variation for the root mean square error
FP	Fridge plant
GRU	Gated Recurrent Unit
HVAC	Heating, Ventilation, and Air Conditioning
KNN	K-Nearest Neighbours
LSTM	Long short-term memory
LSTM-RNN	Long-short-term memory recurrent neural network
MA	Moving Average
MAPE	Mean absolute percentage error
MCU	Mobile Cooling Unit
MHSA of SA	Mine Health Safety Act of South Africa
MLP	Multilayer Perceptron
MSE	Mean square error
PCA	Principal Component Analysis
PLC	Programmable logic controller
ReLu	Rectified Linear Unit
RMSE	Root mean square error
RNN	Recurrent Neural Network
SARIMA	Seasonal auto-regressive integrated moving average
SCADA	Supervisory control and data acquisition
SQL	Structured Query Language

SVM	Support Vector Machines
VRT	Virgin rock temperature

Chapter 1: Introduction

"The beautiful thing about learning is that nobody can take it away from you."

— B.B. King

1. INTRODUCTION

1.1. Preamble

This chapter introduces the background and motivation behind the study, along with an overview of artificial intelligence (AI). Additionally, it includes a comprehensive review of relevant literature, analysing the contributions and limitations of previous studies. A state-of-the-art table summarises the existing knowledge in the field, emphasising the need for further research. The problem statement and this study's specific aims and objectives are addressed. Finally, the chapter concludes by providing an overview of the document's structure.

1.2. Background

Mining is the process of extracting materials or minerals from the earth [1]. This process has been prevalent since pre-historic times. For instance, humans searched for stones to make tools [2]. As time progressed, the need for the materials has changed, and the increased difficulty of retrieving these materials has been observed, where the depth at which mining occurs is a primary reason for it [3]. South Africa has amongst the deepest mines in the world. Six of the top ten deepest mines are found in this region.[1]

South African deep-level mines experience underground rock temperatures of up to 60ºC [4], contributing to harsh working conditions in these environments. Complex energy-intensive cooling systems are used to mitigate these conditions [5]. Furthermore, cooling systems in deep-level mines incur high electricity costs due to their relatively high energy consumption compared to other industries, such as the commercial and retail industries [6].

The high electricity costs have become an increasing problem due to their impact on the production costs of the deep-level mining industry [7]. This has provided opportunities for energy savings initiatives to be implemented. Faster and more

[1] Holder, Kristen, “Discover the Top 10 Deepest Mines in the Entire World”, AZ animals, [Online], Available: https://a-z-animals.com/blog/deepest-mines-in-the-world/, [Accessed: 24-Jul-23]

dynamic solutions have been introduced due to technologies such as AI being set in motion [8].

Due to its complex infrastructure, AI has rarely been utilised in the South African deep-level mining industry. However, decision-making, forecasting, and optimisation using AI give rise to applying dynamic energy savings opportunities [9].

1.2.1. Mining in South Africa

Mining in South Africa has been prevalent since the 19th century when the first diamond was discovered in 1867 in the Hopetown area. The abundance of resources in the country led to the mining industry being the foundation of the South African economy [10]. Moreover, as of 2016, 11% of the world's gold reserves were attributed to South Africa [8].

The gold production in South Africa yielded 92.6 tonnes of gold, ranking it the 13th most gold-producing country in the world[2]. However, it has been observed that gold production has been decreasing year by year since 1990, as seen in Figure 1.

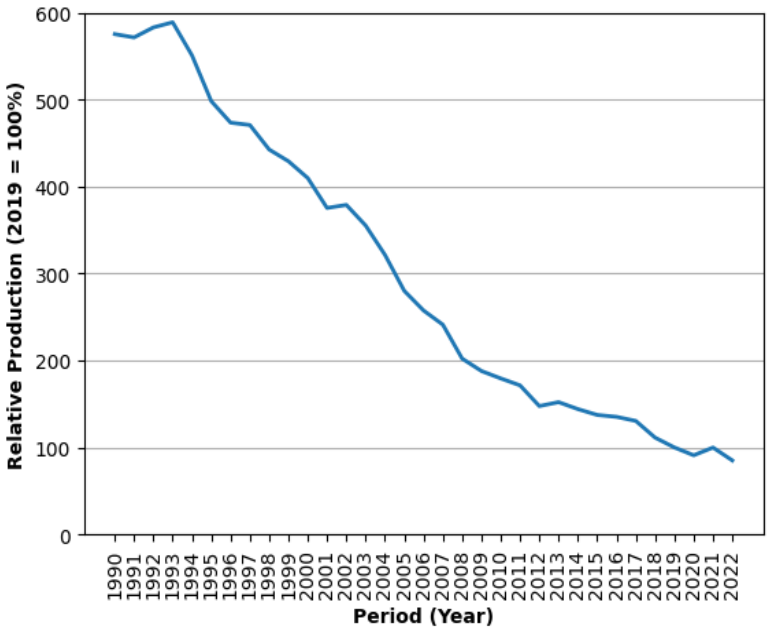

Figure 1: Gold mining historical production in South Africa [11]

[2] "Gold mine production", Goldhub, [Online], Available: https://www.gold.org/goldhub/data/gold-production-by-country, [Accessed: 19-Jul-23]

Furthermore, mining production decreased by 0.8% between May 2022 and May 2023. However, gold was seen as the largest positive contributor [12]. In 2019, the mining industry in South Africa employed 514 859 workers, compared to 538 144 in 2015, where the biggest loss in jobs was found in gold mining (42 091 jobs) [8]. Reasons such as production stoppages, the health of the workforce, the change in infrastructure, and the increase in electricity costs contribute to the loss of jobs in the industry [13]. Although there has been a significant decrease in employability, the gold mining industry remains a notable contributor to the economy regarding employment numbers [12].

1.2.2. Energy consumption of mining systems

Mining electricity costs in South Africa

As mentioned in the preceding section, gold mining production has decreased since 1990. However, it has been observed that these mines are increasing in depth to increase life of mine and to gain more access to the gold reserves [14]. Due to decreases in production and increases in mine depth, the ever-expanding nature of the gold mining industry has significantly contributed to the strain on Eskom's electricity grid [15]. Moreover, the average electricity cost in the mining industry has shown a significant year-on-year increase, as seen in Figure 2 [16].

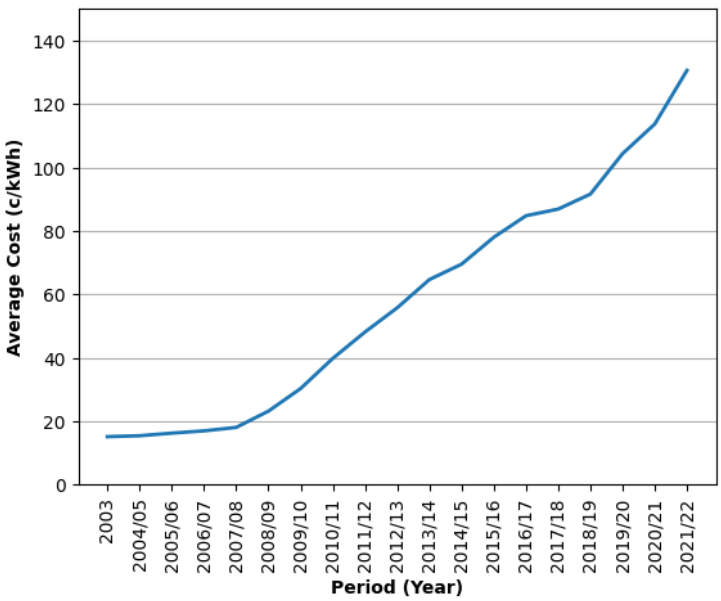

Figure 2: Electricity cost for mining in South Africa [16]

On top of the electricity cost increases, the mining industry must reduce its energy usage during prescribed times due to the country's strained electricity network [17]. This, in turn, leads to losses in production opportunities. Therefore, the implementation of energy efficiency projects will aid in the reduction of production costs in the mining industry.

Energy distribution of mining systems

The main electrical energy consumers consist of [18]:

- Pumping
- Refrigeration
- Compressed air
- Ventilation
- Hoisting and conveying systems

Figure 3 details the predominant energy consumers in a deep-level gold mine [8].

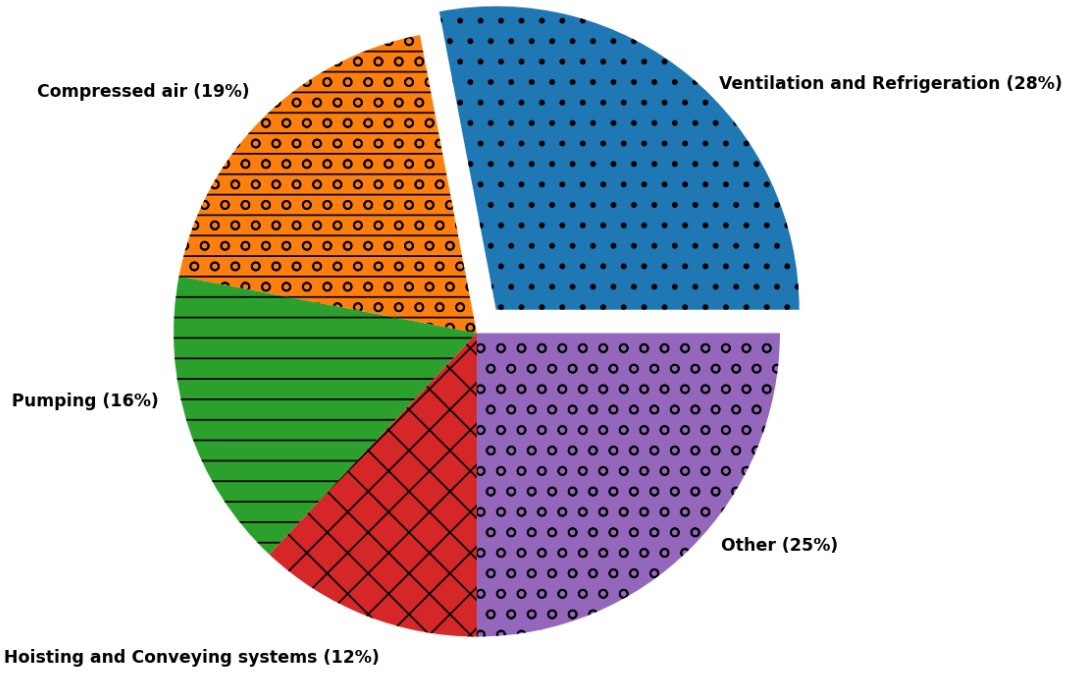

Figure 3: Typical gold mine energy cost distribution (adapted from [8])

As seen in Figure 3, ventilation and refrigeration consume approximately 28% of the energy consumption in deep-level mines.

These commodities are commonly grouped as cooling systems. The objective of cooling systems is to reduce the air temperatures in underground working areas. Ambient air and water are the primary resources for cooling systems. The air is transferred into cold water, reducing the air temperature in these environments [8].

1.2.3. Deep-level mine cooling systems

To maintain suitable working conditions and productivity in deep-level mines, underground temperatures are an imperative parameter that must be considered [19]. Cooling systems in deep-level mines are implemented to reach the objectives mentioned above. Crawford [20] observed that the complexity and capabilities depend on mining depths, which depend on virgin rock temperatures (VRTs). Auto-compression and geothermal heat are key parameters in determining the VRT in an area of the mine. Figure 4 details the relationship between VRTs and mining depths in South Africa.

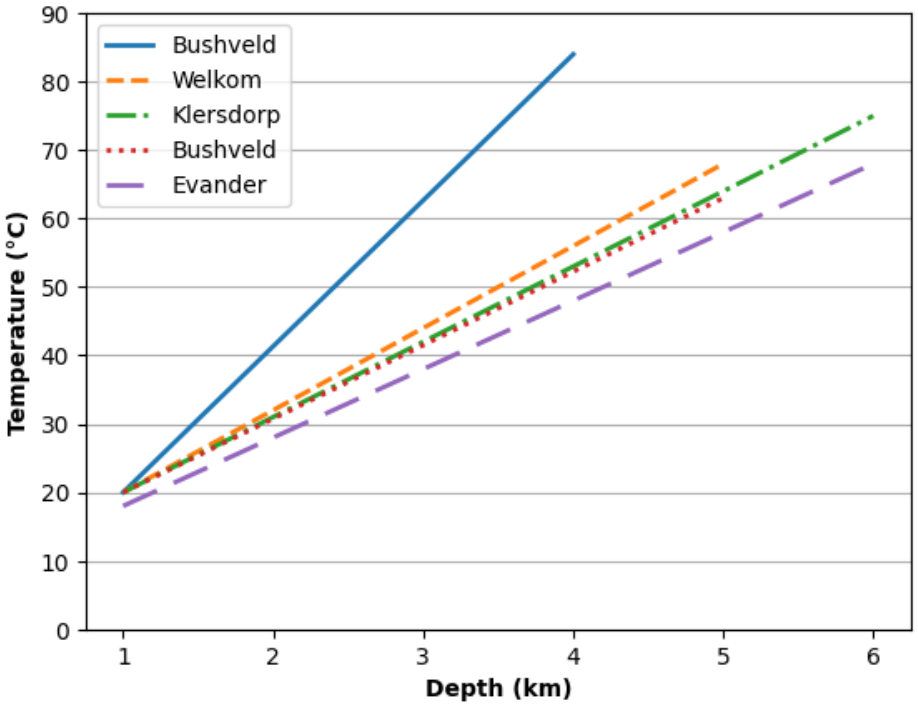

Figure 4: Relationships between VRTs and mining depths in South Africa (adapted from [20])

Figure 4 shows that South African gold mines generally have approximate depths of 4km and experience VRTs around 60ºC.

The Mine Health Safety Act of South Africa (MHSA of SA) forbids work at wet bulb temperatures greater than 32.5ºC and dry bulb temperatures greater than 37ºC [21].

Deep-level mine cooling systems increase in complexity as the depth of the mine increases. The figure below shows the typical configurations of cooling systems, which are dependent on the depth of the mine. As depth increases, additional complexity is added to the system [20].

Deep-level mine cooling systems typically consist of three layers. The first layer consists of surface cooling systems. Surface cooling systems commonly consist of surface bulk air coolers (BACs).

The second layer introduces underground cooling, mainly focusing on underground BACs. The third layer comprises mobile cooling units (MCUs), colloquially categorised as cooling cars [8]. Figure 6 depicts the typical configuration of deep-level mine cooling systems in South Africa.

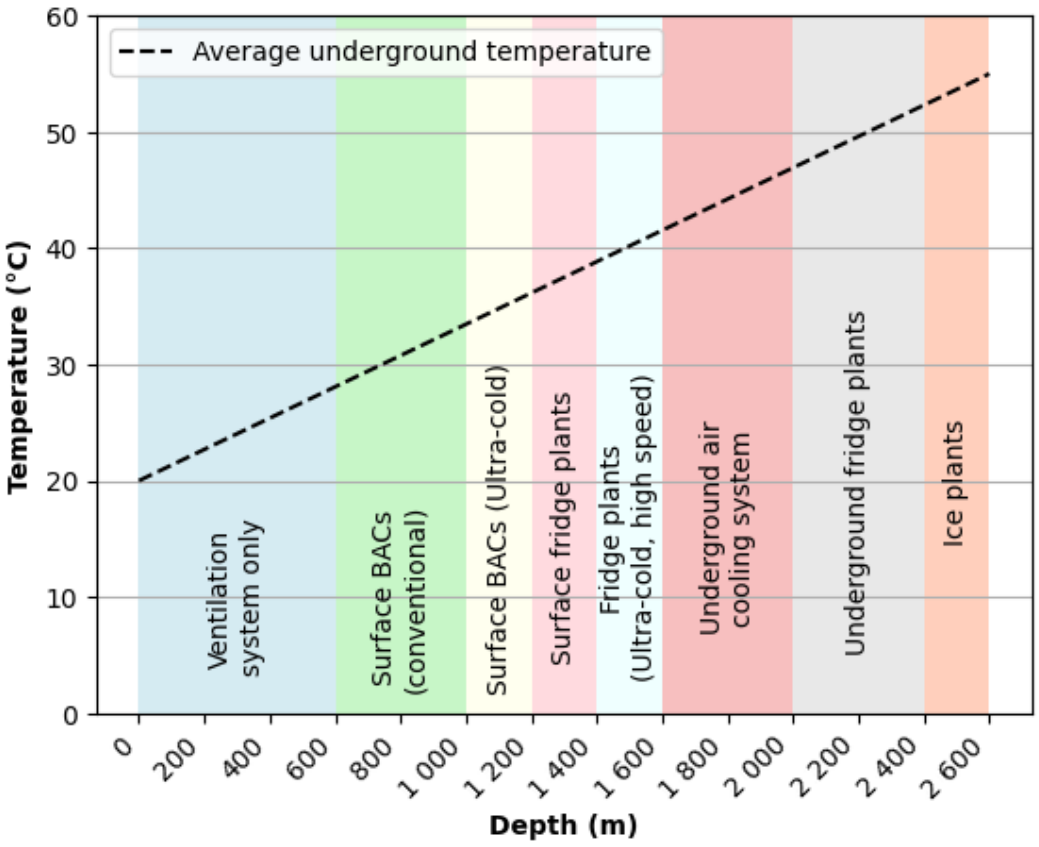

Figure 5: Cooling infrastructure based on depth and temperature (adapted from [22])

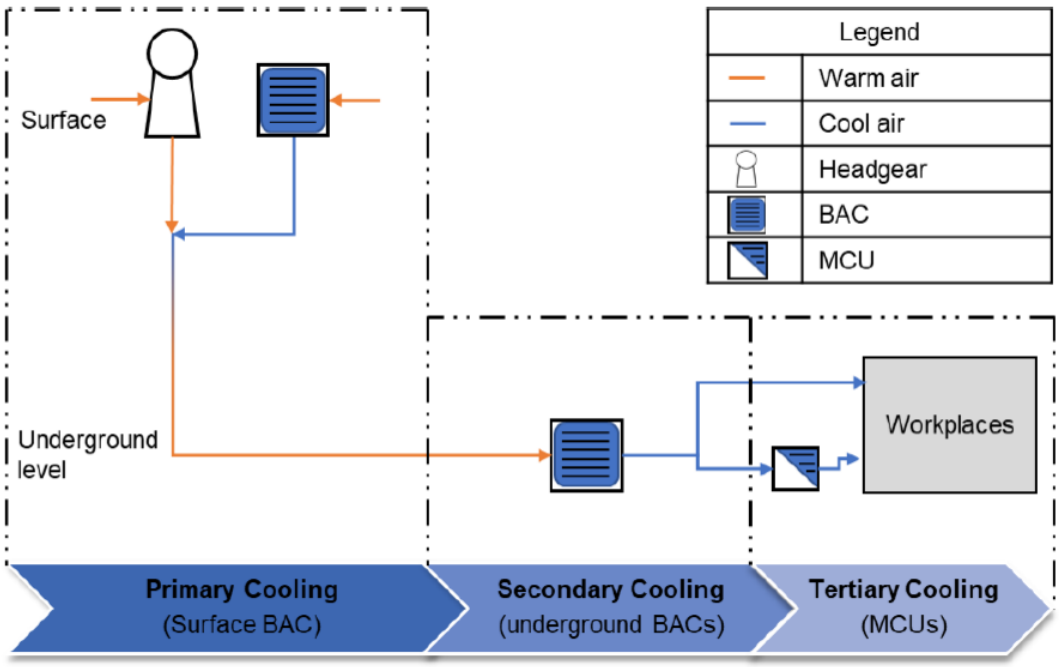

Figure 6: Typical deep-level mine cooling system configuration [8]

Typical cooling systems consist of the following components [15]:

- Refrigeration plants
- BACs
- Pumps
- Dams

Refrigeration plants

Refrigeration plants reduce the temperature of underground hot water. Deep-level mines use the vapour-compression cycle. This is a favoured cycle due to its ease of implementation and low operating costs compared to other existing cycles [23]. Other examples of refrigeration include [24], [25], [26]:

- Thermoelectric effect cycle
- Absorption cycle
- Adsorption cycle

A simple configuration of the vapour-compression cycle can be observed in Figure 7.

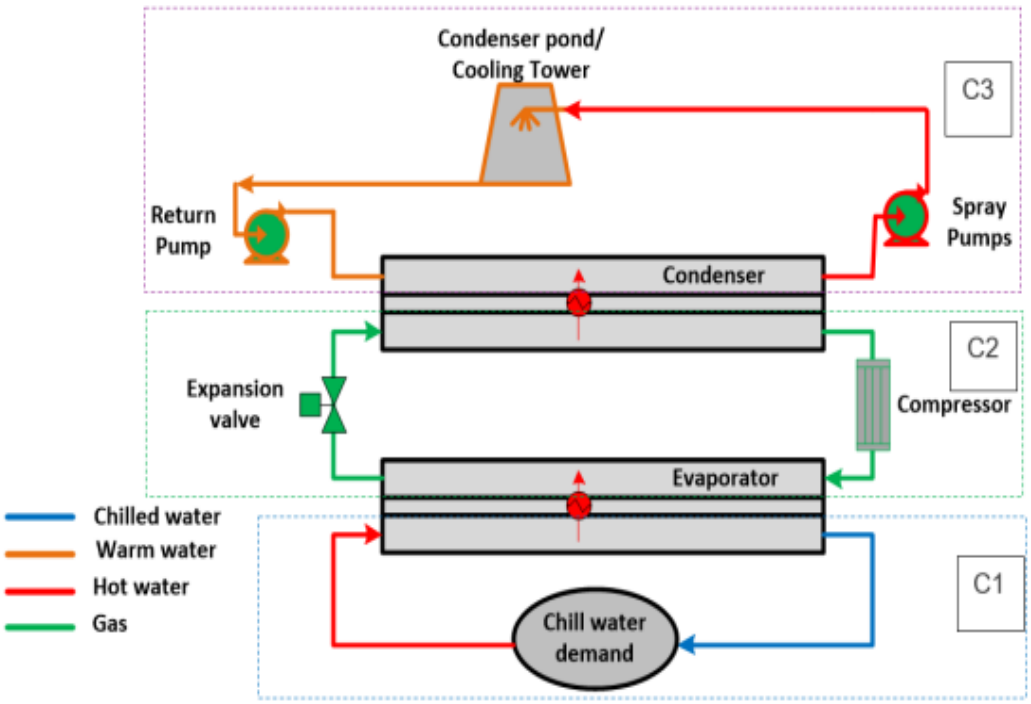

Figure 7: Vapour-compression refrigeration [23]

The vapour-compression cycle consists of three cycles namely, the refrigeration water cooling cycle (C1), the refrigerant gas cycle (C2), and the condenser water cycle (C3). The refrigeration water cooling cycle is responsible for cooling the water with the use of a refrigerant. The water is then sent to the refrigerant gas cycle, where the evaporator extracts water and sends it to the condenser. The condenser water cycle is responsible for extracting heat from the system to the external environment [23].

BACs

BACs use ambient air and cold water to provide cool air to underground working areas [27]. The cold water is either pumped to the BAC or gravity-fed from a dam. Pascoe [28] observed that using BACs is the least expensive component to cool ambient air in underground areas.

This is because less water is required for underground cooling. However, this result is only apparent for deep-level mines that do not require underground refrigeration plants and BACs.

BACs usually have two configurations. These configurations are vertical flow and crossflow [29]. The typical configurations can be observed in Figure 8.

Pumps

The main purpose of pumps is to reticulate the water between cooling system components such as refrigeration plants and BACs [30]. Mines typically use two types of pumps, namely, axial pumps and centrifugal pumps [29].

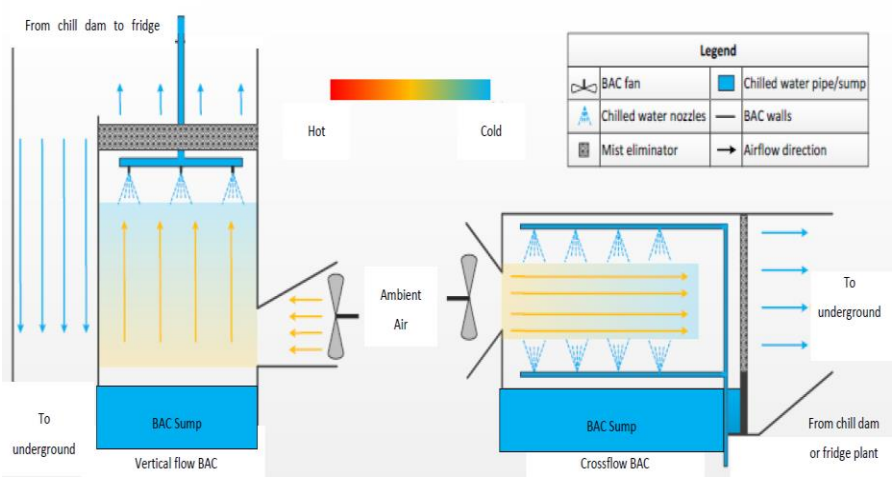

Figure 8: Vertical (left) and crossflow (right) BAC diagrams [27]

Dams

Dams are used to store cold and warm water in deep-level mines. They regulate the water capacity in the cooling systems to adapt to the dynamic characteristics of cold water in deep-level mines [31]. Typical cold dams are covered to maintain the temperature of the water [8], [28].

1.2.4. Deep-level mine cooling system control

Supervisory control and data acquisition

Like many other industries, such as the manufacturing and chemical industries, the mining industry uses control systems named the supervisory control and data acquisition (SCADA) systems [32]. A central controller, sensors, and actuators form the basis of SCADA systems [33]. The typical architecture of SCADA can be observed in Figure 9.

The field sites in the deep-level mine cooling systems consist of the components mentioned above, namely refrigeration plants, pumps, fans, and dams. These components consist of multiple sensors connected to a programmable logic controller (PLC), which is responsible for acquiring data from the sensors [34].

The data is communicated to the SCADA servers via a Wide Area Network (WAN) [32]. Data is then stored on a historian database and displayed in control rooms. A typical SCADA display can be observed in Figure 10.

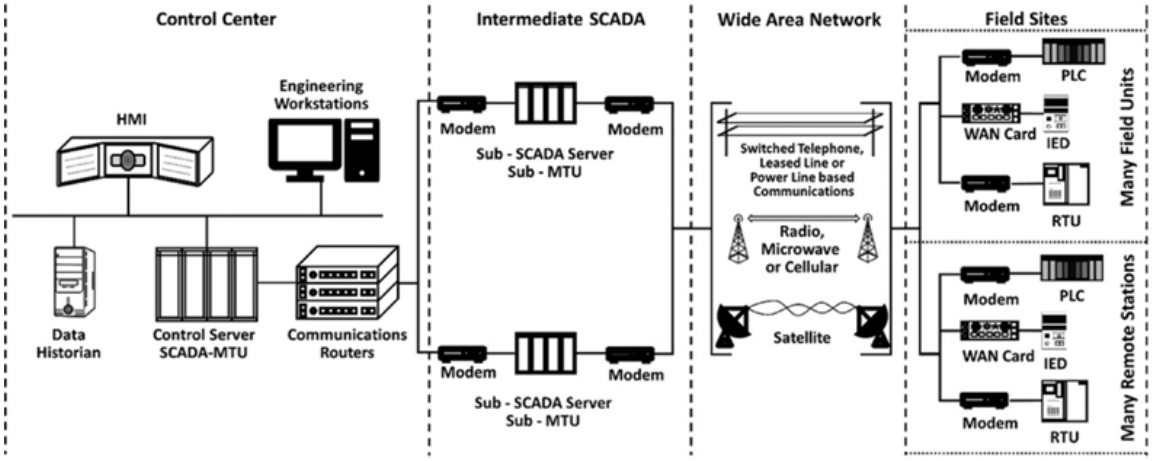

Figure 9: SCADA architecture [32]

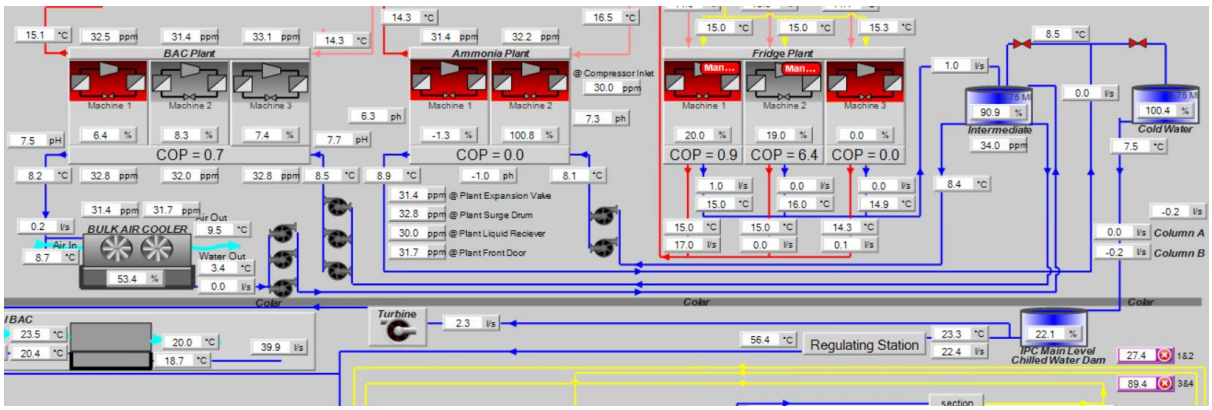

Figure 10: SCADA display example

Set point control

Deep-level mine cooling systems are controlled to meet specific service delivery requirements: temperatures and dam levels. This is done using the step response control method [8].

The step response control method provides an output to a system based on an instantaneous event. This is typically done using the set point control method [20]. The setpoint is an objective that belongs to a specific cooling system parameter of components [8]. For example, a guide vane angle setpoint is determined and implemented on a refrigeration plant compressor. The guide vane angle will be adjusted to meet the set point angle determined for the time of the day [35]. The figure describes the workings of a setpoint control model.

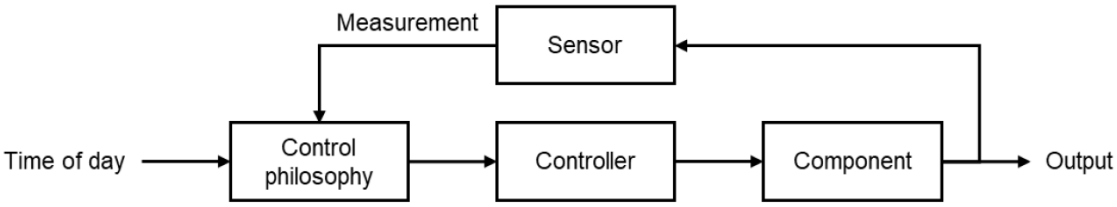

Figure 11: Set point control flow diagram [8]

An advantage of set point control is that it is rather simplistic in implementation [36]. Disadvantages include [8], [37], [38]:

- It does not change based on adjustments to the infrastructure and operations.
- Implementing energy savings becomes difficult if the set point has been adjusted.

Dynamic control

Dynamic control is more complex than setpoint control. The dynamic control could observe multiple inputs to attain a specific objective [37]. It considers the baseline operations as well as the current operations. The response is adjusted based on the difference between the baseline and the current operations [39].

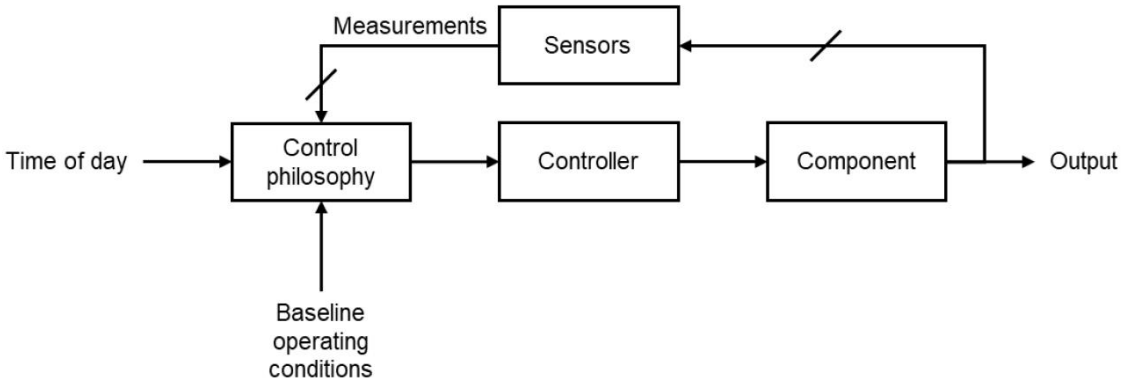

Figure 12: Dynamic control flow diagram [8]

Drawbacks of dynamic control include:

- The complexity of the model requires large computational time and complex computational technologies [38].
- Human inference of the model is limited; hence, it becomes difficult to make corrections to incorrect control models [40]

1.2.5. Energy savings implementations on mine cooling systems

As mentioned in Section 1.2.2, deep-level mine cooling systems account for approximately 28% of the electricity costs in deep-level mines [8]. Therefore, these systems are seen as one of the major contributors to energy consumption in this industry. Thus, it is imperative to implement energy savings strategies to address the mine's increasing electricity costs. Load shifting, peak clipping, and energy efficiency strategies are among the popular approaches for energy savings initiatives [41].

Load shifting

Load shifting energy savings projects shift the energy requirements of a system to different periods of the day while using the same energy usage of the system and maintaining the cooling requirements throughout the day in the context of cooling systems [8]. The shifts in energy are based on the Time-of-use (TOU) tariff structure of the electricity supplier, which is Eskom for South African deep-level mines [16]. The

Eskom TOU tariff structure is divided into three periods of the day: peak, off-peak, and standard, as seen in Figure 13.

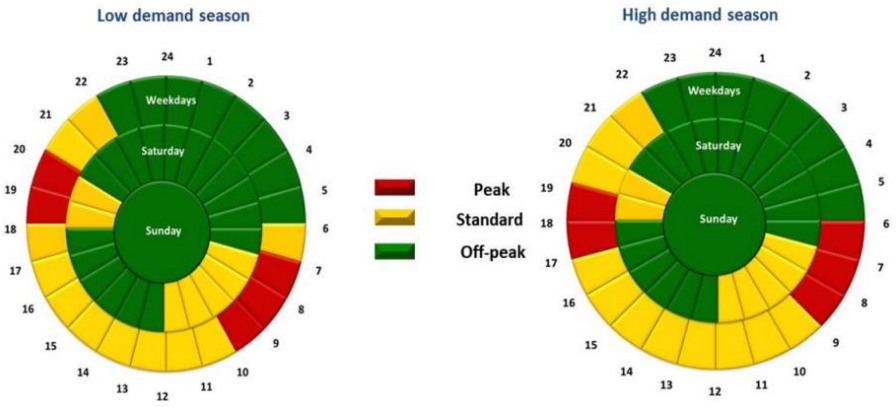

Figure 13: Eskom Megaflex tariff structure [42]

Figure 13 details different tariff structures for the low and high-demand seasons. The high-demand season spans from June to August. The remaining months compose the low-demand season [28].

Peak clipping

Peak clipping aims to reduce energy consumption during specific periods of the day [41]. In the context of cooling systems, this method is often implemented when mining personnel are not underground, as shown in Figure 14 [28].

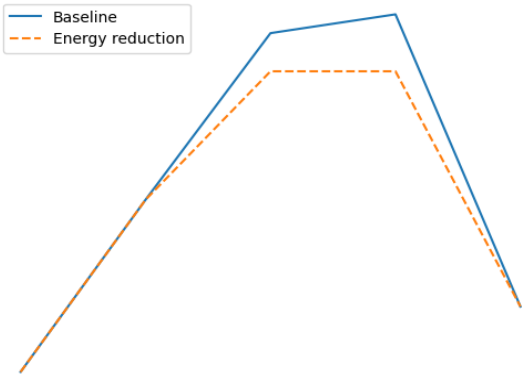

Figure 14: Peak clipping energy reduction

Energy efficiency

Figure 15 indicates the outcome of energy efficiency implementations. Energy efficiency projects aim to use less energy by improving the cooling system's efficiency. These improvements are seen using:

- Adjustments of control philosophies. E.g., Seasonal control [41]
- Installation of new technologies. E.g., the installation of variable speed drives (VSDs) reducing the flow into cooling systems [20]

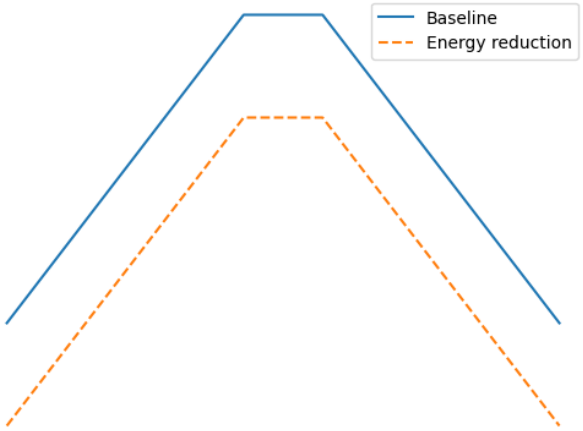

Figure 15: Energy efficiency energy reduction

1.3. Artificial intelligence

Large computational times have been mitigated with the introduction of AI [8]. AI is a vast topic that incorporates many topics, which include computer science, engineering, mathematics, and statistics [43]. AI is commonly known as a "buzzword"; hence, the definition has not been concisely identified. Several AI scientific committees define AI as a tool or resource that contributes to and enhances the daily lives of humans [44].

The application of AI has increasingly become more prevalent in many industries. The medical, media, education, finance, agriculture, and manufacturing industries have made significant gains in the use of AI in applications which do not necessarily require human intervention [45]. Applications of AI include:

- **Automation**: Automation is completing repetitive tasks to allow humans to focus on more complex tasks. Automated assembly lines in factories are an example of automation [43].

- **Robotics**: Robotics is a field akin to automation since they both perform repetitive tasks. Robotics tends to be represented by machines that perform tasks. Research is steadily increasing in the development of artificially intelligent robots. These robots are created to behave and learn similarly to humans [43].
- **Optimisation**: Optimisation uses machine learning, deep learning, and metaheuristic algorithms to make real-time decisions on systems and processes [46].
- **Image Processing**: Makes use of machine learning and deep learning for pattern recognition in images [47]. A common application is the diagnosis of infectious diseases [48].

Although AI has a variety of applications, several drawbacks are, but not limited to [43]:

- Lack of transparency. AI applications are typically classified as “black box” models [49]. “Black box” models know inputs and outputs; however, the inner workings are unknown.
- Trust. Due to the adoption of the “black box” model, it is difficult for stakeholders to trust AI applications in industries.

The mining industry has made significant progress in applying AI technologies—Table 1 details implementations of AI in the mining industry.

Table 1: AI in mining studies

Study	**Description**
Harmse [8]	Utilised AI optimisation techniques for the dynamic control of refrigeration plants.
Ouman [50]	Applied image processing in the mining industry. Image processing was used to identify froth on froth floatation systems.
Nguyen [51]	Implemented AI algorithms to predict and control blast-induced vibration in open-pit coal mines.

Study	Description
Mathee [34]	Used a machine learning model to predict compressed air control parameters in real-time.
Hyder *et al*. [52]	Recognised several AI applications in the industry. Prospecting and exploration, drilling, and autonomous vehicles were identified among the applications.

The table above indicates that AI has been implemented in the mining industry. However, mining is not among the top industries that use AI in their systems and processes [43].

Due to the increased computational performance, AI, specifically machine learning, deep learning, and AI optimisation techniques, has increased in popularity in decision-making processes [52].

1.3.1. Machine learning

The basic principles of machine learning have been present for several decades. Due to the advances in computer technology and the plentifulness of data, machine learning has increasingly become more popular in industrial systems [53].

Mitchell defined machine learning as a computer program that progressively learns a task from experience. The programme's performance is then assessed and improves with experience [54]. Figure 16 details the typical workings of machine learning models [55].

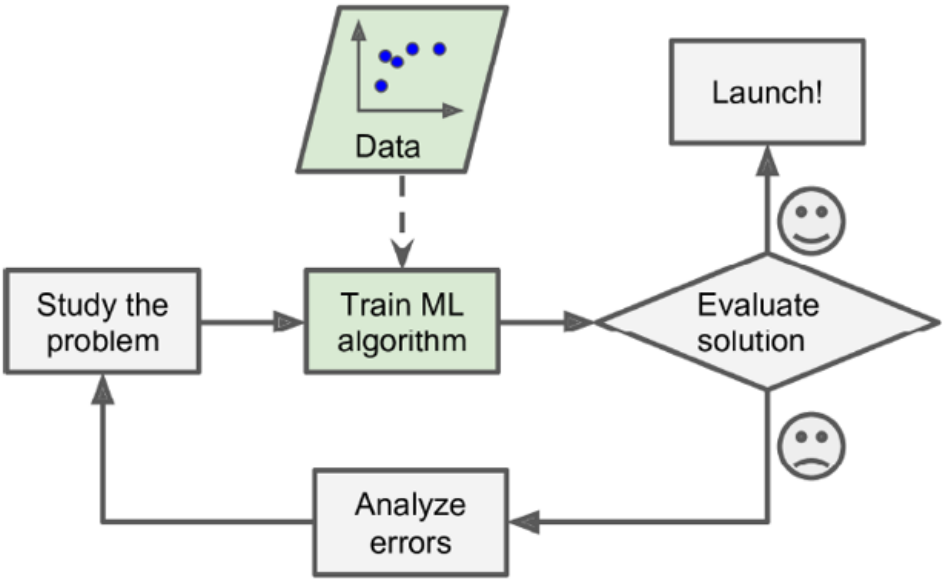

Figure 16: Machine learning process flow diagram [55]

Machine learning is typically divided into supervised, unsupervised, and reinforcement learning [45]. Figure 17 details categories that fall under machine learning.

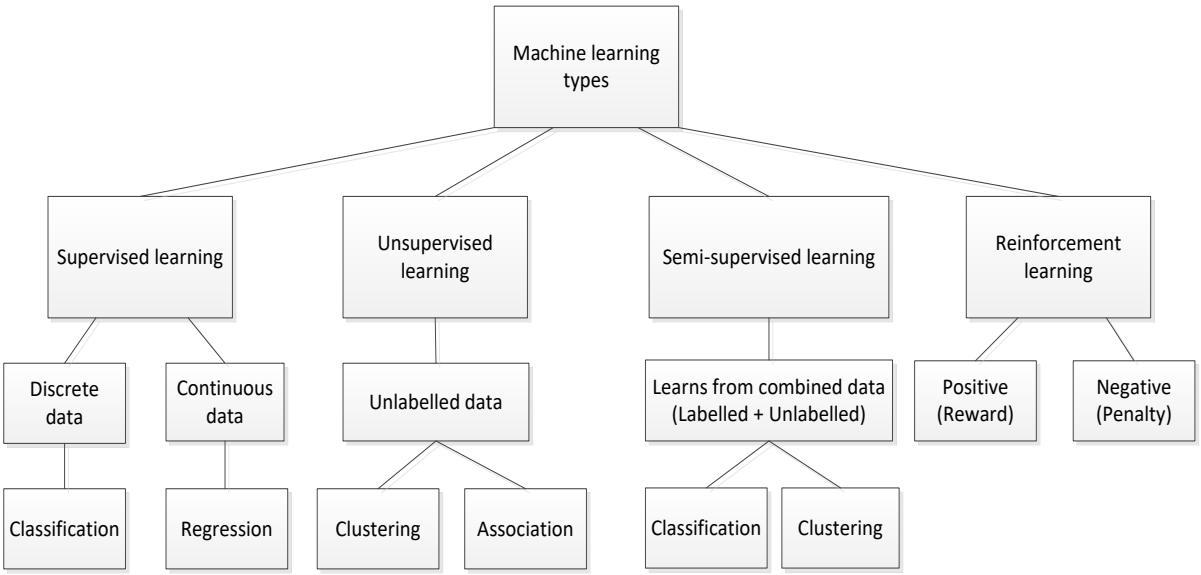

Figure 17: Machine learning types (adapted from [56])

Supervised learning

Supervised learning is the process where learning occurs by using a predetermined relationship between the inputs and outputs [53]. In other words, the data is labelled.

For instance, the mileage, age, and brand are used to determine the price of a vehicle. Examples of supervised learning include [55]:

- Linear Regression
- Logistic Regression
- K-Nearest Neighbours (KNN)
- Support Vector Machines (SVMs)
- Decision Trees and Random Forests
- Neural Networks

Unsupervised learning

Unsupervised learning occurs when data is not labelled [55] [57]. Unsupervised learning is used to identify the underlying relationships between inputs and outputs. Unsupervised learning algorithms cover, but are not limited to [55]:

- Clustering
- One-Class SVM for anomaly and novelty detection
- Principal Component Analysis (PCA) for visualisation and dimensionality reduction
- Apriori for association rule learning

Reinforcement learning

Reinforcement learning is based on observations of the provided data [55]. Sarker observed this as an environment-driven approach [56]. These algorithms learn using a trial-and-error method. A reward is given if the correct insights are observed, whereas a penalty is given for incorrect insights.

If no reward is given, the algorithm re-adjusts to improve the probability of achieving the correct insights [53]. Reinforcement learning has been applied in game theory, robotics, and optimisation [56].

The algorithms mentioned above are not limited to their separate categories. In some cases, the categories are combined to achieve improved insights and complexity [53], [55], [57]. Deep learning is another machine learning algorithm that belongs to the

machine learning family and is incorporated into all the categories mentioned above. This type of learning will be discussed further in Section 1.3.2

1.3.2. Deep learning

Deep learning is a subfield or category of machine learning where the algorithms are based on the brain's architecture [58]. They make use of multiple processing layers to gather insights with the use of large amounts of data [59]. The processing layers are also known as Artificial Neural Networks (ANNs), which form the nucleus of deep learning, as mentioned by Géron [55].

Artificial Neural Networks

ANNs are observed as a representation of complex mathematical equations [49]. Neurons, akin to neurons from the human brain, form the basis of the ANN [34]. These neurons are interconnected, sending a message to each other obtained from an input. These connections form a complex network, which allows it to gain insights based on the messages [58]. The simple architecture of an ANN can be seen in Figure 18.

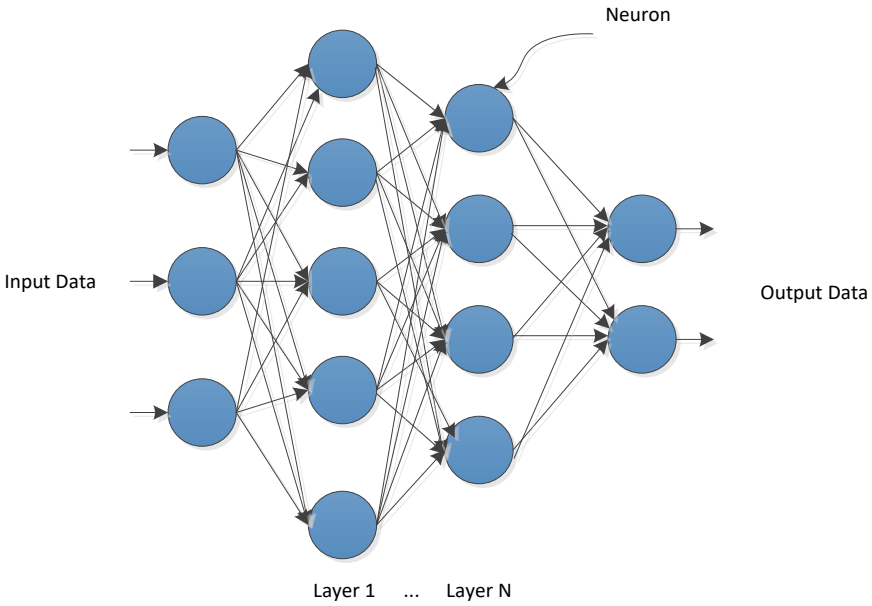

Figure 18: Simple architecture of an ANN (adapted from [58])

ANNs typically consist of three layers, namely the input layer, the hidden layer, and the output layer [34], [49], [60]. The input layer mainly consists of the model's input variables; the output layer represents the desired outcome for the model, and the

hidden layer, where the relationship between the input variables and the desired outcome is determined [61]. The hidden layer determines the relationship between the input and output using weights. These weights dictate the influence each input variable has on the desired outcome [34]. The ANN identifies the weights to produce the desired output with minimal error [60]. The error is typically determined using the mean square error (MSE), which can be observed as follows:

$$MSE = \sum_{i=1}^{N} \frac{(Y_t - Y_o)^2}{N} \quad (1)$$

Where:

- MSE is the mean square error.
- N is the number of parameters.
- Y_t is the desired output.
- Y_o is the model output.

ANNs consist of various algorithms, which differ depending on the desired application of the model. Multilayer Perception (MLP), Convolutional Neural Networks (CNNs), and Recurrent Neural Networks (RNNs) are among the most common ANN algorithms [62].

Multilayer Perception

MLP is a feed-forward network [56], [61]. A feed-forward network is present when information is only processed in one direction through multiple neurons and layers [63]. MLP forms the basis of the majority of existing ANNs.

Convolutional Neural Networks

CNNs have a modified enhancement of the ANN architecture with the addition of convolutional layers [56]. The convolutional layer is made from multiple matrices called kernels, which attempt to identify patterns in the input variables [64]. CNNs are typically used in areas such as image processing, classification, and natural language processing [56], [58]. The architecture of a CNN can be seen in Figure 19 below:

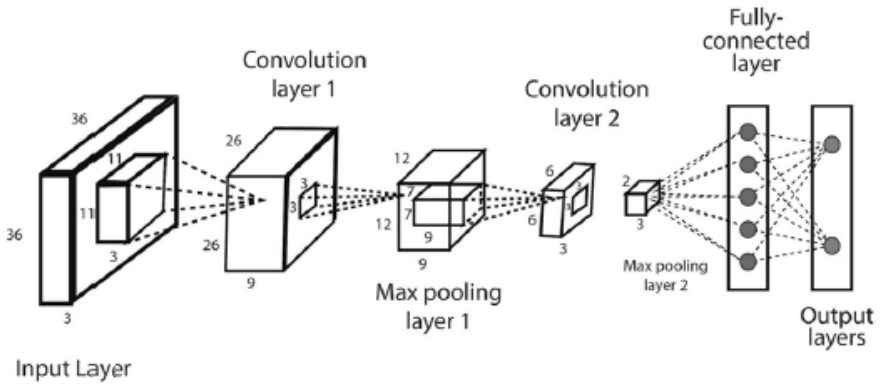

Figure 19: An example of a CNN architecture [56]

Recurrent Neural Networks

RNNs were developed to implement ANNs on sequential data. RNNs contain a hidden layer which recollects the state of the input variables. The desired output is determined by the feed-forward network and the previous states observed [62]. RNNs are typically used when modelling sensor data, typically categorised as time series data.

1.3.3. Time series forecasting

Time series forecasting aims to predict future values using time series input data [65]. Time series data is data that is time-dependent [66]. This technique typically gathers insights by observing the correlation between input data with the same timestamps [67].

Time series forecasting applications include but are not limited to [68] [69]:

- Signal processing
- Biological sciences
- Medicine
- Finance
- Marketing
- Climate modelling

Time series forecasting has become increasingly popular due to the advent of technologies and data growth over recent years. Moreover, the models have also

increased in variety. However, all models do not apply to all types of time series data. Due to the nature of time series data, machine learning techniques, like linear regression models, are popular for time series forecasting due to their simplistic approach.

Linear regression

Linear regression is amongst the most popular machine learning techniques for modelling [67]. A linear regression model determines a linear relationship between independent and dependent variables [34]. A linear regression model in the context of a time series can be described with the following equation [49], [67]:

$$y_t = m_1 x_{t1} + m_2 x_{t2} + \cdots m_n x_{tn} + \varepsilon_t \quad (2)$$

Where:

- y_t is the desired output or dependent variable.
- m_n is the regression coefficient or weight.
- x_{tn} is the independent variable.
- ε_t is the error.

Figure 20 illustrates the linear regression model described in Equation 2 above:

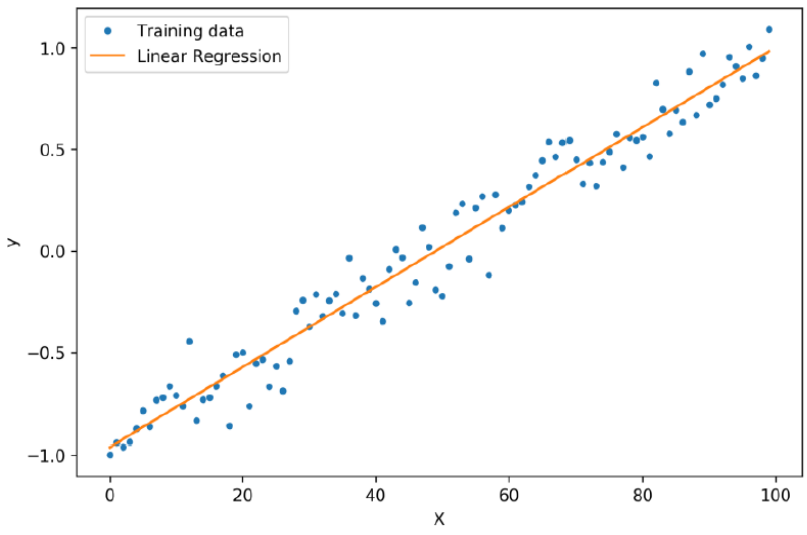

Figure 20: Linear regression model [34]

Although linear regression is observed as a simplistic and effective tool, certain requirements need to be met to implement this technique for time series forecasting. These requirements are [70]:

- Linearity: The relationship between the output and input variables must be linear.
- The input variables must be independent of each other.
- The observations must be independent of each other.
- The error in the model should not be dependent on the previous data, also known as autocorrelation.

Due to the nature of time series data, the error depends on previous data; hence, autocorrelation is present. Models such as the auto-regressive (AR) model, the moving average (MA), auto-regressive moving average (ARMA), and the auto-regressive integrated moving average (ARIMA) mitigate the failed assumptions observed when applying linear regression techniques to time series data [71].

Auto-regressive model

The AR model uses a linear formula to determine the future value of a variable, akin to a linear regression. However, the difference is observed where the formula for the AR model is based on the variable itself, hence being described as “auto-regression” [71]. The AR model can be detailed in Equation 3 below:

$$y_t = c + m_1 y_{t-1} + m_2 y_{t-2} + \cdots m_p y_{t-p} + \varepsilon_t \quad (3)$$

Where:

- c is a constant where no previous values are considered.
- y_t is the desired output or dependent variable.
- m_p is the regression coefficient or weight.
- p is the number of previous values that are considered.
- ε_t is the error.

Moving average model

The MA model is determined by creating a linear formula based on averages of a separate time series [72]. The separate time series is compiled using the error terms of forecasted values and is detailed in Equation 4:

$$y_t = c + \varepsilon_t + m_1\varepsilon_{t-1} + m_2\varepsilon_{t-2} + \cdots m_p\varepsilon_{t-q} \quad (4)$$

Where:

- q is the number of error terms that are considered.

Auto-regressive moving average

The AR and MA models can be combined to form the ARMA model. Zhang and Moore [73] observed that ARMA models yield more effective forecasts than the AR and MA models due to minimising the number of parameters required when forecasting. The ARMA model is given as:

$$y_t = \left(c + m_1 y_{t-1} + m_2 y_{t-2} + \cdots m_p y_{t-p} + \varepsilon_t\right) + \left(\mu + \varepsilon_t + m_1\varepsilon_{t-1} + m_2\varepsilon_{t-2} + \cdots m_p\varepsilon_{t-q}\right) \quad (5)$$

Where:

- p is the number of previous values.
- q is the number of previous error terms.

The models are typically used for stationary time series data. Stationary data refers to data that does not change over time [66]. The ARIMA model was introduced to forecast and model time series dependent on time.

Auto-regressive integrated moving average model

The ARIMA model was popularised in the 1970s by George Box and Gwilym Jenkins [74]. The ARIMA model is a modification of the ARMA model with an integrated section, which allows the model to be implemented on non-stationary data. The integrated section uses differencing, which makes the data stationary by subtracting

an observation value from a previous value [66]. ARIMA model is typically notated as ARIMA (p, q, d) where [66] [71]:

- p and q correspond with the p and q that was mentioned in the ARMA model
- d is the number of iterations of differencing required to make a time series stationary

The ARIMA model has shown promise in forecasting time series data that is linear [75]; however, the same promise was not observed with data that contained seasonal patterns, hence the development of the seasonal ARIMA model (SARIMA) [76].

Seasonal auto-regressive integrated moving average model

The SARIMA model supplements the ARIMA model by including seasonal parameters. The typical notation of the model is shown as SARIMA (p, q, d) (P, Q, D) where [74]:

- p, q, and d correspond with the p, q, d mentioned in the ARIMA model
- P is the seasonal component of the AR (p) parameter
- Q is the seasonal component of the MA (q) parameter
- D is the seasonal differencing (d) parameter

Zhang *et al.* [77] observed that the SARIMA model effectively forecasts time series, including seasonal parameters. However, it was not as effective when forecasting data affected by multiple parameters. Making use of ANN techniques was suggested to forecast this type of data.

ANNs for time series forecasting

ANNs are suitable for forecasting time series data due to the following reasons [78]:

- Non-linearity: Time series data, typically multivariate, tend to be difficult to forecast using the models above. ANNs mitigate this difficulty by identifying the complex non-linear relationships between the input and output variables.
- Use of high-dimensional data: Time series forecast typically performs better when large amounts of data are used. ANNs effectively determine models with such data, which aids in forecasting an output variable.

- Temporal dependencies: Temporal dependencies detail how dependent a previous behaviour is on the current behaviour [79].

Although ANNs have shown significant promise in time series forecasting, they have drawbacks. Drawbacks include [55] [69]:

- Complexity: ANNs are difficult to interpret and understand; thus, there is difficulty in identifying the reasons that affect the model's performance.
- Overfitting: Overfitting is observed when the model performs well during the training phase. However, the model's performance significantly decreases when exposed to unseen data [80]. Overfitting when implementing an ANN will occasionally occur when many parameters are selected.
- Speed: Due to the complexity of the chosen ANN, the model can be computationally intensive during the training phase due to the nature of time series data. The model may require training on multiple occasions, hence unsuitable for real-time response.

Due to recent developments in technologies, the computational intensity of these models has decreased. The application of pre-processing, feature engineering, parameter selection, and model selection should be applied to mitigate the drawbacks that were mentioned [55] [58] [78].

As mentioned above, RNNs are best suited for time series forecasting due to their purpose for modelling sequential data such as time series data. Gated Recurrent Unit (GRU) and Long Short-term Memory (LSTM) are typical types of RNNs due to their ability to handle long-term dependencies [81]. For instance, the temperature changes based on seasonality will be considered when modelling the time series data.

Gated Recurrent Unit

The basic structure of a GRU model has two gates: an update gate and a reset gate. These gates are vectors that determine which information is provided to the output. The update gate determines the amount of previous memory kept [66] [71]. The GRU is made up of the following components along with their respective equations:

- Update gate: $$z = \sigma(W_z x + U_z h) \quad (6)$$
- Reset gate: $$r = \sigma(W_r x + U_r h) \quad (7)$$
- Cell state: $$c = tanh(W_c x + U_c(rh)) \quad (8)$$
- New state: $$h_t = h(1 - z) + z.c \quad (9)$$

Where:

- σ is the sigmoid function.
- W_z is the weighted matrix for the input state.
- x is the input vector.
- U_z is the weighted matrix for the hidden state.
- h is the hidden state vector.
- h_t is the output vector.

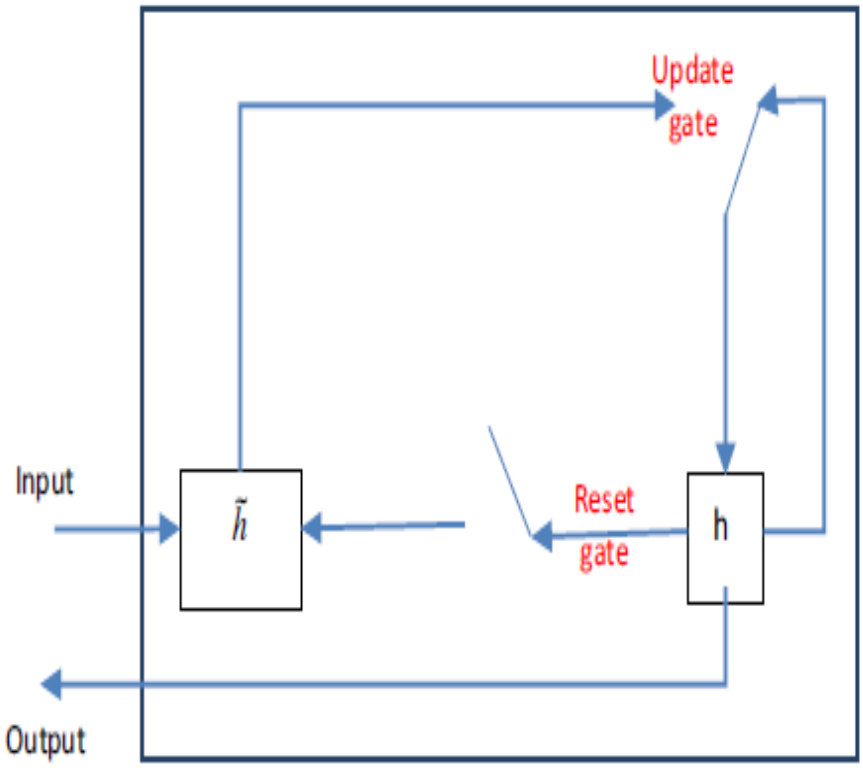

Figure 21: GRU network architecture [71]

Long Short-term Memory Recurrent Neural Network

Faustryjak *et al*. [82] observed that LSTM models are one of the best-performing models for time series forecasting. These models can identify patterns from input variables over a long sequence [71]. The LSTM model is represented as a memory cell. The memory cell is divided into two segments.

The first segment contains the input gate, a forget gate and an output gate. The multilayer perceptron is typically used as the output gate. These gates are responsible for determining which data is important to the model. The second segment contains the cell state and a hidden state. These states are used for gathering data for the next time step [66]. Figure 22 details the structure of the LSTM cell.

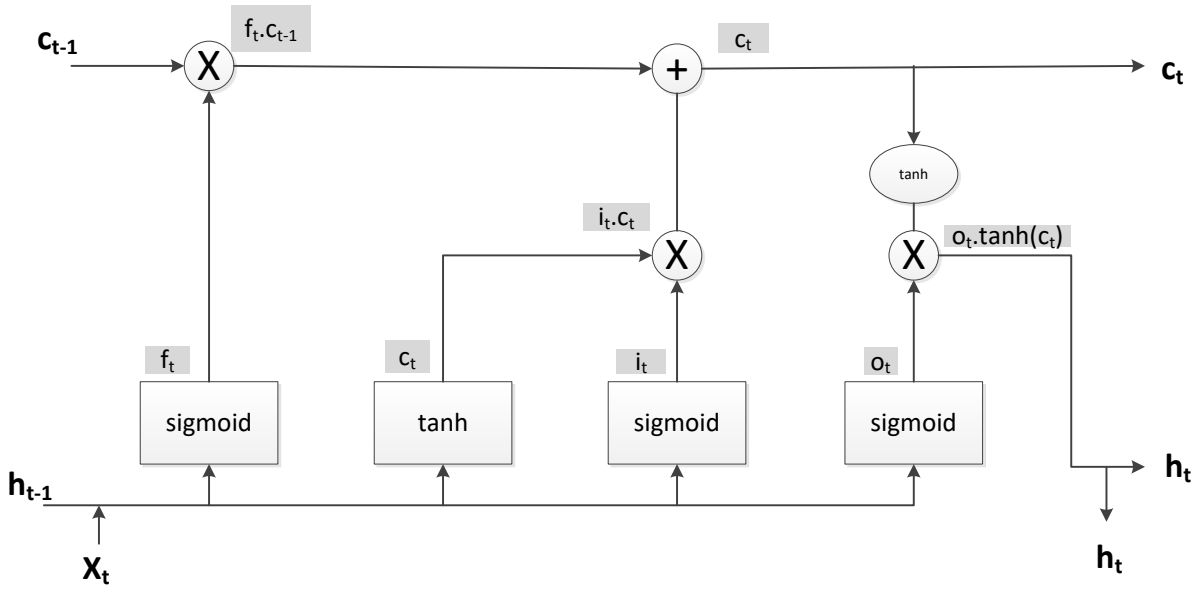

Figure 22: LSTM cell structure (adapted from [66])

The gates and states are described mathematically as follows:

- Input gate: $$\mathrm{i}_t = \sigma(W_i h_{t-1} + W_i h_t) \quad (10)$$
- Forget gate $$f_t = \sigma\left(W_f h_{t-1} + W_f h_t\right) \quad (11)$$
- Output gate $$o_t = \sigma(W_o h_{t-1} + W_o h_t) \quad (12)$$
- Hidden cell state $$C = tanh(W_c h_{t-1} + W_c h_t)\big) \quad (13)$$
- Cell state $$c_t = (i_t C) + (f_t c_{t-1}) \quad (14)$$
- New state $$h_t = o_t\, tanh(c_t) \quad (15)$$

Where:

- h_t is the output vector.
- W_i, W_f, W_o, and W_c are the parameter matrices for each of the gates and states

The LSTM model is well-suited for time series forecasting; however, it does contain several drawbacks, which include:

- They require larger amounts of data during the training phase.
- LSTM models can be computationally intensive since the LSTM cell's parameters must be calculated.
- They may perform poorly with data that contains large amounts of noise.

1.4. Air temperature forecasting

As mentioned by Yamak *et al*., time series data is time-dependent [66]. Temperature is observed as a sequential measurement that varies over time, thus falling into the category of time series data [83]. Classical or numerical air temperature forecasting is done with the use of atmospheric models based on current ambient conditions [65].

The determination of unforeseen events, such as tornados, the prediction of soil surface temperature, and energy consumption are use cases for air temperature forecasting [84]. The use of air temperature has been an integral parameter in the implementation of control strategies in HVAC systems in residential buildings [85]. Table 2 details existing literature on the use of air temperature forecasting in HVAC systems:

Table 2: Summary of literature based on air temperature forecasting.

Study	**Description**
Hietaharju *et al*. [85]	Developed a mathematical model to predict the indoor temperature to perform demand side management of the HVAC system within an office building.
Aliberti *et al*. [86]	Applied an RNN model with the demand response and demand side management on smart buildings.

Study	Description
Elmaz *et al*. [87]	Introduced a combination of the CNN-LSTM model to determine the operating conditions of HVAC systems in buildings.
Mtibaa *et al*. [88]	Made use of an LSTM model to predict the indoor air temperature to determine a control strategy for HVAC systems in indoor buildings.
Bellagarda *et al*. [89]	Implementing an energy management strategy of HVAC systems through smart building indoor air temperature forecasting using ANNs.

Bellagarda *et al*. [89] observed that the LSTM-RNN model is the most common approach used for air temperature forecasting. This is also observed in Table 2.

1.5. Literature study

1.5.1. Summary of literature

The focus of this study is the implementation of control strategies in deep-level mine cooling systems. Several studies focused on implementing static setpoint control strategies on such systems. Although these strategies were successful, these strategies are not implemented dynamically due to the uncertainty of conditions during all periods of the year.

Studies indicate the possibility of implementing AI for decision-making in the deep-level mining industry. For instance, Harmse [8] used AI to optimise deep-level mine refrigeration systems. Table 3 below summarises related studies discussed and indicates gaps in the current literature. The following criteria were determined as relevant to the study:

- **Deep-level mining industry**: Does the study take place in the mining industry? It is important to note the requirements of the deep-level industry as they may differ from other industries.
- **Cooling systems**: Is the study focused on cooling systems? Cooling systems have a set of parameters to determine the system's operating status.
- **Control Philosophy**: Was a control philosophy or strategy implemented?
- **Artificial Intelligence**: Does the study implement AI technologies and tools into a control philosophy?
- **Temperature forecasting**: Was temperature forecasting used as decision-making as the primary medium for control strategies?
- **Cost savings**: Does the study result in energy cost savings?

The literature study was conducted by using various databases. It was identified by searching the criteria above deep-level mining, cooling, refrigeration, and ventilation systems, control, AI, temperature forecasting, and cost savings. Science Direct[3], IEEE Explore[4], ResearchGate[5], Springer[6], and general searches using Google Scholar were the databases examined for the search. The following sections shall discuss the outcomes and shortcomings of the studies focusing on one or more of the criteria.

Enhancing mine cooling efficiency using optimised control strategies [4 - 6], [15], [20], [26 - 30], [35] [41]

The studies focused on enhancing the efficiency of deep-level mine cooling systems. Mathematical models and simulation software were used to identify and develop control strategies accounting for seasonal variations and peak demand. The strategies included the installation of VSDs, peak clipping, and load shifting strategies.

However, these studies did not monitor the underground air temperatures at deeper levels. Moreover, some of the strategies required additional infrastructure to be installed in the mine to improve the accuracy of the developed models. The lack of instrumentation can be addressed by implementing AI techniques.

[3] ScienceDirect, [Online], Available: https://www.sciencedirect.com/, [Accessed: 2022]
[4] "IEEE Xplore", [Online], Available: https://ieeexplore.ieee.org/Xplore/home.jsp, [Accessed: 2022]
[5] ResearchGate, [Online], Available: https://www.researchgate.net/,[Accessed: 2022]
[6] Springer Link, [Online], Available: https://link.springer.com/, [Accessed: 2022]

Utilising AI to optimise refrigeration systems in deep-level mining [8]

This study applied an AI optimisation technique, particle swarm optimisation, to develop a dynamic control strategy on deep-level mine refrigeration systems. A mathematical model was used to characterise the refrigeration plant and was applied to the optimisation algorithm. Most of the cost savings were observed by a load shifting and efficient plant selection recommended by the strategy. The study did not include the effect of air temperatures in the solution. Moreover, AI techniques such as ANNs could characterise the plants more accurately and incorporate additional parameters with minimal effort.

Application machine learning models for prediction and forecasting [9], [51], [77], [82]

These studies explored the application of machine learning models in various industries, such as the environmental, medical, mining, and financial industries. Cabaneros *et al.* [9] reviewed the application of ANNs in the context of air pollution. Zhang *et al.* [77] compared the performance of ANNs, RNNs, and the SARIMA for predicting monthly typhoid fever incidence, with the neural network models outperforming the SARIMA model.

Faustryjak *et al.* [82] implemented an LSTM-RNN model to offer stock market increase recommendations for the future. Lastly, Nguyen [51] utilised a KNN algorithm to predict blast-induced ground vibration in open-pit coal mines, outperforming the traditional mathematical models.

These studies indicate the application of AI techniques in various industries. However, there is an indication of the implementation of AI in the mining industry. These studies did not apply the methods developed in the deep-level mining industry.

An Improved compressed air control solution using machine learning in deep-level mining [34]

This study developed an ANN model to predict the pressures of the compressed air network. It used the predictions with an energy management system to implement a dynamic control solution for the compressed air system. However, this solution was not applied to other systems, such as cooling systems.

Application of ANNs for temperature forecasting and HVAC system control [39], [53], [61], [85-89]

These studies applied machine learning models for HVAC system control, mainly in the building sector. Temperature forecasting was seen as the primary parameter for the HVAC controller [88], [89]. Ntakolia *et al.* [53] observed that machine learning models were implemented for heating demand prediction, load forecasting and control. ANNs, LSTM and a combination of CNNs and LSTMs were primarily used for indoor temperature forecasting models to implement the control strategies.

The studies identified that the neural networks mentioned could handle multiple input and output parameters better than traditional methods. Moreover, the models yielded superior response speed and efficiency results.

Due to the similarity to HVAC systems, this indicates the potential for implementing AI-based temperature forecasting methods for deep-level mine cooling systems [30]. However, a lack of literature pertains to implementing these methods in the mining industry.

Evaluating different machine learning models for energy measurement and verification in deep-level mines [49]

This study evaluated the use of machine learning models, namely linear regression, ANNs, SVMs, and KNNs, for the measurement and verification (M&V) of energy usage in the deep-level mining industry.

The models predict energy usage and calculate energy savings for M&V applications. Although the method was applied in the deep-level mining industry, the study did indicate whether machine learning models apply to industry control strategies.

Application of machine learning for air temperature forecasting [62], [65], [84]

These studies evaluated the feasibility of using machine learning models for air temperature forecasting. The studies focused on using SARIMA, ANN, RNN, and LSTM-RNN models. Although the studies indicate that these models are feasible for air temperature forecasting, the forecasting methods did not use the models for a dynamic control solution. Moreover, the studies focused on making long-term

forecasts, which does not apply to applying the models on cooling systems in the deep-level mining industry.

Table 3 summarises the related studies discussed and indicates a gap in the present literature.

Table 3: State-of-the-art matrix detailing gaps in previous research

Reference	DEEP-LEVEL MINING	COOLING SYSTEMS	CONTROL PHILOSOPHY	ARTIFICIAL INTELLIGENCE	TEMPERATURE FORECASTING	COST SAVINGS
[4 - 6], [15], [20], [26 - 30], [35] [41]	✓	✓	✓	✗	✗	✓
[8]	✓	✓	✓	✓	✗	✓
[9], [51], [77], [82]	✗	✗	✗	✓	✗	✗
[34]	✓	✗	✓	✓	✗	✓
[39], [53], [61], [85-89]	✗	✓	✓	✓	✓	✓
[49]	✓	✗	✗	✓	✗	✓
[62], [65], [84]	✗	✗	✗	✓	✓	✗

1.5.2. Shortcomings of existing literature

Section 1.5.1 indicates the existing literature related to the study. The studies indicate the literature gap and the shortcomings applicable to the study.

Shortcomings of the existing literature include:

- The underground ambient conditions were not accounted for in developing the control solutions.
- Additional infrastructure is required to improve the performance of the traditional models used for the cooling system control strategies.

- There is a lack of literature on using AI-based temperature forecasting methods for deep-level mine cooling systems.

1.6. Need for the study

Attention to electricity costs is imperative to sustain the profitability of deep-level mines.

The cooling systems found in deep-level mines are complex and integrated, contributing to approximately 28% of the mine's total electricity consumption. Literature indicates that these systems have implemented control strategies to reduce energy costs. However, these strategies have shortcomings, where potential energy savings opportunities are missed.

One of the shortcomings observed with cooling system control strategies is that these strategies are static. Cooling systems depend on ambient conditions, for instance, underground air temperatures, which are dynamic; thus, the existing strategies need to be evaluated based on these conditions. AI has shown the ability to predict these conditions. Thus, the need exists to develop a control strategy that addresses the challenges of re-evaluating static control strategies to gain the full potential for energy savings.

AI-inspired temperature forecasting is needed to develop a dynamic control solution for deep-level mine cooling systems.

1.7. Study objectives

Defining and addressing the research objectives provide a comprehensive understanding of the research problem. AI, specifically a machine learning and/or deep learning model, would need to be implemented to forecast surface and underground air temperatures. These models will serve as the basis for a dynamic control solution of a surface mine BAC, indicating the possible cost savings that can be achieved.

Table 4 indicates the research objectives that will be considered to address the need for the study mentioned in Section 1.6.

Table 4: Research objectives

Research objective	Statement	Description
1	Identify the mine's system parameters closely related to the surface BACs.	The system parameters must be identified to avoid scope creep and mitigate the model's complexity.
2	Determine, develop, and evaluate an appropriate temperature forecasting model.	A suitable model for forecasting temperatures in the mining industry needs to be determined based on existing literature. Moreover, the model needs to be evaluated to ensure that the selected model is sufficient to be implemented for a dynamic control solution.
3	Develop a dynamic control solution for the surface BAC cooling plants and the BAC.	The dynamic control solution shall be developed based on the model developed for research objective 2 and predefined targets.
4	Validate the control solution which addresses the research problem.	This is addressed by evaluating whether the previous objectives have been sufficiently addressed. Moreover, it indicates whether the developed control solution can yield possible electricity cost savings.

1.8. Research methodology

A solution methodology will be developed to address the research objectives. The solution developed in the study will result in quantitative data. Therefore, the quantitative research methodology is required to validate the proposed methodology. Moreover, the developed solution must be applied to similar deep-level mine cooling systems.

Therefore, a case study research design forms the basis of the study [90]. This will show that the solution can be generalised with a single case study. Moreover, the

research design shall eliminate bias regarding the validation process [90]. Figure 23 details the case study's research design procedure.

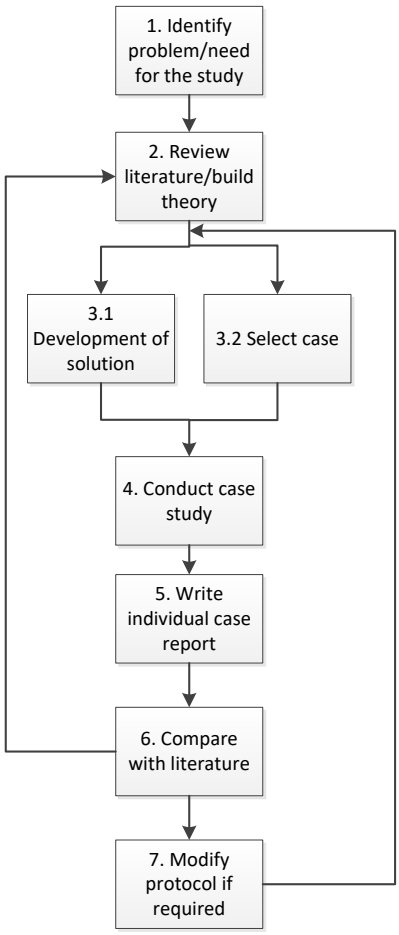

Figure 23: Case study research design (adapted from [90])

1.9. Dissertation overview

Chapter 1 provides a comprehensive overview of South Africa's mining industry and energy consumption patterns, focusing on cooling systems as a significant contributor to energy usage in deep-level mines. The chapter explores existing energy reduction strategies and reviews relevant technologies and studies from various industries. Through this review, the need for the study is identified. The chapter concludes with a summary of the relevant literature and clearly states the research problem and objectives. This forms Steps 1 and 2 in Figure 23 and Figure 24.

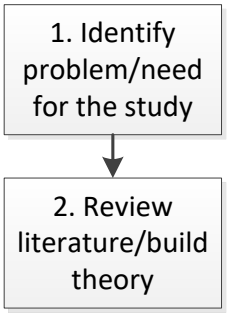

Figure 24: Problem identification and literature review – steps 1 and 2

Chapter 2 outlines a method to approach the need for the study and objectives described in Chapter 1.

The approach to address research objective 1 is to determine the boundaries of the study. Additionally, the parameters within the boundaries are identified. Research objective 2 is addressed by determining the most suitable model to forecast the surface and underground temperatures. The chosen model will be used for the development of a dynamic control solution for a mine cooling system. A method is determined to fulfil research objective 3. A dynamic control strategy for the system is developed based on the developed model to address research objective 2.

The method derives the processes from the literature detailed in the previous chapter to develop a temperature forecasting model for a control strategy on deep-level mine cooling systems. This forms Step 3.1 in Figure 23 and Figure 25.

Figure 25: Development of solution – Step 3.1

The results based on the implementation of the methodology will be depicted on a specific mine in **Chapter 3**. The relevant objectives will be validated and verified by comparing the results with the literature and compared to the present operation to indicate the financial benefit. Thus, addressing research objective 4. This forms steps 3.2, 4, 5, and 6 in Figure 23 and Figure 26.

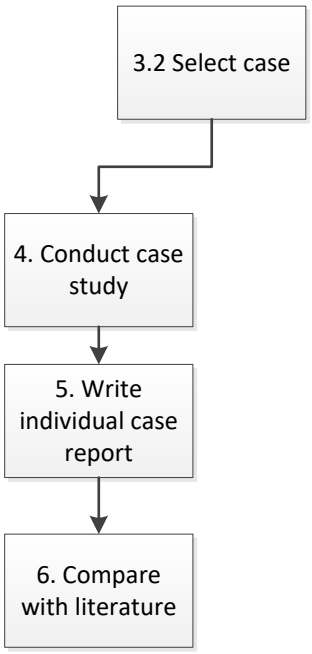

Figure 26: Results analysis – steps 3.2 - 6

Chapter 4 will provide a summary of the study, an analysis of the study's objectives, recommendations, shortcomings, and future work relevant to this study. This forms Step 7 in Figure 23 and Figure 27.

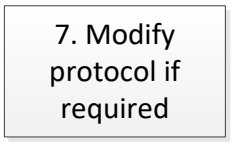

Figure 27: Conclusion – Step 7

1.10. Conclusion

One of the main challenges for deep-level mines is reducing electricity costs to remain profitable. Research indicates that mining cooling systems, which include ventilation and refrigeration systems, account for approximately 28% of a deep-level mine's energy consumption due to their complexity.

These systems must ensure that temperatures do not exceed wet bulb temperatures of 32.5°C and dry bulb temperatures of 37°C, as deep-level mines experience VRTs of up to 60°C. To reduce energy consumption, control strategies have been developed

and implemented to optimise the operating conditions of cooling systems while meeting service delivery requirements.

However, existing control strategies are often static and fail to capitalise on the potential for additional energy savings based on the dynamic nature of the mine. The use of AI allows the opportunity to control these systems dynamically.

To address this limitation, this study proposes an AI-based temperature forecasting model that will enable the development of a dynamic control strategy for deep-level mines. By predicting the temperature trends in the mine, the model can determine the daily operation of cooling systems, resulting in significant financial benefits.

Chapter 2: Development of method

“Simplicity is the ultimate sophistication."

– Leonardo da Vinci

2. DEVELOPMENT OF METHOD

2.1. Introduction

Chapter 1 provided the necessary background and literature review, identifying the research problem and need, as discussed in Section 1.7. The research objectives, specified in Section 1.8, informed the method described in this chapter, which comprises the following:

- **Step 1**: System parameter identification
- **Step 2**: Selection of an appropriate model for temperature forecasting
- **Step 3**: Development and evaluation of the selected temperature forecasting model
- **Step 4**: Dynamic control solution development
- **Step 5**: Validation methodology

Each step will be followed to ensure the successful implementation of the proposed methodology, designed to address the research objectives. The method of this study shall be developed from multiple cooling systems, namely, an open-loop two-stage cooling plant system and a semi-closed-closed loop cooling plant system. These systems are combined to depict the cooling systems typically found in deep-level mines [8], [28], [41]. Figure 28 shows a typical example of a multi-stage open-loop cooling system.

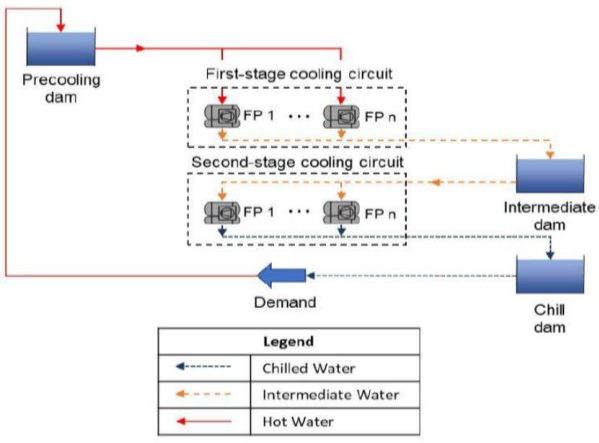

Figure 28: Multi-stage open-loop cooling system [41]

An intermediate dam is used between two cooling circuits for two-stage cooling systems. The water from the pre-cooling circuit is directed to the first stage cooling circuit, initiating the primary heat extraction phase.

Moreover, it is deposited in the intermediate dam and routed through the second-stage circuit for additional heat extraction. The water is then stored in the chill dam for underground operations. The water temperature increases after underground operations and is returned to the pre-cooling dam.

Figure 29 indicates the system layout for a semi-closed loop cooling plant system. The water from the pre-cooling dam is sent through cooling plants, where heat extraction occurs and stored in a chilled dam.

The water sourced the chill dam is utilised for BAC operations and additional underground cooling. The water from the BAC is stored in a BAC dam and then returned to the pre-cooling dam. Thus, the characterising the system as a semi-closed loop system.

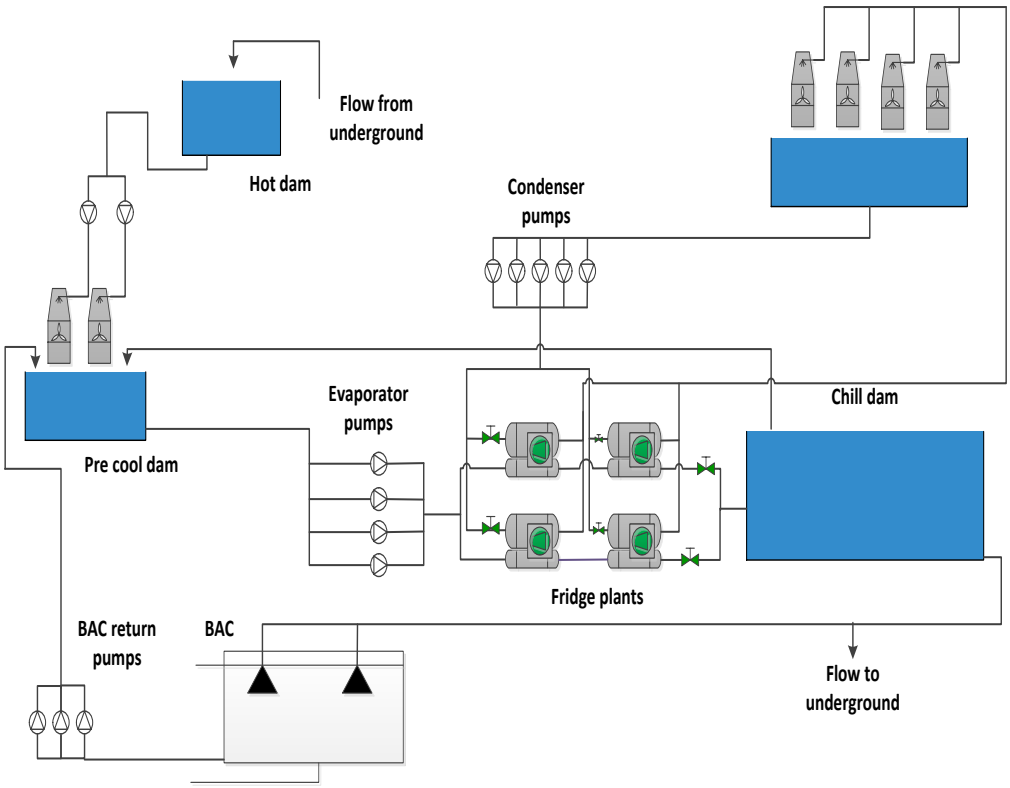

Figure 29: Gold mine cooling system (adapted from [91])

Figure 30 shows the layout, which is derived from the preceding layouts.

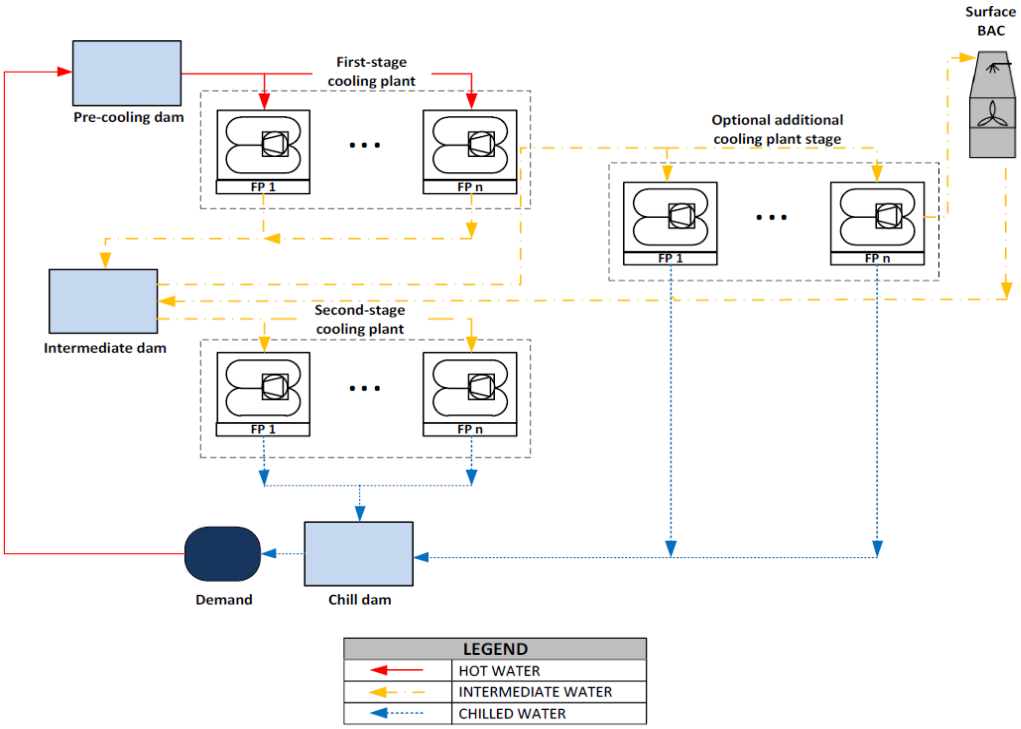

Figure 30: Multi-stage cooling system with optional supplementary cooling [41]

Figure 30 describes a multi-stage cooling system with a supplementary cooling circuit. The supplementary cooling circuit provides water to the BACs but can send water to the chill dam if additional cooling is required.

2.2. Step 1: System parameter identification

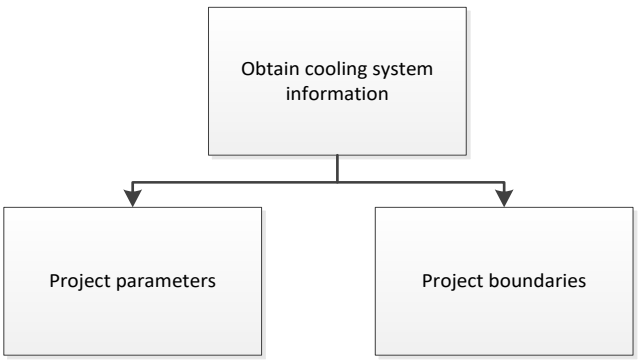

Figure 31: Project scope (adapted from [34])

This section discusses an approach to fulfil research objective 1, detailed in Section 1.7.

Research objective 1: Identify the system parameters closely related to the surface BACs.

Before developing an AI model, the parameters and boundaries must be identified initially [34]. This is imperative to avoid scope creep and mitigate the complexity of the model [92]. The study's boundaries are kept to the optional cooling circuit, the BAC, a working area on one of the underground levels and the deepest station. The instrumentation collects all the data and is only available in these areas.

After the boundaries have been determined, the parameters relevant to the surface and underground air temperatures must be identified. Suppose these parameters are not available or inaccurate. In that case, the model cannot predict the temperatures, thus not implementing a dynamic control solution on the surface of BAC plants and fans.

The main control parameters are the surface and underground air temperatures. Other parameters include the surface ambient conditions, the BAC cooling plant power consumption, the surface BAC cooling plant, fan running statuses, the surface BAC inlet and outlet air temperatures, and any underground cooling auxiliaries which impact the underground air temperatures. Table 5 shows the parameters required for traditional control approaches and AI-inspired approaches.

Table 5: Parameter requirements for mine cooling systems [20], [23], [41]

Parameter Description
Surface BAC plant refrigerant
Surface BAC plant current meter
Surface BAC plant voltage meter
Surface BAC fan inlet air velocity
Ambient barometric pressure
Evaporator inlet water temperature
Evaporator outlet water temperature
Condenser inlet water temperature
Condenser outlet water temperature
BAC inlet water temperature
BAC inlet dry bulb air temperature

Parameter Description
BAC inlet wet bulb air temperature
BAC outlet dry bulb air temperature
Evaporator Inlet water flow rate
Condenser inlet water flow rate
BAC outlet water flow rate
Number of surface BAC plants
Number of evaporator pumps
Number of condenser pumps
Number of BAC return water pumps
Motor and pump specifications for the return BAC pumps
Motor and pump specifications for the evaporator pumps
Motor and pump specifications for the condenser pumps
Motor and pump specifications for the plant compressor
Valve sizes and position
Pipe Cladding
Bends on the condenser and evaporator pumps
Number of condenser towers
Motor and pump specifications for the condenser fans
Evaporator pump locations
Condenser pump locations
Surface BAC location
Number of BAC fan units
Specifications for the motors and pumps of the BAC fans
Pipe dimensions for the evaporator circuit
Pipe dimensions for the condenser circuit
Pipe dimensions for the surface BAC
Surface ventilation fan current meters
Surface ventilation fan voltage meters
Surface ventilation fan frequency meters
Surface ambient airflow sensor
Underground ambient airflow sensor
Underground ambient dry bulb air temperature
Underground ambient wet bulb air temperature

2.3. Step 2: Machine learning model selection

As discussed in Section 1.4, ANNs, CNNs, and LSTM-RNN models were developed to forecast temperatures to implement dynamic control solutions for cooling systems in residential and office buildings. However, the LSTM-RNN is the most popular model [84-88]. Moreover, some studies indicate that the use of neural networks performed better for multiple input and output parameters compared to traditional forecasting methods, such as SARIMA, as discussed in Section 1.7.

Bellagarda *et al*. [89] evaluated various temperature forecasting models for smart buildings and identified that the LSTM-RNN model was the most common approach. Badenhorst [30] mentioned that mine cooling systems are like office and residential HVAC systems and the control strategies implemented on these systems used temperature as the main parameter [88], [89]. Thus, it can be inferred that the best model for office and residential buildings would be the best for deep-level mine cooling systems.

Thus, against this backdrop, the LSTM-RNN model shall be developed to forecast temperatures in the mining industry.

2.4. Step 3: Machine learning model development

This section shall discuss the method that will address research objective 2, detailed in Section 1.7. The LSTM-RNN model was determined as the model to be developed, as discussed in Section 2.3. Different models shall be developed that forecast towards different horizons, i.e., forecasting one day (48 timesteps) ahead. The models will be developed based on the following models:

- Model A: trained to forecast 48 timesteps (30-minute intervals) ahead.
- Model B: trained to forecast n timesteps (30-minute intervals) ahead of a MAPE 10% on the test set.
- Model C: trained to forecast n timesteps (30-minute intervals) ahead, yielding a MAPE of 5% on the test set.
- Model D: trained to forecast 1 timestep ahead.

Research objective 2: Determine, develop, and evaluate an appropriate temperature forecasting model.

The following steps are used to develop the temperature forecasting model:

- **Step 3.1:** Data acquisition [8], [34];
- **Step 3.2:** Data cleaning [34], [49], [55], [93], [94], [95], [96], [97];
- **Step 3.3:** Feature Selection [34];
- **Step 3.4:** Data pre-processing [34], [55], [98], [99];
- **Step 3.5:** Model development [34], [55], [58], [100];
- **Step 3.6:** Model evaluation [34], [84], [101], [41].

2.4.1. Step 3.1: Data acquisition

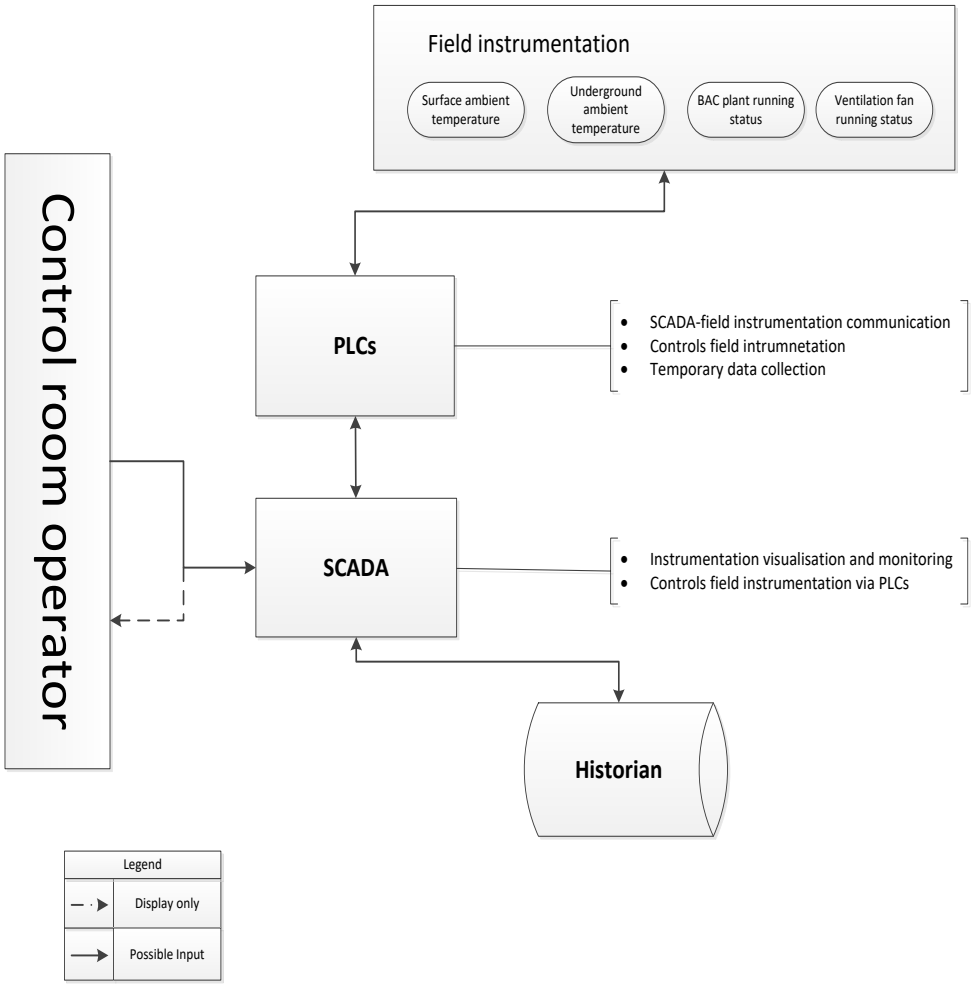

Figure 32: The SCADA and instrumentation communication link (adapted from [34])

Figure 32 details the process flow diagram of the acquisition process in deep-level mines. Deep-level mines contain large, complex, energy-intensive, integrated cooling systems, thus generating substantial amounts of data [8].

The data from these systems consistently generate data from sensors which measure the parameters mentioned in Table 5. The data from these parameters are transmitted to PLCs.

The PLC acts as connection between the sensor data from the PLCs and SCADA. The SCADA also displays real-time data stored for a limited period. The data is then stored in the historian for longer periods.

This data stored in the historian is used to develop the temperature forecasting model. This data is in its raw format. This data will need to be transformed to be suitable for the model.

2.4.2. Step 3.2: Data cleaning

As mentioned in the preceding section, the acquired raw data must be transformed into a suitable format. The first step is data cleaning [34].

Data cleaning identifies inaccuracies in the dataset [34], [49]. The inaccuracies can be dealt with by doing the following [55]:

- Removing the inaccurate data point.
- Removing the parameter that contains inaccuracies.
- Replacing the inaccurate data with an arbitrary value.

Inaccuracies in the dataset also include missing values of the dataset. This process is imputation if the third option is taken [55]. There are multiple methods for imputing missing values. The following imputation methods have been observed in previous machine learning-related studies [94], [95] :

- Mean imputation. This involves replacing missing values with the mean value of the dataset.
- Median imputation: replacing missing values with a median value of the dataset.

- Regression imputation: implementing regression to predict the data point based on the non-missing values.
- KNN imputation uses the k closest data points, or neighbours to the missing data points, to determine the data point in question.

The imputation methods mentioned only detail the most common imputation methods. Figure 33 shows other existing methods.

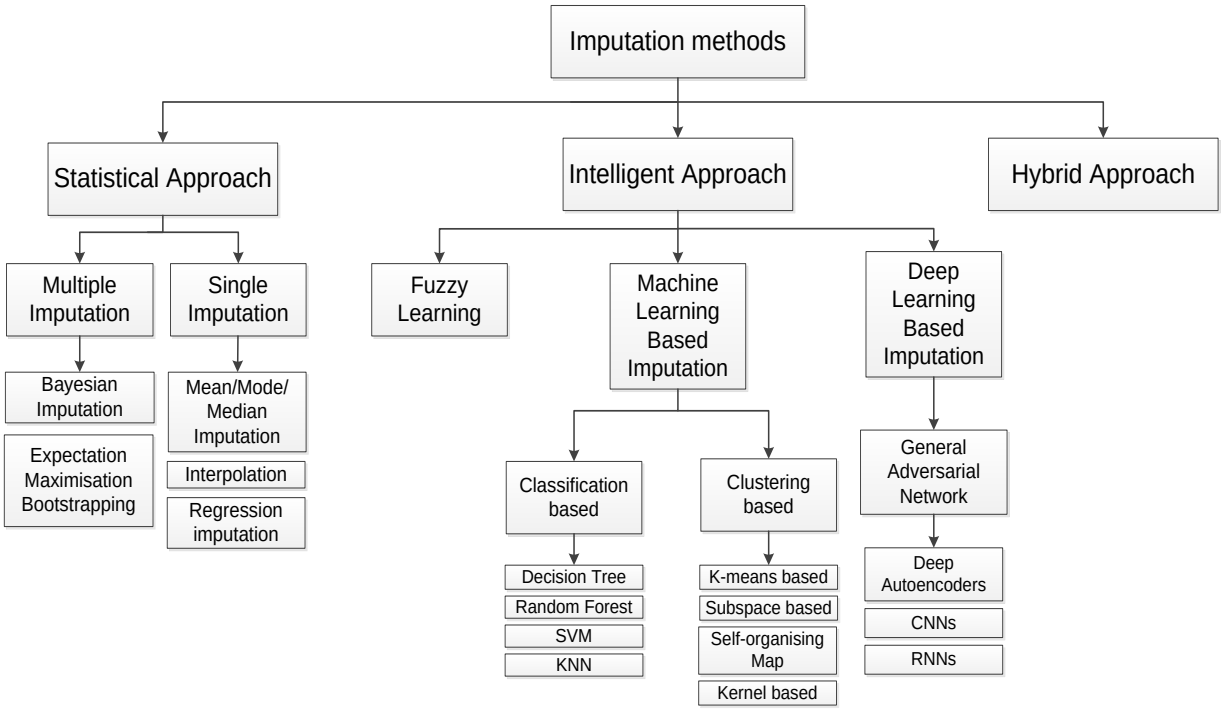

Figure 33: Missing data imputation methods (Adapted from [93])

Table 6 details the advantages and disadvantages of the popular imputation methods [94], [95], [96].

Table 6: Advantages and disadvantages of popular imputation methods

Method	**Advantages**	**Disadvantages**
Mean/Median	Easy to interpret and implement.	Poor performance and bias on high-dimensional data sets containing large amounts of missing values.

Method	Advantages	Disadvantages
Regression	Performs well for multivariate data.	It only performs well if the data set has a linear relationship.
KNN	Flexible, can be used for continuous and discrete data.	High computational time due to working through the whole data set.

Cooling systems in deep-level mines are non-linear, contain continuous and discrete data, and are high-dimensional due to the system complexity and the real-time data collection. Thus, KNN imputation is the most appropriate method for this data set. The imputation technique will be implemented on each parameter to mitigate the limitation of high computation [97].

2.4.3. Step 3.3: Feature selection

After the data cleaning process on the raw data is completed, the feature selection process can be completed. This determines the most relevant parameters for forecasting the temperatures. Due to the application of the model, there is no process to determine the most relevant parameters [34].

The least amount of parameters closely related to the temperatures are initially selected, and additional parameters shall be included if the model's performance is insufficient [34], [49]. The feature selection process reduces the model training time and potentially improves the prediction performance.

2.4.4. Step 3.4: Data pre-processing

Now that the data has been cleaned and the most relevant features have been selected, the data needs to undergo further transformation, known as data pre-processing [102].

The further transformations include the implementation of a sliding window, data scaling and data portioning [34]. This will be done for the parameters selected in Step 3.3, mentioned in Section 2.4.3.

Sliding window implementation

A sliding window needs to be implemented since time series forecasting using an LSTM-RNN model is being implemented [103]. The sliding window indicates how the model should learn to predict future output values [104]. This indicates the number of previous time values used to predict the next output time value, as seen in Figure 34.

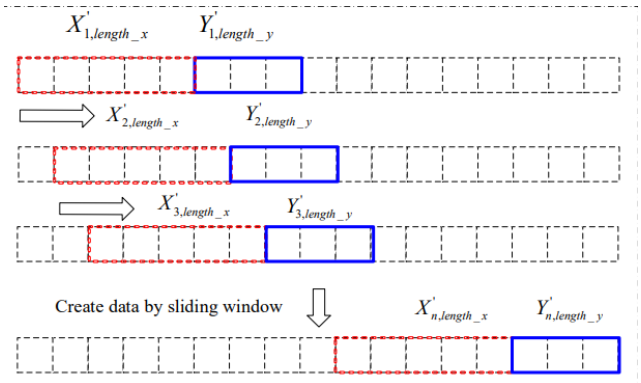

Figure 34: Example of a sliding window technique [103]

Figure 34 indicates that five previous time values will predict the next three output values. The window “slides” to the next window to predict the next three output values.

Data partitioning

The data will now undergo data partitioning. Data partitioning splits the dataset into a training, validation, and test set [34]. The test set is used to train the model. The learn the features of the set to forecast the temperatures. The validation set evaluates the model's performance during the training phase.

The model's performance on this set lets the model know whether the model is improving or not and prevents the model from overfitting. The test set evaluates the model's performance after training [105]. Moolayi [58] indicates that there is no mandatory split ratio. However, Joseph [105] observed that the most common split is 80% for the training set, 10% for the validation and 10% for the test set.

Data scaling

The data now needs to be scaled or normalised [34]. When the parameters have different scales, this negatively affects the performance of machine learning models [55].

Therefore, it is imperative to apply data scaling methods to ensure the data set is scaled. Multiple data scaling techniques result in different distributions or scales for the parameters in the data set. The most common techniques are min-max scaling, standardisation, and normalisation [55] [99].

Min-max scaling occurs when the parameter values are scaled between zero and one, where the minimum value is scaled to zero, the maximum value is scaled to one, and the rest of the data set is scaled to values between zero and one based on the distance from the maximum and minimum values [99]. Min-max scaling can be explained mathematically using the following equation [34] [99]:

$$x_{i_{scaled}} = \frac{x_i - x_{min}}{x_{max} - x_{min}} \tag{16}$$

The standardisation method, also known as variance scaling, subtracts the mean value of the dataset from the parameter value and then divides the value by the variance [99]. This results in the values having zero mean. Equation 16 details the mathematical explanation of standardisation:

$$x_{i_{scaled}} = \frac{x_i - x_{mean}}{\sqrt{x_{variance}}} \tag{17}$$

Normalisation divides the parameter value by the Euclidean norm [99]. It is defined mathematically as:

$$x_{i_{scaled}} = \frac{x_i}{\|x\|_2} \tag{18}$$

The Euclidean norm determines the length of a vector in a coordinate space. The Euclidean norm takes the square root of the sum squared parameter values and is detailed as follows:

$$\|x\|_2 = \sqrt{\sum_{i=0}^{m} x_i^2} \tag{19}$$

Zheng *et al.* [99] mention that if the parameters differ drastically, it is recommended to implement the standardisation method. However, Géron [55] observed that neural networks expect the input parameters to have values ranging between 0 and 1; thus, min-max scaling is the most appropriate method to implement.

2.4.5. Step 3.5: Model development

As mentioned in Section 1.4, it has been observed that the use of LSTM-RNN is the most appropriate model for temperature forecasting. The LSTM-RNN model shall aim to predict the temperatures by identifying patterns from the parameters mentioned in Section 2.2.

The first step in the development of the LSTM model is the selection of hyperparameters. These parameters determine the model's learning process and structure, thus influencing the model's performance in terms of accuracy [34] [58]. The parameters are initially chosen arbitrarily, and then the model's performance is evaluated. If the model accuracy requires improvement, the hyperparameter values may need to be adjusted. This process is known as hyperparameter tuning [55] [58]. The number of hidden layers and neurons per hidden layer, the activation function, the number of epochs, the batch size, and the learning rate are the primary hyperparameters for an LSTM-RNN model.

Number of neurons

The number of neurons in the first hidden layer is typically based on the number of input parameters. Moolayi [58] suggests that the number of neurons for the first hidden

layer is selected by choosing a multiple of eight closest to the number of input parameters. The number of neurons per layer should decrease with each layer [55].

Number of layers

Increasing the number of layers improves the performance of the model. However, it may not be necessary for RNN models [100].

Géron [55] suggests that the number of layers can be increased gradually until the model starts to overfit the training set.

Activation function

The activation function is the function that is used to transform the neuron input [34]. Generally, the Rectified Linear Unit (ReLu) function will be appropriate for most cases. Experimenting with other activations is possible if the ReLu function does not yield sufficient results [58]. Table 7 indicates some available activation functions.

Table 7: Tensorflow activation functions [100]

Activation function	**Equation**
Tanh	$f(x) = \frac{e^x - e^{-x}}{e^x + e^{-x}}$
ReLu	$f(x) = \begin{cases} x; & x > 0 \\ 0; & x \leq 0 \end{cases}$
Elu	$f(x) = \begin{cases} x; & x > 0 \\ \alpha(e^x - 1); & x \leq 0 \end{cases}$
SeLu	$f(x) = \lambda \begin{cases} x; & x > 0 \\ \alpha(e^x - 1); & x \leq 0 \end{cases}$
ReLu6	$f(x) = \begin{cases} 6; & 6 < x \\ x; & 0 < x \leq 6 \\ 0; & x \leq 0 \end{cases}$
CreLu	$f(x) = \begin{cases} max(0, x); & x > 0 \\ max(0, -x); & x \leq 0 \end{cases}$
Softmax	$f(x_i) = \frac{e^{-x_i}}{\sum_i e^{-x_i}}$
Softsign	$f(x) = \frac{x}{1 + \lvert x \rvert}$

Activation function	Equation
Softplus	$f(x) = \ln(1 + e^x)$

Number of epochs

The number of epochs is the number iterations that the model observes the training data [34]. The selection process follows the same principle as the selection process used to determine the number of hidden layers. Thus, there is a certain number of epochs where the model will start to overfit the training data. Callback functions are used to avoid overfitting the model. These functions are applied during the Early stopping, and model checkpoint methods are the popular call backs functions during the training phase of the model[7].

Batch size

The batch size is the number of samples provided to the network per epoch. This eases the learning process for the model [58]. The selection process is based on the nature of the input parameters.

Learning rate

The learning rate determines the size of weight updates of each iteration in the training phase [34]. It is a positive value which ranges between 0 and 1. This hyperparameter determines the rate at which the model adapts to the modelling problem. During the training phase, the mode will converge too quickly, thus leading to a suboptimal solution [78]. Moolayi [58] observed that using a learning rate 0.001 is common for machine learning algorithms.

After the model hyperparameters have been determined, the model can begin training. This is done by training the model with the training set, the validation set is used to determine the most appropriate model, and the test set evaluates the model's

[7] "Callbacks API", Keras, [Online], Available: https://keras.io/api/callbacks/, [Accessed: 23-Jul-2023]

performance [106]. The performance of the model shall be discussed in the subsequent section.

The solutions mentioned generally work for determining the hyperparameters, but this is usually based on a trial-and-error basis, which can become time-consuming if the incorrect hyperparameters are selected; this process is known as a manual search [34]. Other approaches are the grid search and random search [58].

The grid search method evaluates the model's performance for all combinations for a defined set of parameters. This approach will determine the hyperparameters that will provide the best-performing model for the defined set of hyperparameters. However, if the incorrect hyperparameters are not selected, the best model may not be observed [55].

The random search follows the same methodology as the grid search, but the hyperparameters are chosen randomly from a distribution. A larger range of values can be selected for each hyperparameter, increasing the possibility of obtaining a better-performing model [58]. The random search method will determine the hyperparameters for the LSTM-RNN model’s architecture.

2.4.6. Step 3.6: Model evaluation

After the model's training is complete, the model needs to be evaluated. The model's performance is based on its ability to predict surface and underground air temperatures. The model performance should show sufficient results to be used for implementation.

The most common metrics used to evaluate the performance of LSTM-RNN are the coefficient of variation for the root mean square error (CV(RMSE), the root mean squared error (RMSE), the MSE as mentioned in Section 1.4.2, and the mean absolute percentage error (MAPE) [34] [84] [101].

CV(RMSE) quantifies the error size relative to the mean of the observations. A low CV (RMSE) score indicates a low error range; thus, the performance would be sufficient [101]. The ASHRAE Guideline 14 considers a value less than 5% for half-hourly data

acceptable for model performance [107]. RMSE determines the difference between the predicted and actual values [34].

The RMSE of the training and test set shall be compared to determine whether the model is overfitting. MAPE is the mean value of the sum of absolute differences between the predicted and actual values [101]. A value that converges to zero is the most desirable. However, a maximum of 10% is sufficient according to the literature [49], [34], [41]. The evaluation metrics are defined as follows:

$$\mathrm{CV}(RMSE)\% = \sqrt{\frac{\frac{1}{N}\sum_{i=1}^{N}(y_i - \hat{y}_i)^2}{\bar{y}}} \times 100 \tag{20}$$

$$RMSE = \sqrt{\frac{\sum_{i=1}^{N}(y_i - \hat{y}_i)^2}{N}} \tag{21}$$

$$MAPE = \sqrt{\frac{\sum_{i=1}^{N}|y_i - \hat{y}_i|}{n}} \times 100 \tag{22}$$

Where:

- y_i is the actual value.
- $\hat{y}_i$ is the predicted value.
- $\bar{y}$ is the mean value of the actual values.

The model can be implemented using the evaluation metrics when sufficient performance has been accomplished. The performance of the LSTM-RNN model tends to deteriorate based on the number of timesteps that are forecasted [87] [89] [101]. The following models will be used to develop different dynamic solutions:

- Model A: trained to forecast 48 timesteps (30-minute intervals) ahead.
- Model B: trained to forecast 24 timesteps (30-minute intervals) ahead.

- Model C: trained to forecast n timesteps (30-minute intervals) ahead, yielding a MAPE of 10% on the test set.
- Model D: trained to forecast n timesteps (30-minute intervals) ahead, yielding a MAPE of 5% on the test set.
- Model E: trained to forecast 1 timestep ahead.

Although the model's performance deteriorates as the number of timesteps forecasted increases, providing the control solution to the mine well ahead of time would be more beneficial. This will allow the mine to implement the suggested solution adequately.

This is imperative, mainly if the mine lacks the infrastructure to implement a control strategy on the cooling system quickly. Therefore, the different models will be used to develop different control strategies whereby the most appropriate solution of the case study mine shall be selected.

2.5. Dynamic control solution

After completing the training and evaluation phases, the model is ready to be implemented for the dynamic control strategy. The objective of the model is to make future predictions based on real-time data. The real-time data needs to undergo data pre-processing so that the data is a suitable format for the model. For instance, outliers must be removed and scaled based on the methods used in the preceding section.

Periodic updates to the solution and model may be required if significant changes are made to the mine or if the performance of the predictions deteriorates. For instance, one of the ventilation fans is not operational.

This will require retraining the model using the same training procedure discussed in Section 0. This section will discuss the development of a dynamic control solution based on the underground temperature forecasting model. The reason for this approach is to identify potential periods of the day where the surface BAC plants and fans may not need to be operational.

The temperature forecasting model will determine the operating conditions of the surface BAC plants and fans. After gathering the data relevant to predicting the surface

and underground air temperatures, the data must be manipulated into a suitable format for the model. The model shall forecast the temperatures and determine the desired operation of the surface BAC plants and fans.

Figure 35 details the basic functioning of the dynamic control system. Three solutions will be presented as possible to apply to the case study. The following solutions shall be presented as possible solutions based on the developed and evaluated models mentioned in Section 2.4.6:

- Solution A: based on model A.
- Solution B: based on model B.
- Solution C: based on model C.
- Solution D: based on model D.
- Solution E: based on model E.

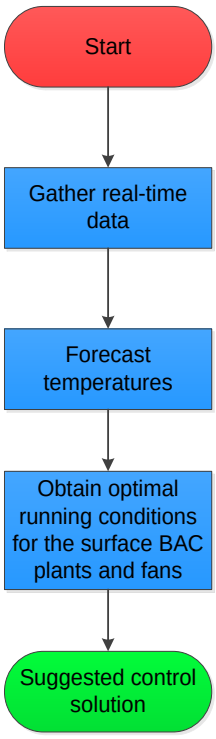

Figure 35: Overview of the dynamic control solution

Each solution shall follow the same procedure, as shown in Figure 35. Data is gathered from SCADA. Data is then manipulated into the same format as the data used to train and evaluate the temperature forecasting model. The temperatures will be forecasted

n timesteps ahead based on the chosen model discussed in Section 2.4.6, where multiple iterations of the running conditions of the input parameters will be evaluated to determine the optimal running conditions of the surface BAC plants and fans. The optimal operation of the forecasted period will be used as the control solution.

According to the literature, static, seasonal control strategies have been implemented on surface BAC plants and fans [4] [41]; however, potential savings are missed during the transitional seasonal periods of the year.

A dynamic approach must be developed to improve the control strategy. The following specifications are derived to address this section of the methodology:

- Specification 1: Data gathering.
- Specification 2: AI-based forecasting.
- Specification 3: Operation suggestion.

The background details about each specification shall be discussed in this section. Some of the processes within the specifications were discussed in Section 0.

Figure 36 shows the detailed process of the dynamic control solution development. Moreover, the specification will be discussed as subsections with the assistance of the figure.

2.5.1. Specification 1: Data gathering.

The data is gathered from the historian database of the mine's SCADA system using the same procedure in Step 1 from Section 2.2 and Step 3.1 from Section 2.4.1. The data required to forecast the temperatures is extracted in half-hourly periods. Only the necessary parameters will be extracted using Step 3.3 from Section 2.4.3. The data will then be cleaned and pre-processed using Step 3.2 from Section 2.4.2 and Step 3.4 from Section 2.4.4. This data will be stored if any historical analysis is required.

2.5.2. Specification 2: AI-based forecasting

Once the data is in the forecasting model's preferred format, the temperatures are ready to be forecasted. The temperatures will then be forecasted and evaluated against a temperature target using Step 3.5 from Section 2.4.5 and Step 3.6 from Section 2.4.6. The surface air wet bulb temperature target **7°C,** determined by Lodewyk [41], where the surface BAC equipment can be switched off based on that target temperature. The target for the 7 level air wet bulb underground temperatures is **32°C**, based on the MHSA of SA's underground temperature requirements. Suppose the forecasted temperatures are below the temperature target for the whole day. In that case, the control strategy for the forecasted period will indicate that the BAC plants and fans will be off for that period.

2.5.3. Specification 3: Operation suggestion

As seen in Figure 36, when the forecasted temperatures do not reach the temperature requirements, the development process will progress to additional steps to determine the optimal running conditions for the surface BAC plants and fans for the forecasted period. The process is derived from Mathee [34] and Lodewyk [41]. The strategy process is detailed in Figure 36.

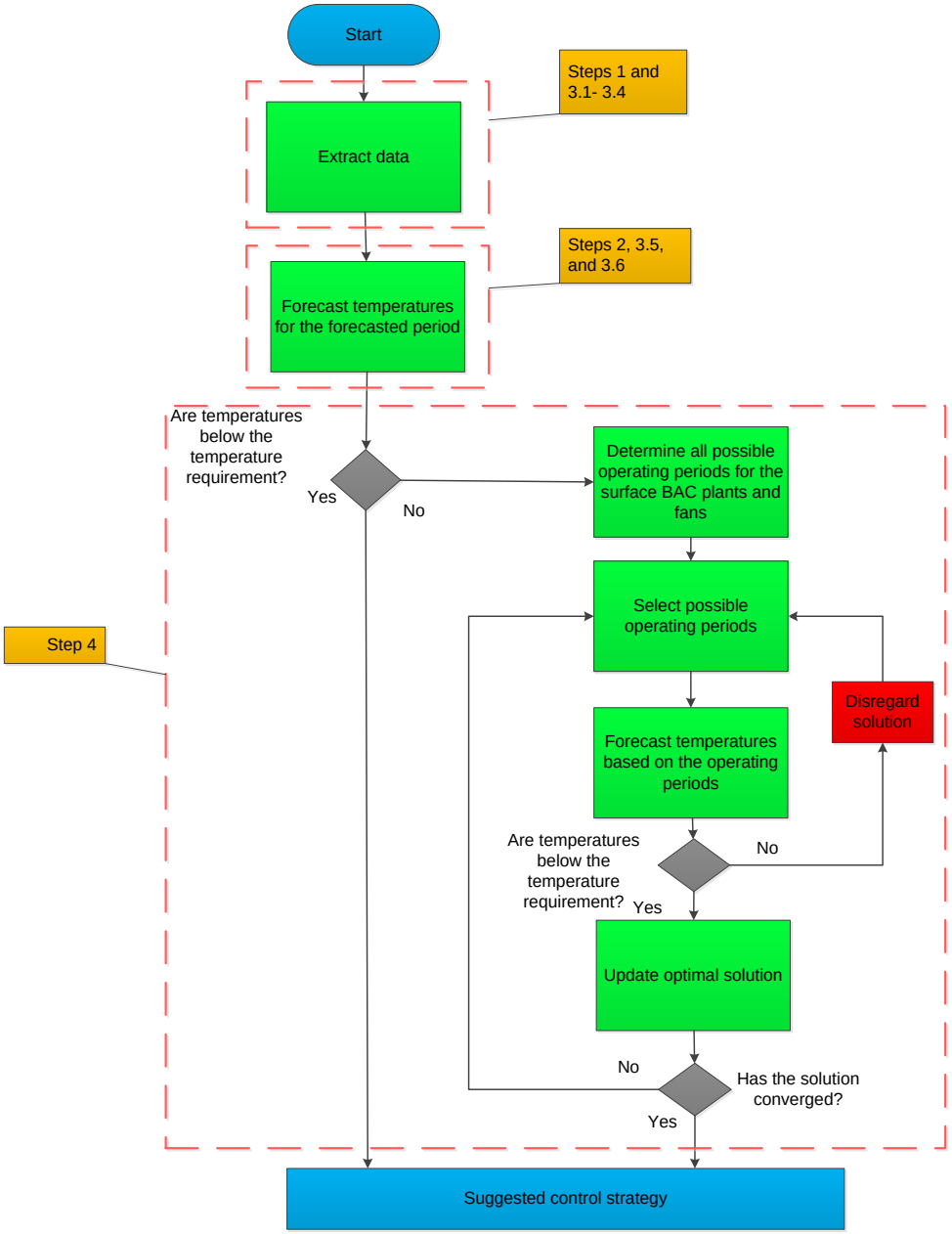

Figure 36: Proposed dynamic control strategy methodology

2.6. Step 4: Validation methodology

The development of the control solution method required numerous aspects. This is to ease the process of developing a solution which addresses the study's research objectives, mentioned in Sections 1.7 and 2.1, respectively.

Research objective 1 identifies and determines the mine cooling system parameters relevant to the surface BAC plants and fans. The method to address this objective is

demonstrated in Section 2.2. Research objective 2 is to identify, develop and evaluate the feasibility of implementing an appropriate model to forecast the surface and underground air temperatures. The LSTM-RNN model was chosen and developed. The application the method in Section 0 addresses the objective. Research objective 3 is to develop a dynamic control solution for the surface BAC cooling plants and the BAC. Section 2.5 discusses the method applied to fulfil this objective.

Specifications were determined in Section 2.5 to ensure that the control solution is suitable for the study. The following specifications were determined:

- Specification 1: Data gathering.
- Specification 2: AI-based forecasting.
- Specification 3: Operation suggestion.

Once all specifications have been addressed, it can be confirmed that the developed solution is suitable to address the need for the study. Adjustments to the solution may be altered if the study objectives have not been addressed adequately.

The solution developed will suggest the operating conditions of the mine's cooling system. The suggested strategy shall be compared with the actual operating conditions to indicate the possible cost savings achieved if the solution is implemented.

2.7. Conclusion

The methodology applied to address the studies' research objectives was discussed in this chapter. The methods were derived from previous literature where the methods investigated were implemented successfully.

The first research objective was to identify the system parameters. The approach to fulfil this objective was detailed in Section 2.2. The method was derived from studies focusing on deep-level mine cooling systems. This method identified the project boundaries and parameters required to develop an underground temperature forecasting model.

The second research objective involved the development and evaluation of an appropriate model to forecast the surface and underground air temperatures. The process involves data acquisition, pre-processing, model development, and evaluation. These are the generic steps required for most machine learning and deep learning models. It was determined that the LSTM-RNN is the most suitable model based on the literature and the nature of the data obtained from the relevant system parameters.

The model was evaluated using statistical metrics. This is to ensure that the model can forecast the surface and underground air temperatures adequately. The CV(RMSE) indicates the error range or variability. The RMSE indicates the difference between the actual and forecasted temperatures. The MSE is typically used to indicate the error during the development of the model. The MAPE is another error metric used for the model evaluation. Based on the literature, the model should achieve a value of less than 10% for the MAPE.

During the development of the model, if it does not yield acceptable results based on the model's initial structure, the random search algorithm implementation shall be used to improve the model's performance.

The third research objective was to develop a dynamic control solution on the surface BACs based on the temperature forecasting model developed from the second research objective. Data gathering, periodic temperature forecasting and periodic operation suggestions were followed to develop the control solution. The operation suggestion uses temperature targets to determine the most suitable running operations of the Surface BACs.

Lastly, the validation methodology was discussed. This detailed the key points of how each research objective was addressed. After validating the research objectives, the suggested operating conditions are compared to the actual operations, indicating the possible cost savings that can be achieved if the solution is implemented.

Chapter 3: Implementation and results

"A good traveller has no fixed plans and is not intent on arriving."

– Lao Tzu

3. IMPLEMENTATION AND RESULTS

3.1. Introduction

3.1.1. Preamble

This chapter aims to detail and evaluate the results of the proposed dynamic control solution of mine cooling systems in deep-level mines. Moreover, the results obtained from a case study are based on the methodology discussed in Chapter 2. The results indicate that the proposed solution addresses the need for the study (Section 1.6) and the research objectives (Section 1.7). The research objectives are verified. A comparison of the actual operation of the mine's cooling system and the proposed solution was used to validate the proposed solution.

3.1.2. Case study background information

The section covers the first research goal, as outlined in Section 1.7.

Research objective 1: Identify the parameters of the system that are closely related to the surface BACs.

The approach detailed in Section 2.2 was employed to address this objective, identifying the system's boundaries and parameters related to the surface BAC plants and fans.

The first step is to determine the cases as discussed in Section 1.9. This focuses on one mine case study. The dynamic control solution is specific to the case study mine. Moreover, all the research objectives are addressed using this single case study. Finally, this case study mine has sufficient data availability for developing the temperature forecasting model.

Mine A is the case study deep-level mine where the proposed solution is developed, situated in South Africa. The deepest working level reaches a depth of 3 700m. Complex integrated cooling systems are present for such mines that reach these depths due to the high VRTs. Figure 37 details a basic level arrangement of Mine A.

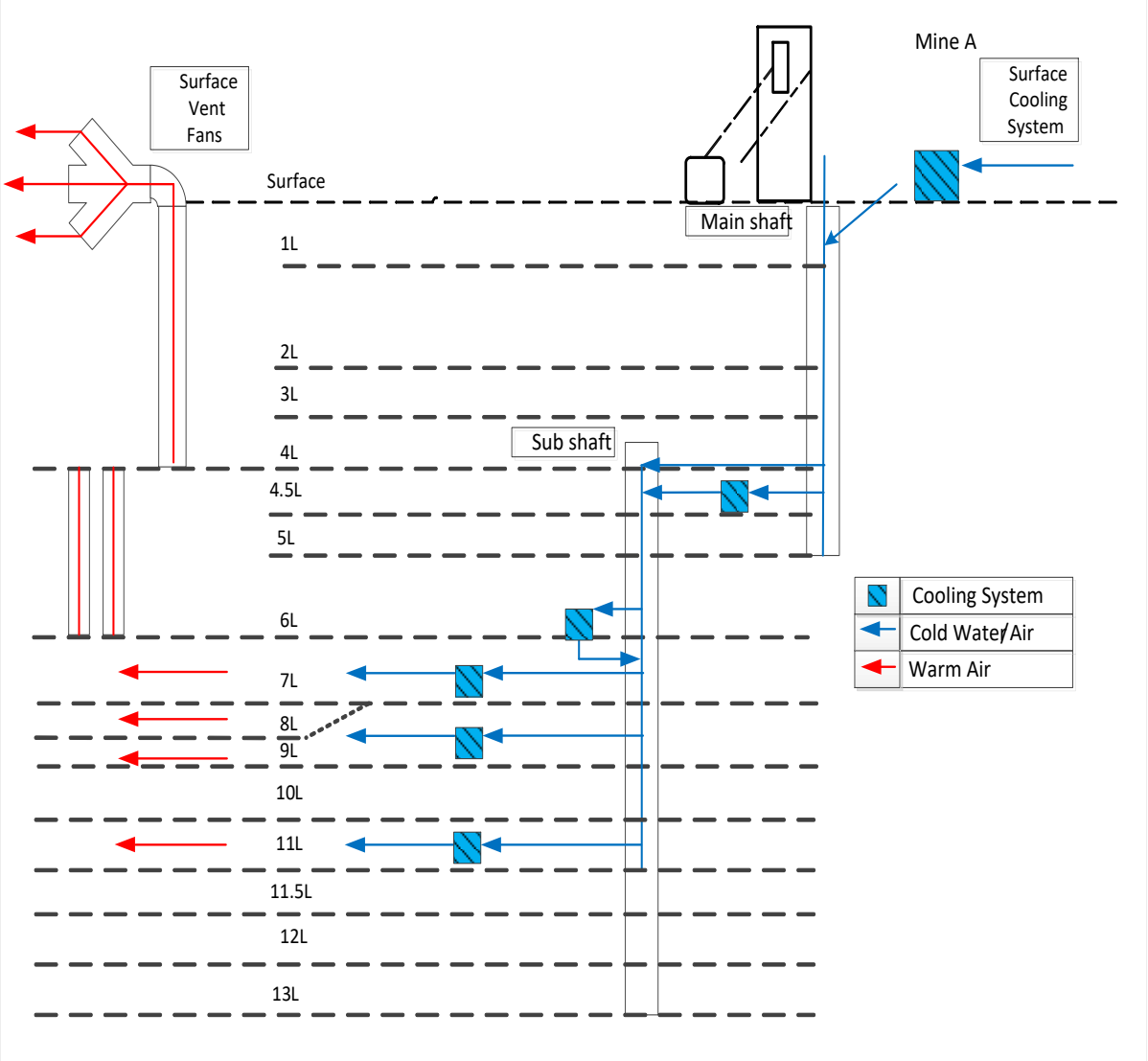

Figure 37: Mine A-level arrangement

Mine A contains a total of 15 working levels, which include two half-levels. It contains surface and underground cooling systems on levels 4.5, 7, 9, and 11. The water temperature is reduced by the surface cooling system and transported underground for mining and cooling.

The water undergoes further cooling underground before being sent to the deeper working levels due to the high VRTs at those depths. Smaller cooling systems such as BACs, ACUs and cooling cars are used deeper to reduce the working areas' temperatures.

This study focuses on developing a dynamic control solution on a section of the surface cooling system of Mine A. A general layout of the surface cooling system can be observed in Figure 38.

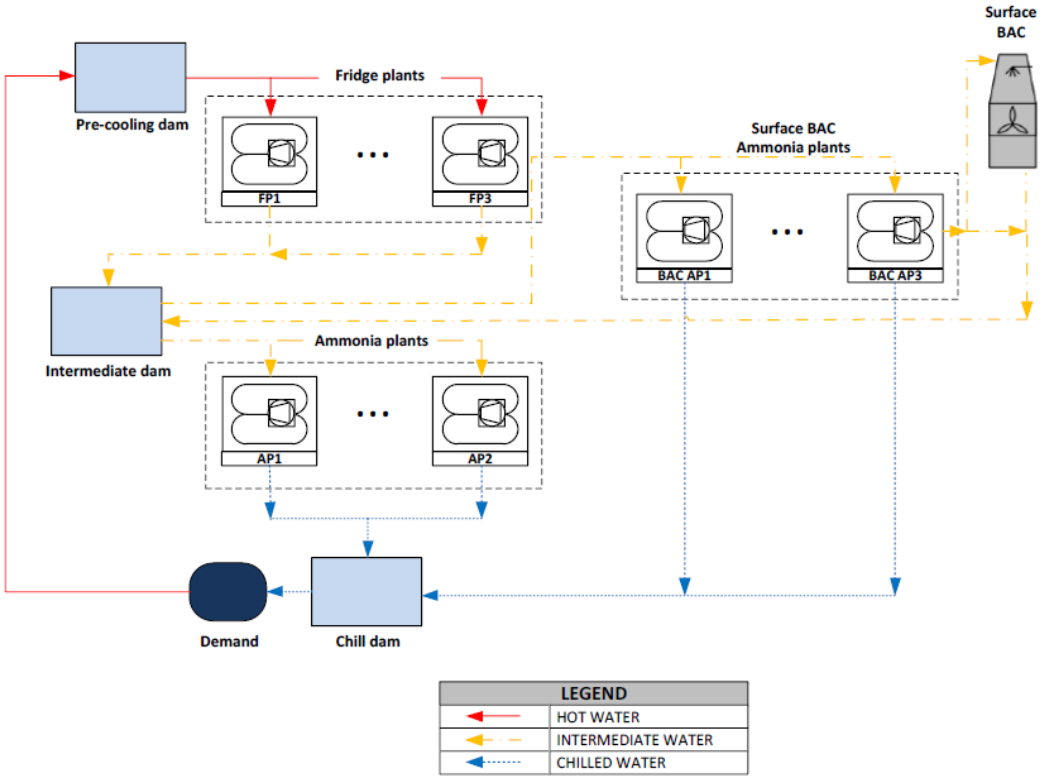

Figure 38: Mine A cooling system layout

The surface cooling system consists of three first stage fridge plants (FPs), two second-stage ammonia plants (APs) and optional cooling plants, BAC ammonia plants (BAC APs), as illustrated in Figure 38.

Hot water is transported from underground to the pre-cooling dam via pumping. Subsequently, the water is directed through pre-cooling towers, where the water is pre-cooled before being sent to FPs for further cooling. The water is transported to the intermediate dam and then to the APs for additional cooling. The BAC APs draw water from the intermediate dam to facilitate water temperature reduction. The water from the BAC APs is returned to the intermediate dam and the BAC. Mine A's cooling system consists of eight cooling plants: a pre-cooling dam, an intermediate dam, a chill dam, and a BAC. The BAC APs can send water to the intermediate or chill dam. The study will only focus on the BAC APs and the BAC.

3.1.3. System parameter identification

The BAC APs and the BAC are the focus of the study. Thus, the parameters related to the mine cooling system components are only considered. Table 8 indicates the required parameters to develop an AI model. The required parameters were compared to those required using a traditional simulation method.

Table 8: Parameter requirements of Mine A's cooling system

Parameter Description	**Traditional Method**	**AI-based Method**
Surface BAC AP refrigerant	✓	
Surface BAC AP current meter	✓	
Surface BAC AP voltage meter	✓	
Surface BAC AP energy consumption		
Surface BAC fan inlet air velocity	✓	
Surface ambient dry bulb air temperature		✓
Surface ambient wet bulb air temperature		✓
Surface Ambient barometric pressure	✓	
Surface BAC AP evaporator inlet water temperature	✓	✓
Surface BAC AP evaporator outlet water temperature	✓	✓
Surface BAC AP condenser inlet water temperature	✓	✓
Surface BAC AP condenser outlet water temperature	✓	✓

Parameter Description	Traditional Method	AI-based method
Surface BAC fan inlet water temperature	✓	
Surface BAC fan inlet dry bulb air temperature	✓	
Surface BAC fan inlet wet bulb air temperature	✓	
Surface BAC fan outlet dry bulb air temperature	✓	✓
Surface BAC AP evaporator Inlet water flow rate	✓	
Surface BAC AP condenser inlet water flow rate	✓	
Surface BAC AP running status		✓
Surface BAC fan outlet water flow rate	✓	✓
Number of surface BAC plants	✓	✓
Quantity of evaporator pumps	✓	
Quantity of condenser pumps	✓	
Number of BAC return water pumps	✓	
Motor and pump specifications for the return BAC pumps	✓	
Motor and pump specifications for the evaporator pumps	✓	
Motor and pump specifications for the condenser pumps	✓	
Motor and pump specifications for the plant compressor	✓	

Parameter Description	Traditional Method	AI-based method
Valve sizes and position	✓	
Pipe Cladding	✓	
Bends on the condenser and evaporator pumps	✓	
Number of condenser towers	✓	
Motor and pump specifications for the condenser fans	✓	
Evaporator pump locations	✓	
Condenser pump locations	✓	
Surface BAC location	✓	
Surface BAC fan running status		✓
Number of BAC fan units	✓	✓
Specifications for the motors and pumps of the BAC fans	✓	
Pipe dimensions for the evaporator circuit	✓	
Pipe dimensions for the condenser circuit	✓	
Pipe dimensions for the surface BAC	✓	
Surface ventilation fan current meters	✓	
Surface ventilation fan voltage meters	✓	
Surface ventilation fan frequency meters	✓	

Parameter Description	Traditional Method	AI-based method
Surface ambient airflow sensor	✓	
Surface ventilation fan running status		✓
Underground ambient airflow sensor	✓	
Underground ambient dry bulb air temperature	✓	✓
Underground ambient wet bulb air temperature	✓	✓

The following parameters were considered:

- Surface ambient dry bulb air temperature (°C)
- Surface ambient wet bulb air temperature (°C)
- BAC AP evaporator inlet water temperature (°C)
- BAC AP evaporator outlet water temperature (°C)
- BAC AP condenser inlet water temperature (°C)
- BAC AP condenser outlet water temperature (°C)
- BAC AP evaporator outlet water flow (L/s)
- Surface BAC outlet dry bulb air temperature (°C)
- BAC AP running status (0/1)
- Surface BAC fan running status (0/1)
- BAC AP energy consumption (kWh)
- Surface ventilation fan running status (0/1)
- Surface ventilation fan frequency (Hz)
- Underground dry bulb air temperature (°C)
- Underground wet bulb air temperature (°C)

The parameters for the AI model were identified through a thorough investigation of the SCADA system for Mine A's cooling system. The traditional method parameters were identified from Lodewyk [41], which was applied to the cooling system of the

same case study mine, where the parameters are measured using sensors, and these measurements are stored as data in the historian, as discussed in Section 2.4.1.

It can be observed that the AI model will require fewer parameters to develop a model than the traditional model. It is important to note that the parameters required for the AI model may be increased or decreased based on the evaluation of the model during the training phase. Thus, this section confirms the fulfilment of research objective 1.

3.2. Case study machine learning model development

3.2.1. Preamble

This section is related to the second goal, outlined in Section 1.7.

Research objective 2: Determine, develop, and evaluate an appropriate temperature forecasting model.

The method detailed in Section 2.3 and 0 was implemented to address this objective, to develop and evaluate LSTM-RNN models to forecast the surface and underground air temperatures. The following LSTM-RNN models shall be developed and evaluated:

- Model A: trained to forecast 48 timesteps (30-minute intervals) ahead.
- Model B: trained to forecast 24 timesteps (30-minute intervals) ahead.
- Model C: trained to forecast n timesteps (30-minute intervals) ahead, yielding a MAPE of 10% for all outputs on the test set.
- Model D: trained to forecast n timesteps (30-minute intervals) ahead, yielding a MAPE of 5% for all outputs on the test set.
- Model E: trained to forecast 1 timestep (30 minutes) ahead.

3.2.2. Step 3.1: Data acquisition

This data from the parameters identified in Section 3.1.3 will be used to develop the temperature forecasting model. An existing SCADA and historian are available at Mine A. The data was extracted from the historian in 30-minute intervals. This was done by obtaining the credentials for the historian database. The data is extracted using SQL

query. Figure 39 details the representation of the SQL query used to extract data from the historian database.

```
1   SELECT TagName, DateTime, Value
2   FROM History
3   WHERE TagName LIKE '{tag}'
4   AND DateTime > '{from_}' AND DateTime <= '{to}'
5   AND RetrievalMode = 'Average'
6   AND Resolution = 1800000
```

Figure 39: SQL query to extract data from Mine A's historian.

As observed in Figure 39, the “TagName”, “DateTime”, and “Value” columns were selected from the “History” table in the historian database.

Each parameter is represented as a tag in the database. Each parameter is extracted by using line 3 in the figure above. Other specified parameters were the date interval, retrieval mode and data resolution. The retrieval mode specifies the type of aggregation. In this case, the “Average” aggregation is selected. The data from the SCADA is stored in second increments. This allows for real-time control of systems using the SCADA, as seen in Figure 32.

The model will require the data to be in 30-minute intervals; therefore, the data needs to be aggregated. The average of the data points within the 30-minute intervals was extracted for each parameter. The resolution indicates the time intervals between each data point.

The database reads this in the microseconds unit; thus, the 30-minute interval is converted to 1 800 000 microseconds. This is done for all parameters iteratively. Once the data is extracted, it is saved in a CSV file.

3.2.3. Step 3.2: Data cleaning

The data pre-processing step was done using Python[8]. The Pandas[9], NumPy[10], and Scikit-Learn [11] libraries were specifically used. The data stored in a CSV file is in its raw format and needs to be transformed into a suitable format for the development of the model.

The data was observed in a graphical format of scatter and time series plots. The scatter plot was used to identify outliers for each parameter. The outliers were identified by observing the parameter's normal operating ranges. The outliers found in the scatter plot are removed from the parameter dataset. Figure 40 indicates a scatter plot for the BAC outlet air temperature.

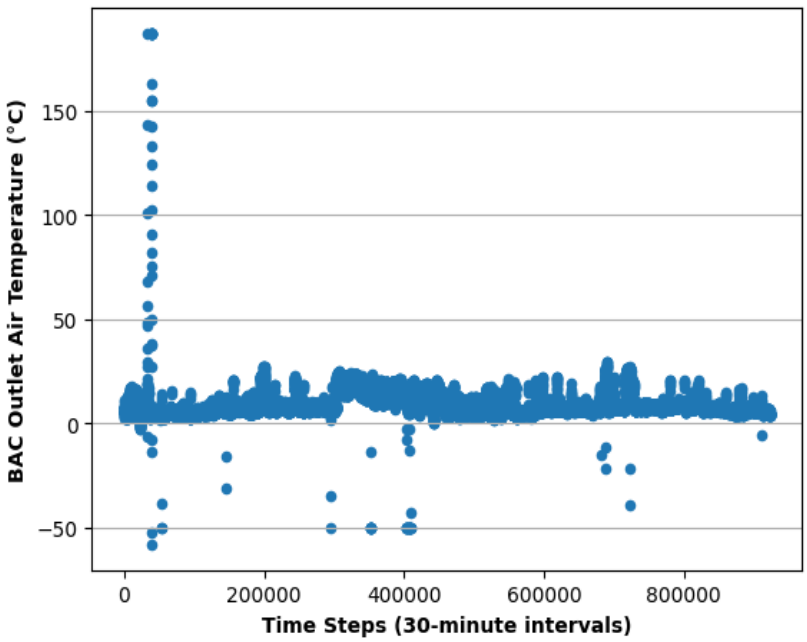

Figure 40: BAC Outlet Air Temperature - Raw data

From Figure 40, the scatter plot details how the outliers can be observed for the BAC outlet. The standard operating range for this parameter from 0°C to 30°C. This range is due to the operating conditions of the BAC, the operating conditions of the BAC

[8] Python, [Online], Available: https://www.python.org/, [Accessed: 29-Aug-2023]
[9] Pandas, [Online], Available: https://pandas.pydata.org/, [Accessed: 29-Aug-2023]
[10] NumPy, [Online], Available: https://numpy.org/, [Accessed: 29-Aug-2023]
[11] "scikit-learn, Machine Learning in Python", Scikit-learn, [Online], Available: https://scikit-learn.org/stable/, [Accessed: 29-Aug-2023]

plants and ambient conditions. The outliers are the data points that are not within the operating range and are removed from the dataset, as seen in Figure 41

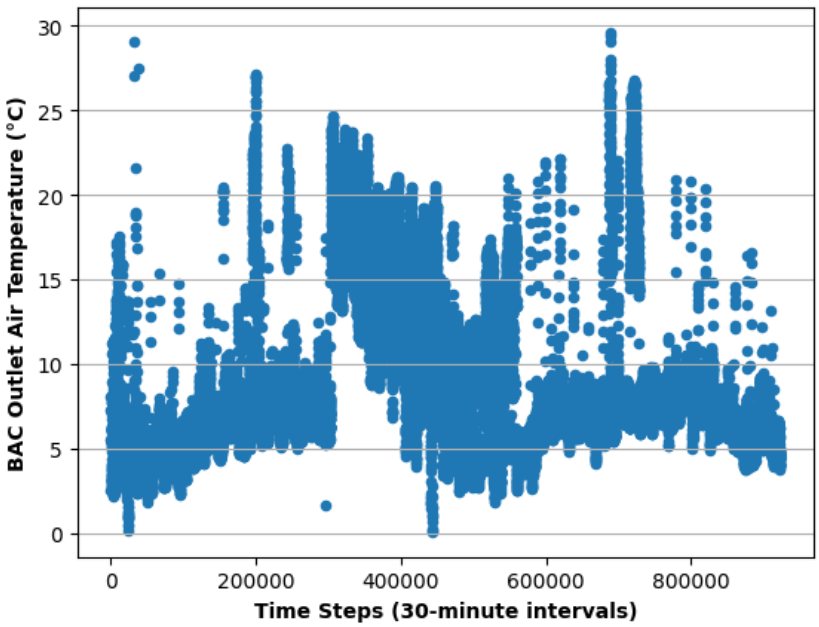

Figure 41: BAC Outlet Air Temperature - After removal of outliers

The next part deals with parameters that contain missing data. Time series plots identify whether a parameter contains missing data points in the data set. This is observed in Figure 42

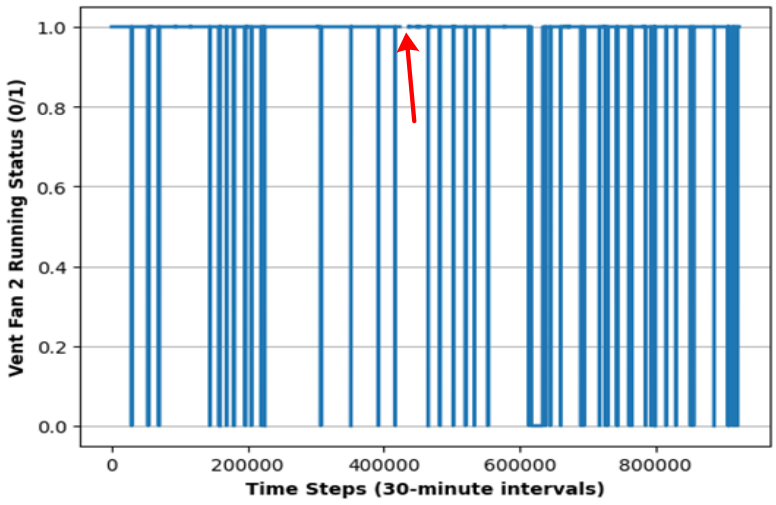

Figure 42: Ventilation Fan 2 Running Status - Raw Data

Figure 42 indicates that missing values are present for the running status of surface ventilation fan 2. The missing data is usually due to a communication error between the instrumentation and the SCADA. As mentioned in Section 2.4.2, imputation will

replace the missing values in the data set. KNN imputation method was chosen as the imputation method. The five nearest neighbours were used to determine the value that replaces the missing data point. The number of neighbours can be adjusted if the model's performance is insufficient. The figure below details ventilation fan 2's data after imputation has been implemented.

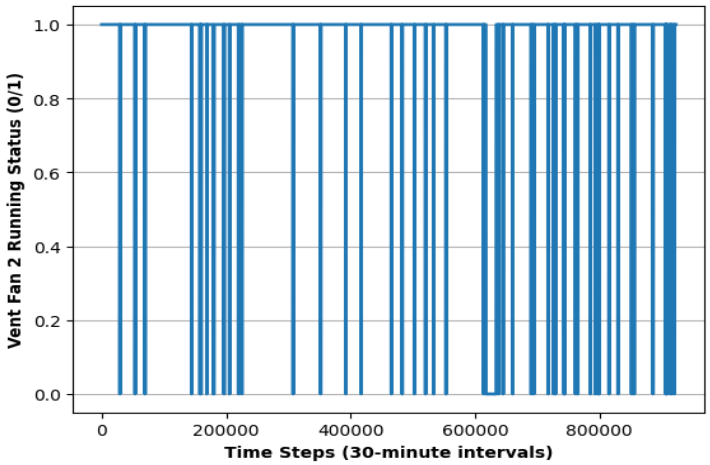

Figure 43: Ventilation Fan 2 Running Status - After imputation.

Due to the large number of data points for each parameter, there is some difficulty visually observing whether missing data is present. The Pandas library allows functions to determine if there are missing data points in the data set. Figure 44 shows a code snippet detailing how to check for missing data. The function results in a true value if none of the parameters contains missing values and false otherwise. Figure 45 details that all parameters have false values. Therefore, all missing data points have been removed from the data set.

```
data.notna().all()
```

Figure 44: Code snippet to check for missing data in the dataset.

```
BAC Fan 1 Running Status                          True
BAC Fan 2 Running Status                          True
BAC Plant 1 Running Status                        True
BAC Plant 2 Running Status                        True
BAC Plant 3 Running Status                        True
Vent Fan 1 Running Status                         True
Vent Fan 2 Running Status                         True
Vent Fan 3 Running Status                         True
6 Level Fridge Plant 3 Running Status             True
6 Level Fridge Plant 4 Running Status             True
7 Level BAC Fan 1 Running Status                  True
7 Level BAC Fan 2 Running Status                  True
7 Level BAC Fan 3 Running Status                  True
7 Level BAC Fan 4 Running Status                  True
BAC Outlet Air Temperature                        True
Ambient Air Wet Bulb Temperature                  True
Ambient Air Dry Bulb Temperature                  True
BAC Plant Condenser Inlet Water Temperature       True
BAC Plant Condenser Outlet Water Temperature      True
BAC Plant Evaporator Inlet Water Temperature      True
BAC Plant Evaporator Outlet Water Temperature     True
Vent Fan 1 Frequency                              True
Vent Fan 2 Frequency                              True
Vent Fan 3 Frequency                              True
Day                                               True
Hour                                              True
Month                                             True
7 Level Air Wet Bulb Temperature                  True
7 Level Air Dry Bulb Temperature                  True
```

Figure 45: Code snippet output when checking for missing values.

3.2.4. Step 3.3: Feature selection

Feature selection can be applied once all the data is cleaned, as discussed in Section 2.4.3. The following parameters were determined as input parameters for the development of the model:

- Surface ambient wet bulb air temperature (°C)
- Surface ambient dry bulb air temperature (°C)
- Day of the month
- Hour of the day
- Month of the year
- 7 Level air wet bulb temperature (°C)
- 7 Level air dry bulb temperature (°C)

A total of 7 individuals of the selected features are deemed sufficient to forecast the temperatures, specifically on the surface and 7 levels. Additional features discussed in Section 3.1.3 can be potentially added to the selection if the model is inaccurate.

Data scaling shall only be implemented on the features that were selected. This will reduce the implementation time of the succeeding step.

3.2.5. Step 3.4: Data pre-processing

After cleaning the data and selecting the desired features, the data needs to be transformed into a format suitable for the model's training. As discussed in Section 2.4.4, The data pre-processing method was done for the following models:

- Model A: trained to forecast 48 timesteps (30-minute intervals) ahead.
- Model B: trained to forecast 24 timesteps (30-minute intervals) ahead.
- Model C: trained to forecast n timesteps (30-minute intervals) ahead, yielding a MAPE of 10% on the test set for all temperatures.
- Model D: trained to forecast n timesteps (30-minute intervals) ahead, yielding a MAPE of 5% on the test set for all temperatures.
- Model E: trained to forecast 1 timestep (30 minutes) ahead.

Sliding window implementation

The first step was to transform the data into sliding windows. This indicates how the models will learn how to predict the future timesteps. The following sliding windows were implemented for each model:

- Model A: previous timesteps = 48; future outputs = 48 timesteps
- Model B: previous timesteps = 24; future outputs = 24 timesteps
- Model C: previous timesteps = 4; future outputs = 4 timesteps
- Model D: previous timesteps = 2; future outputs = 2 timesteps
- Model E: previous timestep = 1; future output = 1 timestep

Data partitioning

The data is now ready to undergo data partitioning. The data was then split into training, validation, and test sets. Of the data, 80% is the training set, 5% is the validation set, and 15% is the test set. This was done for all the models where the sliding window was implemented.

Data scaling

The data is now ready to be scaled using the min-max scaling method. This is done by implementing Equation 15. Figure 46 shows the unscaled data for the ambient dry bulb temperatures.

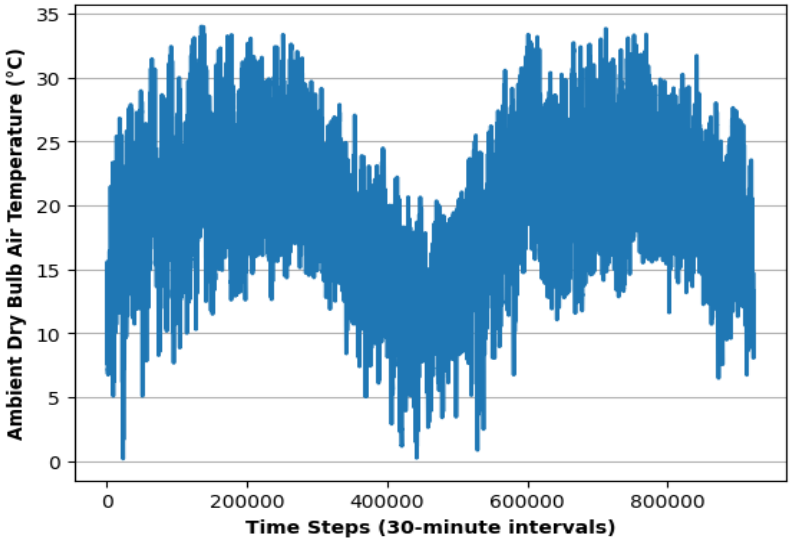

Figure 46: Ambient dry bulb air temperature

Figure 47 indicates that the data from Figure 46 is scaled to depict values between 0 and 1. This was done to ensure that the parameters are suitable for model training; as mentioned in Section 2.4.4, parameters containing larger scales than the rest make it difficult for the neural networks to determine relationships between the inputs to forecast the outputs. Figure 47 details scaled ambient dry bulb air temperatures.

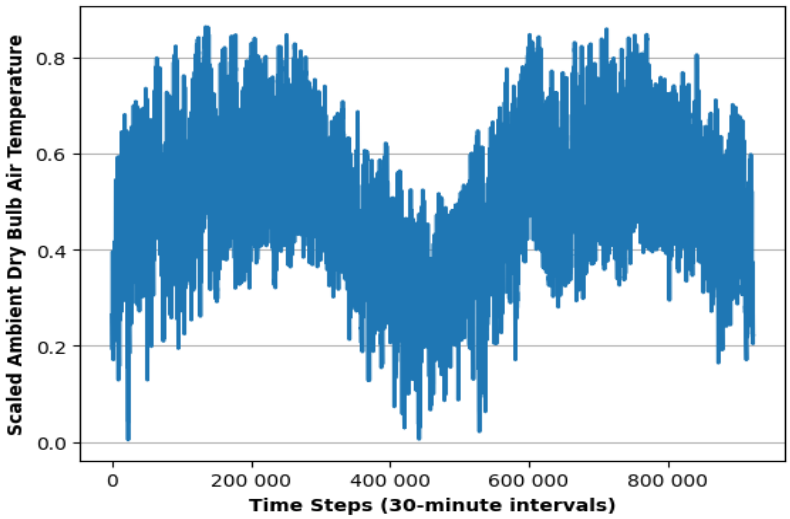

Figure 47: Ambient dry bulb Air Temperature – scaled.

3.2.6. Step 3.5: Model development

The model can be developed now that all the data is in its desired format. The first step is determining the model's hyperparameters, as discussed in Section 2.4.5. The hyperparameters deemed important for the model structure were the number of hidden layers and neurons per hidden layer, the activation function, the number of epochs, the batch size, and the learning rate.

The number of neurons in the first hidden layer is typically based on the number of input parameters. As discussed in Section 3.2.4, 7 input parameters were selected. If the number of input parameters was multiplied by 2, then the following equation is used to determine the number of neurons in the first hidden layer:

$$x = \log_2(14) \tag{27}$$

Where x lies between 3 and 4, the upper bound of 4 is selected, as discussed in Section 2.4.5. Therefore, 32 neurons were selected for the first hidden layer and were calculated using Equation 27.

This structure was arbitrarily chosen for the initial structure of the model, as discussed in Section 2.4.5. The output layer is a linear function. This indicates to the model that continuous time series data is forecasted.

The initial structure of the model was determined for the model; then, the model performance was evaluated. The random search hyperparameter tuning method will be implemented to determine the model structure, yielding acceptable results. The concluding hyperparameters determined for all the models are as follows:

- Hidden layer activation function: LSTM (hidden 1)
- Output layer activation function: Linear
- Number of neurons: 7 (input layer), 32 (hidden layer) and 4 (output layer)
- Number of epochs: 300
- Callback function: Model checkpoint (save best performance)
- Batch size: 32
- Learning rate: 0.0001

Training of the model can commence once the hyperparameters have been determined. The model was trained using the data set's training and validation split. The model accuracy was confirmed using the test split data set was used to verify the model's accuracy. Figure 48 indicates the improvement in model loss throughout the training phase for model A.

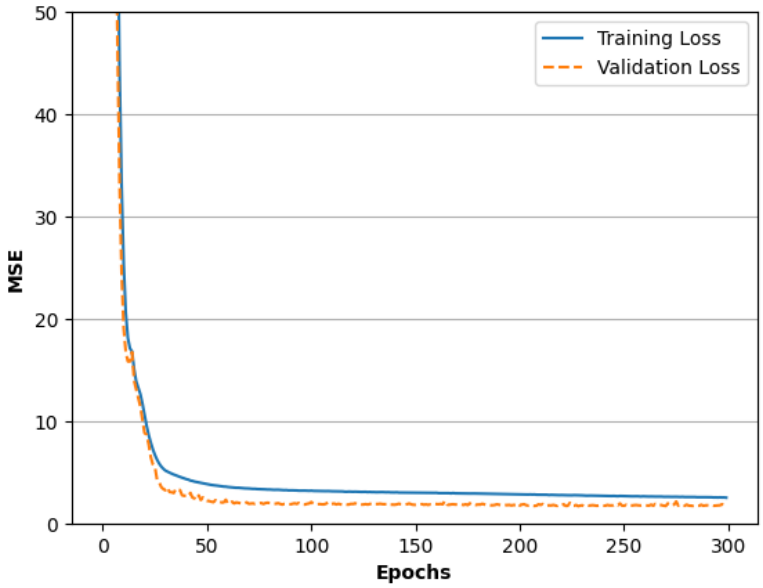

Figure 48: Model A mean square error during the training phase.

Figure 48 shows the MSE loss through each epoch of training. This indicates that the model improves in identifying input parameter patterns and predicting the training and validation set temperatures. The validation set has a smaller MSE than the training set. This indicates that the model was able to predict well with unseen data. The model checkpoint was used to discard the training after the best validation MSE was obtained. After training, the model must be evaluated throughout the training and validation set. This is done by evaluating both sets' CV(RMSE), RMSE and MAPE.

As discussed in Section 3.2.5, the following models were developed:

- Model A: Used the previous 48 timesteps (1 day) to forecast 48 timesteps (1 day) ahead.
- Model B: Used the previous 24 timesteps (12 hours) to forecast 24 timesteps (12 hours) ahead.
- Model C: Used the previous 4 timesteps (2 hours) to forecast 4 timesteps (2 hours) ahead.

- Model D: Used the previous 2 timesteps (1 hour) to forecast 2 timesteps (1 hour) ahead.
- Model E: Used the previous 1 timestep (30 minutes) to forecast 1 timestep (30 minutes) ahead.

Figure 49 indicates the CV(RMSE) values, Figure 50 indicates the RMSE values, and Figure 51 indicates the MAPE values for the training and validation split datasets after the training is complete for the developed models. This indicates the training performance for each model.

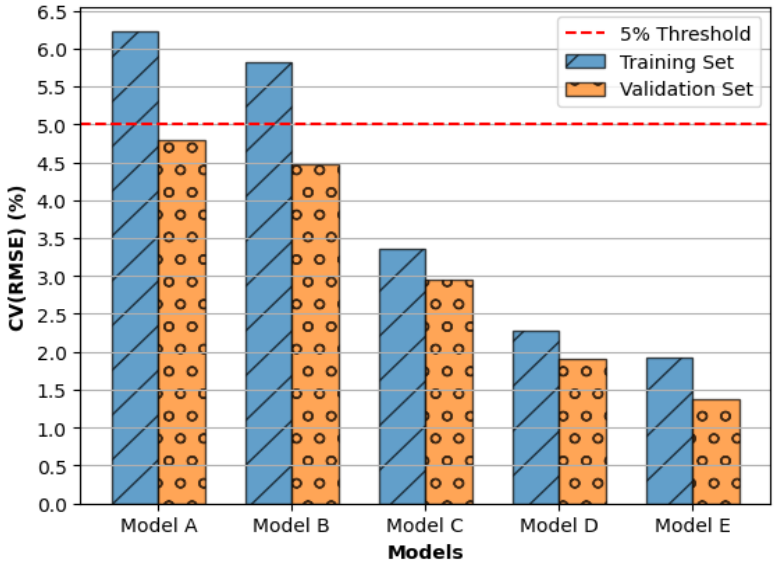

Figure 49: CV(RMSE) values for the training and validation sets

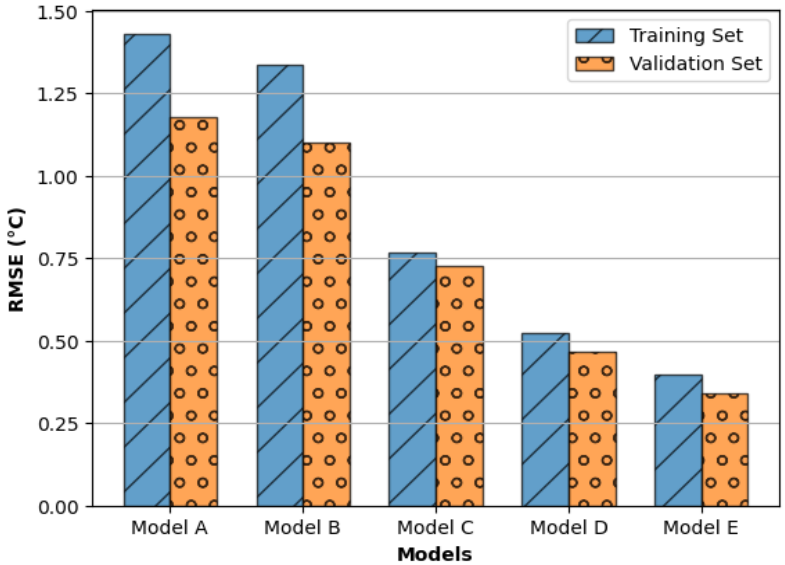

Figure 50: RMSE values for the training and validation sets

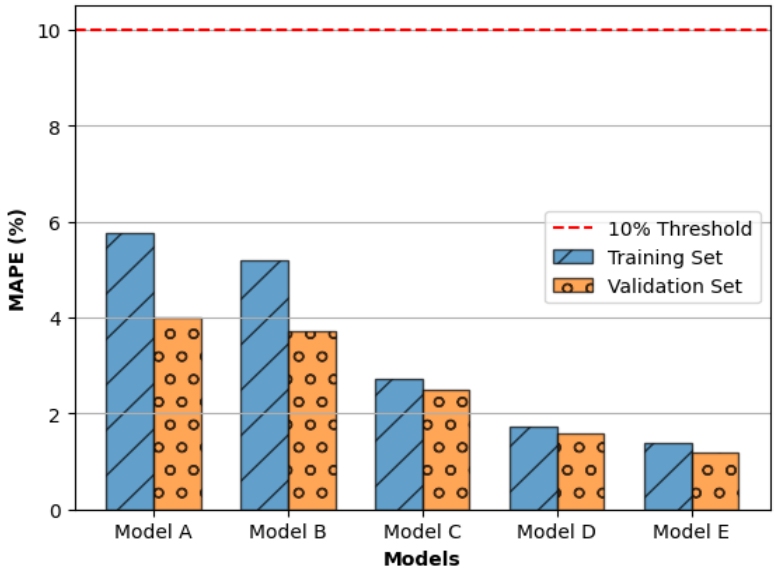

Figure 51: MAPE values for the training and validation sets

As observed in Figure 49, Figure 50, and Figure 51, the CV(RMSE), RMSE, and MAPE values are the highest for model A, with CV(RMSE) values of 6.23% and 4.78%, RMSE values of 1.43°C and 1.18°C, and MAPE values of 5.78% and 4% for the training and validation set. The lowest values are observed for model E, which are 1.92% and 1.38% for the CV(RMSE), 0.40°C and 0.34°C for the RMSE, and 1.38% and 1.2% for the MAPE. This indicates that the model's ability to learn how to predict temperatures improves as the forecasting horizon decreases, with a forecasting horizon of 48 timesteps (1 day) for model A and one timestep (30 minutes) for model E.

Moreover, the figures above show that the values for the validation set are lower than those for the training set for all models. This indicates that the models can predict well on unseen data. Finally, a greater variation between the training and validation set values is observed for the models with the greatest forecasting horizon. This indicates that the models slightly overfit the predictions, thus generalising the predictions for greater forecasting horizons. Although this is a good indication of the performance of the models, the true performance of the models needs to be evaluated using the test set. The test set was not involved during the training phase. Thus, the evaluation with this set eliminates bias in the results.

3.2.7. Step 3.6: Model evaluation

Although the validation set can indicate the model performance on unseen data, the validation set is small compared to the training and test sets. Moreover, the validation set is used during the training phase of the model. Thus, it is not a true reflection of the model's performance. The evaluation metrics of the test set validate the accuracy of the model. The following figures compare the test set model's predicted values of the underground wet bulb temperatures for each developed model. This shows the model's ability to predict the temperatures based on unseen data. The set contains 4 602 data points, equivalent to approximately three months.

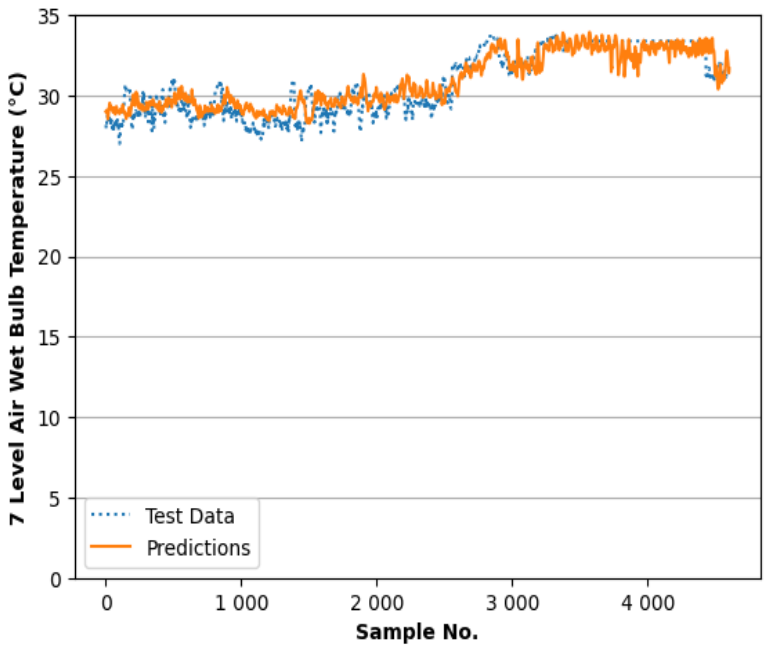

Figure 52: Model A 7-level air wet bulb temperature predictions on test set.

Figure 52 compares model A's predicted and 7 level air wet bulb temperatures. CV(RMSE) of 4.19%, a RMSE of 1.57°C and a MAPE of 4.02% was obtained. The CV(RMSE) is above the recommended 5% threshold, as mentioned in Section 2.4.6. However, the MAPE is below the 10% threshold.

The RMSE value of the 7 level air wet bulb temperature for the training set was 0.78°C and 1.57°C for the test set, leading to a difference of 0.79°C. This indicates that the model does not overfit the data, thus not generalising for predictions.

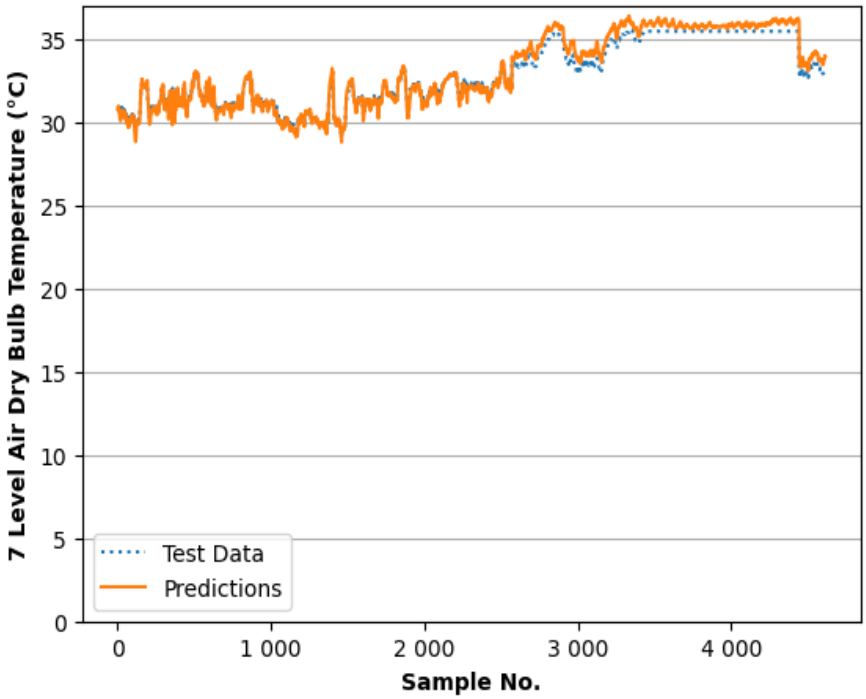

Figure 53: Model E 7 level air wet bulb temperature predictions on the test set

Figure 53 compares model E's predicted and actual 7 level wet bulb temperatures. Model E yielded a CV(RMSE) of 1.55%, an RMSE of 0.37°C and a MAPE of 1.01%. The CV(RMSE) is below the recommended 5% threshold, and the MAPE is below the 10% threshold.

The RMSE value of the 7 level wet bulb temperature for the training set was 0.27°C and 0.37°C for the test set, leading to a difference of 0.1°C. This indicates that the model does not overfit the data. Moreover, smaller errors are observed in model E compared to model A. Therefore, it is more difficult to forecast the temperature over a greater horizon.

This is more apparent when there are irregular data points in the set since the models with larger forecasting horizons may not use an irregular data point to determine the forecasted outcome. All outputs of the model need to be evaluated to determine each model’s performance.

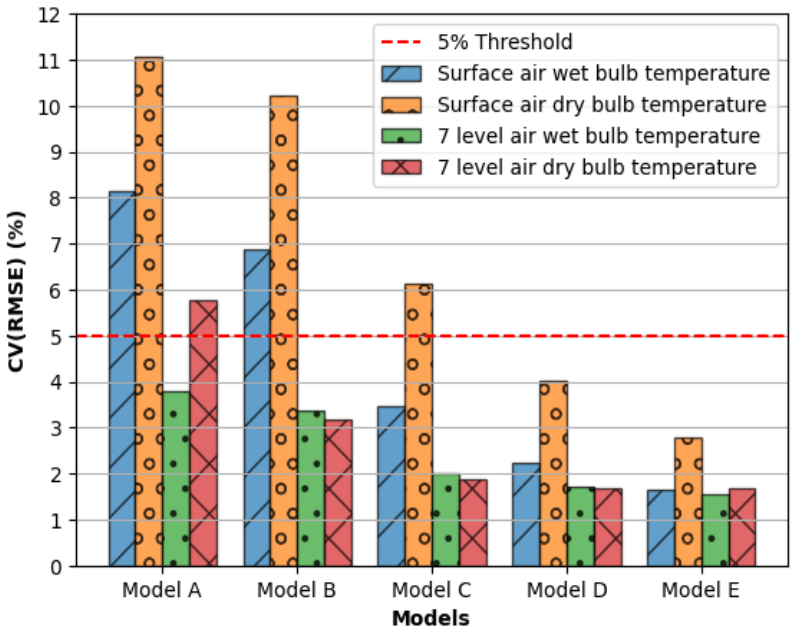

Figure 54: CV(RMSE) values for the test set

Figure 54 indicates the CV(RMSE) values for the test set for each model. It can be observed that the CV(RMSE) decreases as the forecasting horizon decreases, where model A has a forecasting horizon of 1 day and model E has a forecasting horizon of 30 minutes. The +-5% threshold is reached for the following models:

- Model A
  - 7 level air wet bulb temperature (3.79%)
  - 7 level air dry bulb temperature (5.78%)
- Model B
  - 7 level air wet bulb temperature (3.37%)
  - 7 level air dry bulb temperature (3.17%)
- Model C
  - Surface air wet bulb temperature (3.47%)
  - 7 level air wet bulb temperature (2.00%)
  - 7 level air dry bulb temperature (1.88%)
- Model D
  - Surface air wet bulb temperature (2.23%)
  - Surface air dry bulb temperature (4.03%)
  - 7 level air wet bulb temperature (1.73%)
  - 7 level air dry bulb temperature (1.66%)

- Model E
    - Surface air wet bulb temperature (1.66%)
    - Surface air dry bulb temperature (2.78%)
    - 7 level air wet bulb temperature (1.55%)
    - 7 level air dry bulb temperature (1.68%)

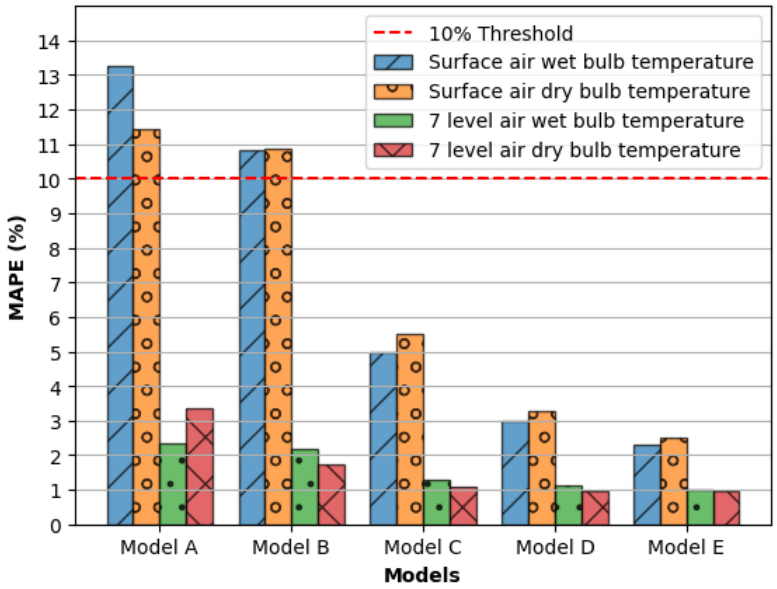

Figure 55: MAPE values for the test set

Figure 55 details the MAPE values for the test set for each model. The MAPE values follow the same trend as the CV(RMSE) values for the test set, where they improve as the forecasting horizon decreases.

The +-10% threshold for the MAPE is reached for the following models:

- Model A
    - 7 level air wet bulb temperature (2.33%)
    - 7 level air dry bulb temperature (3.37%)
- Model B
    - Surface air wet bulb temperature (10.84%)
    - Surface air dry bulb temperature (10.88%)
    - 7 level air wet bulb temperature (2.17%)
    - 7 level air dry bulb temperature (1.73%)
- Model C
    - Surface air wet bulb temperature (4.98%)

    - Surface air dry bulb temperature (5.49%)
    - 7 level air wet bulb temperature (1.28%)
    - 7 level air dry bulb temperature (1.07%)
- Model D
    - Surface air wet bulb temperature (2.99%)
    - Surface air dry bulb temperature (3.29%)
    - 7 level air wet bulb temperature (1.11%)
    - 7 level air dry bulb temperature (0.95%)
- Model E
    - Surface air wet bulb temperature (2.29%)
    - Surface air dry bulb temperature (2.49%)
    - 7 level air wet bulb temperature (1.01%)
    - 7 level air dry bulb temperature (0.95%)

Models D and E achieved CV(RMSE) values below the 5% threshold for all forecasted temperatures. Models C, D, and E achieved MAPE values below the 10% threshold for all forecasted temperatures. Therefore, these models, C, D, and E, are deemed accurate for forecasting temperatures. Moreover, it can be observed that it is more difficult to forecast the surface temperatures due to the larger variability in the data.

Finally, model A (1-day forecast) and model B (12-hour forecast) do not meet the thresholds for CV(RMSE) and MAPE. This indicates that an alternative method of forecasting temperatures should be developed for larger forecasting horizons. Thus, this section verifies that research objective 2 was fulfiled.

3.3. Dynamic control solution verification

3.3.1. Preamble

This section covers the third research objective, outlined in Section 1.7.

Research objective 3: Develop a dynamic control solution for the surface BAC cooling plants and the BAC.

This objective is accomplished by implementing the method illustrated in Section 2.5: developing and applying a dynamic control solution using an AI-based temperature forecasting model. The solution overview is detailed in the figure in Section 2.5.

The method contained specifications which are addressed in Section 2.5 and are listed below:

- Specification 1: Daily data acquisition.
- Specification 2: AI-based forecasting.
- Specification 3: Daily operation suggestion.

The dynamic control solution was proposed to be developed for the case study mine detailed in Section 3.1.2. The control solution used the verified temperature forecasting models and the parts of the model development procedure for the control solution (Section 0). The dynamic control solution was developed from the following models:

- Model C (two-hour forecast)
- Model D (one-hour forecast)
- Model E (30-minute forecast)

3.3.2. Specification 1: Daily data acquisition

The data acquisition process was done using the method mentioned in Sections 2.4.1 and 3.2.2. The data is extracted based on the required data to forecast each model. The data is extracted with a 30-minute frequency. After this data was extracted, the data was stored in a CSV file locally on a PC.

The following extraction periods were done for each model:

- Model C (extract data for the previous two hours from the present time)
- Model D (extract data for the previous hour from the present time)
- Model E (extract the present time data)

The data is extracted for the parameters discussed in Section 3.2.4. Figure 56 indicates an example of data extraction for the surface ambient dry bulb air temperatures required for model C.

Model C was developed to forecast temperatures two hours ahead based on the previous two hours. In this example, the present time is 09:00:00. Thus, model C will forecast temperatures at 11:00:00 (4 timesteps ahead).

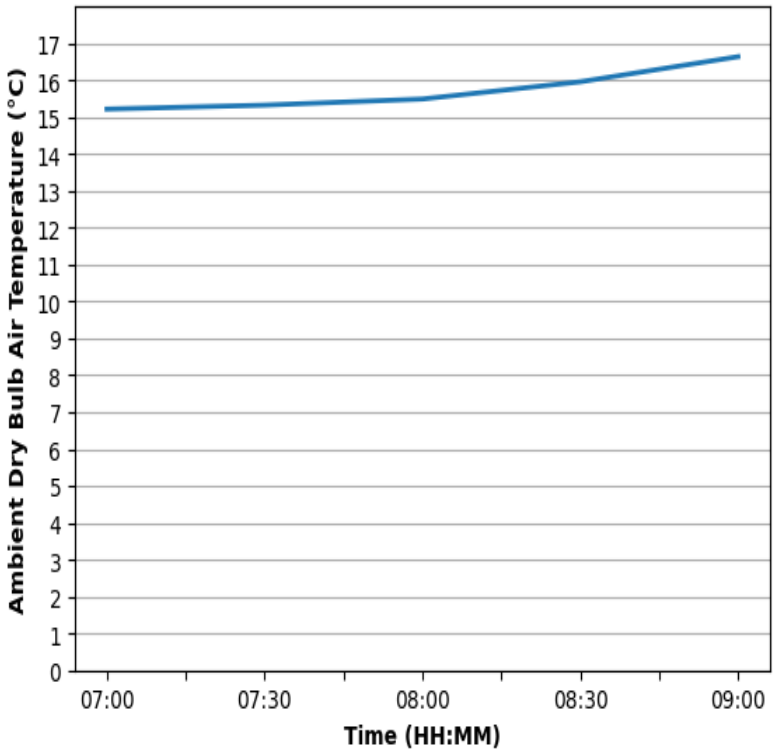

Figure 56: Surface dry bulb air temperature extraction for model C

The data extraction procedure was done for models C, D, and E, thus concluding the data acquisition phase for the control solution.

This verifies that Specification 1 was addressed to ensure the correct data is acquired to forecast temperatures based on each model.

3.3.3. Specification 2: AI-based forecasting

The extracted data was still in the raw format from Section 3.3.2. The extracted data was cleaned and processed using the same procedure used in Sections 3.2.3 and 3.2.5 without the data partitioning to develop the temperature forecasting models.

The following figures show the results of the developed models for a typical day outside of the training, validation, and test set.

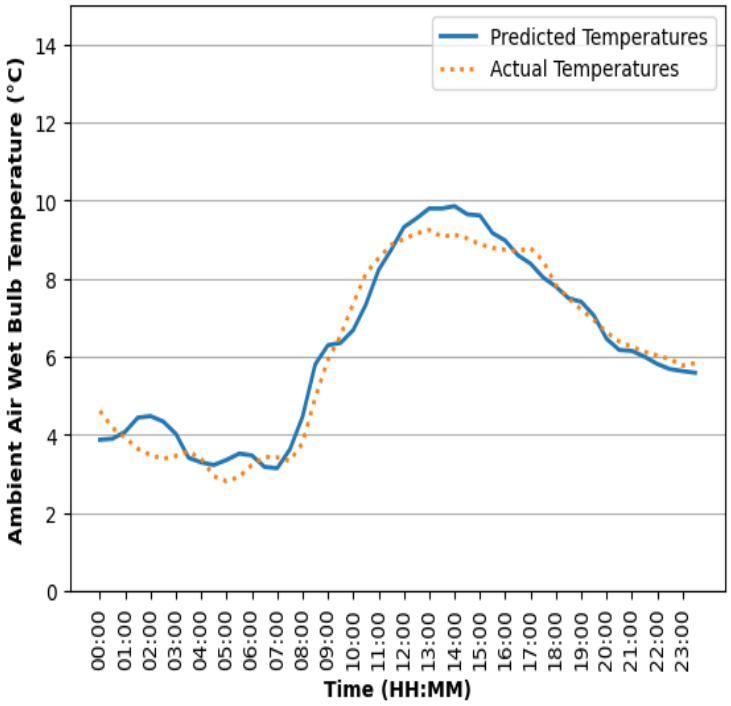

Figure 57: Real-time forecast of the surface air wet bulb temperature using model C

Figure 57 shows the forecasted surface air wet bulb temperatures compared to the actual temperatures. Each timestep indicates the temperatures forecasted two hours ahead of its actual time, as stated in Section 3.3.1.

A MAPE of 7.72% was achieved for model C's forecast of the surface air wet bulb temperatures. Moreover, the forecasting accuracy improves later in the day, as it relies less on the previous day's data.

Figure 58 shows the forecasted 7 level air wet bulb temperatures compared to the actual temperatures. It can be observed that there is less variation in the data as compared to the surface temperatures. This is due to the additional cooling auxiliaries found underground. A MAPE of 2.32% was achieved for the 7 level air wet bulb temperatures.

The results discussed in Figure 57 and Figure 58 indicate that model C can forecast temperatures accurately since they are below the 10% threshold. Thus, model C can be a dynamic control solution for the surface BAC plants and fans. The following figures detail the results obtained for model D.

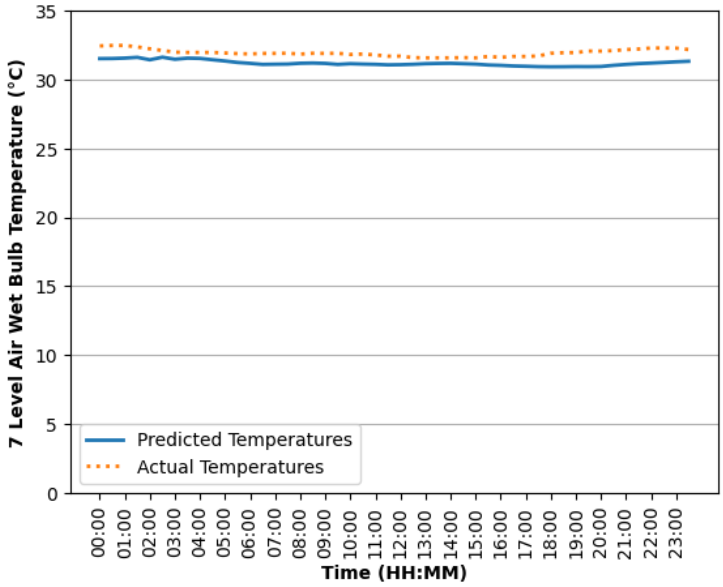

Figure 58: Real-time forecast of the 7-level air wet bulb temperature using model C

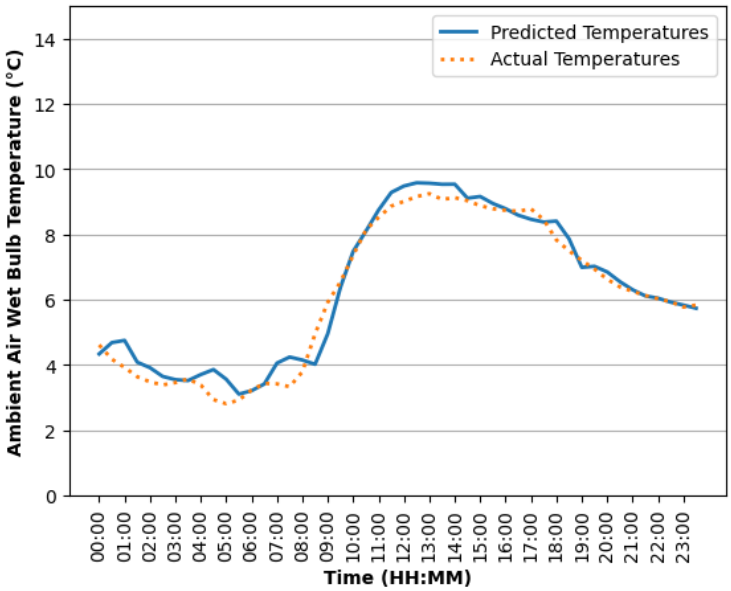

Figure 59: Real-time forecast of the surface air wet bulb temperature using model D

Model D yielded a MAPE of 6.57% when comparing the forecasted and actual surface wet bulb temperatures (Figure 59), which is lower than the MAPE observed for model C (7.72%). This follows the same trend shown in Section 3.2.7 when evaluating the models on the test set, where the MAPE is smaller for smaller forecasting horizons.

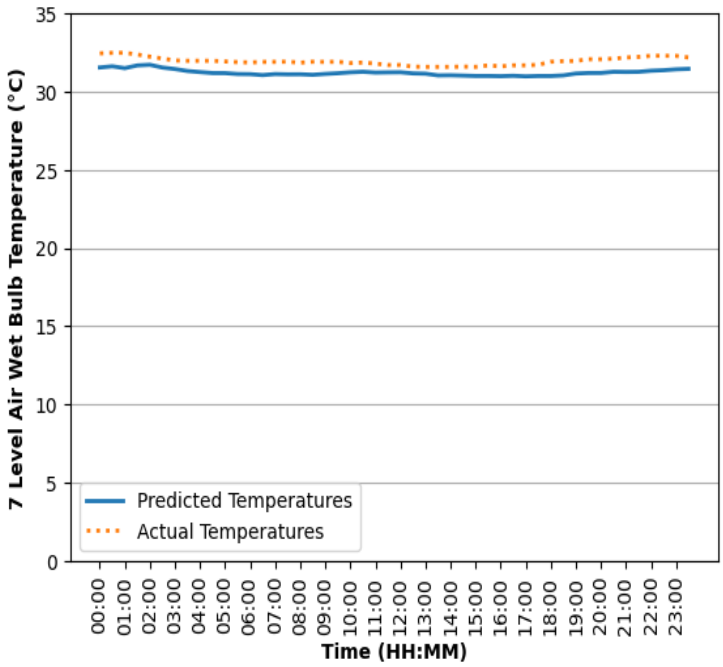

Figure 60: Real-time forecast of the 7 level air wet bulb temperature using model D

The forecasted 7 level air wet bulb temperatures achieved a MAPE of 2.27% compared to the actual temperatures. The results obtained are similar to those observed for model C (Figure 58). This is due to the lack of temperature variation throughout the day. The results obtained for model E are shown in Figure 61 and Figure 62.

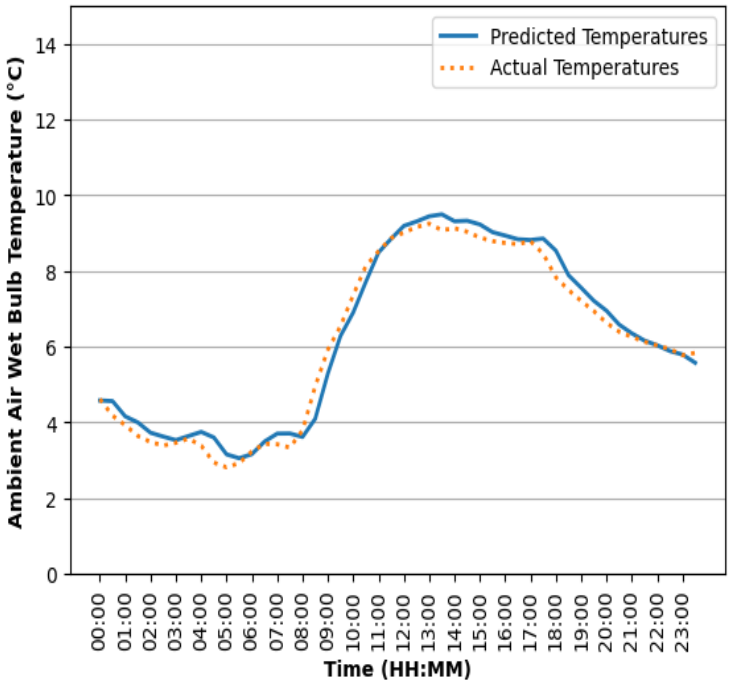

Figure 61: Real-time forecast of the surface air wet bulb temperature using model E

A MAPE of 4.9% is observed in Figure 61, yielding a similar trend in the comparisons of Figure 57 and Figure 59, where the MAPE decreases as the forecasting horizon decreases. Figure 62 yielded a MAPE of 2.13%, similar to the results obtained for models C and D.

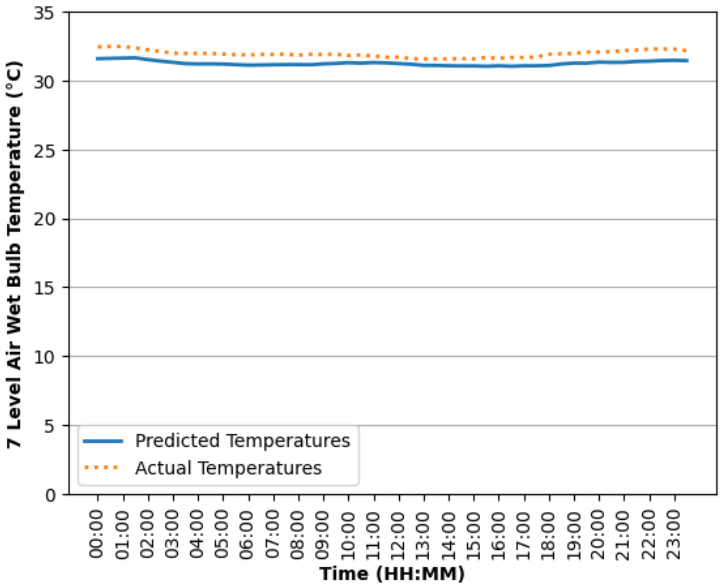

Figure 62: Real-time forecast of the 7 level air wet bulb temperature using model E

The results above indicate that the MAPE values are below the 10% threshold, thus deeming the models accurate. The following figure shows the MAPE values for models C, D, and E for real-time forecasting.

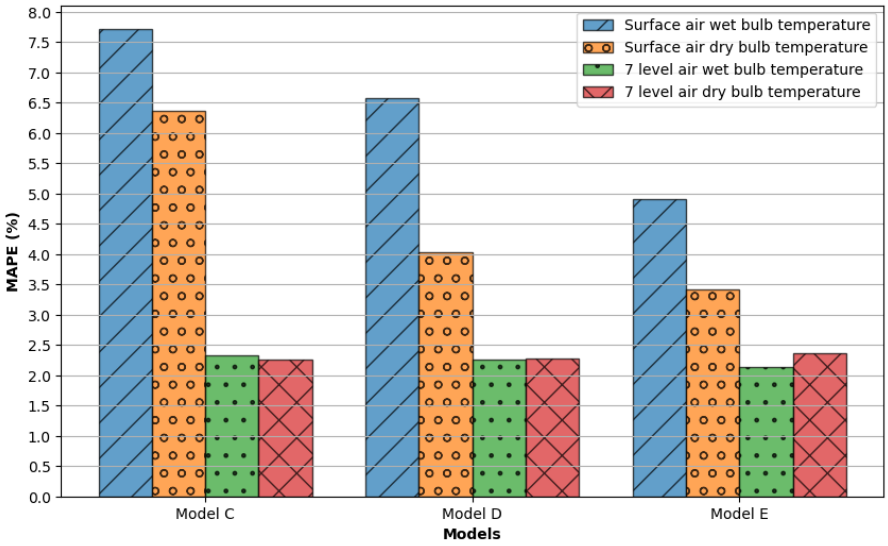

Figure 63: MAPE values for real-time temperature forecasts

Figure 63 shows that MAPE values achieved for all the forecasted temperatures are below the 10% threshold. Thus, the models are accurate for real-time temperature forecasting. However, the models struggle to forecast temperatures that converge to zero, as seen in Figure 64

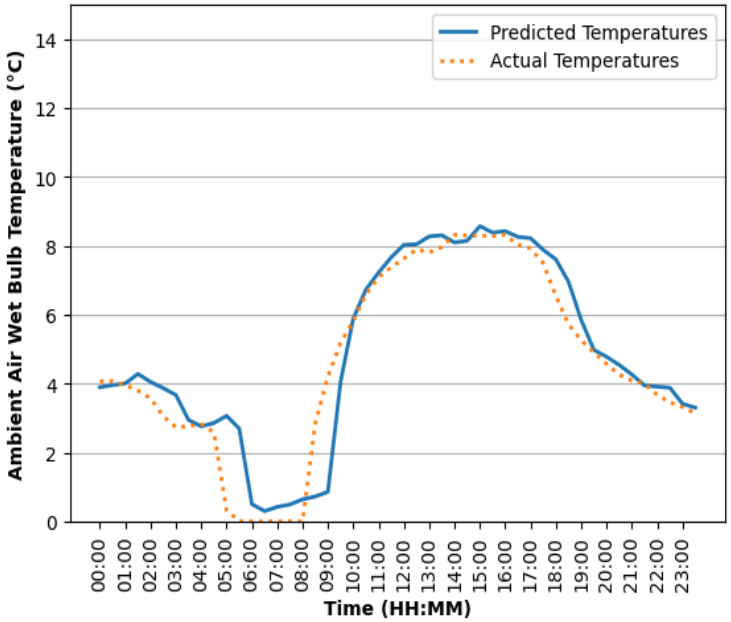

Figure 64: Real-time forecast of the surface air wet bulb temperature with zero values

Since the models are accurate, as seen in Figure 63, this indicates that the models can accurately forecast temperatures in real-time. Therefore, the models can be successfully implemented to determine the dynamic control solutions.

Thus, Specification 2 has been addressed. Specification 2 shall be used in the solution developed for Specification 3.

3.3.4. Specification 3: Operation suggestion

The dynamic operation suggestion is based on the real-time forecasted temperature. As discussed in Section 2.5.3, the thresholds for the surface air wet bulb temperature are **7°C** and **32°C** for the 7 level air wet bulb underground temperatures.

These objectives form the basis of the dynamic control solution. The dynamic control solution was developed for models C, D, and E.

Summer operation suggestion

Figure 65 shows the real-time forecasted temperatures with the 7°C threshold based on a day outside the winter months (June, July, and August).

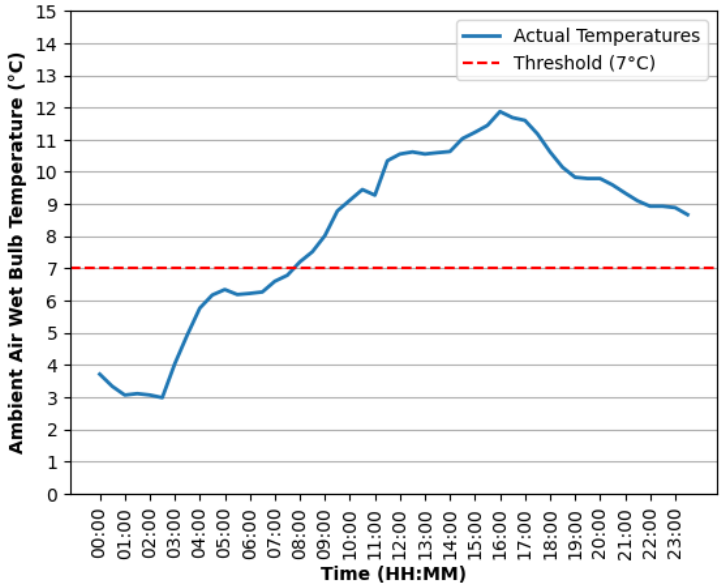

Figure 65: Forecasted summer surface air wet bulb temperatures using model E with the threshold

Figure 65 yielded a MAPE of 3.75%. The forecasted temperatures are below 7°C between 00:00 and 08:00. Thus, the BAC fans and plants can be switched off during this period.

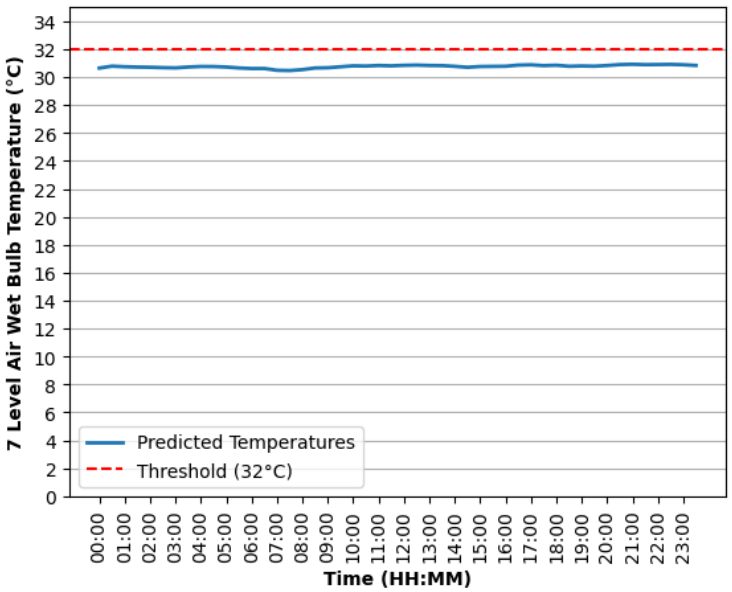

Figure 66: Forecasted summer 7 level air wet bulb temperatures using model E with the threshold

A MAPE of 1.42% was achieved, as shown in Figure 66. The forecasted temperatures are below 32°C.

Thus, the temperatures indicate the possibility of switching off the BAC fans and plants with the assumption that the operations of the underground cooling auxiliaries remain the same throughout the day.

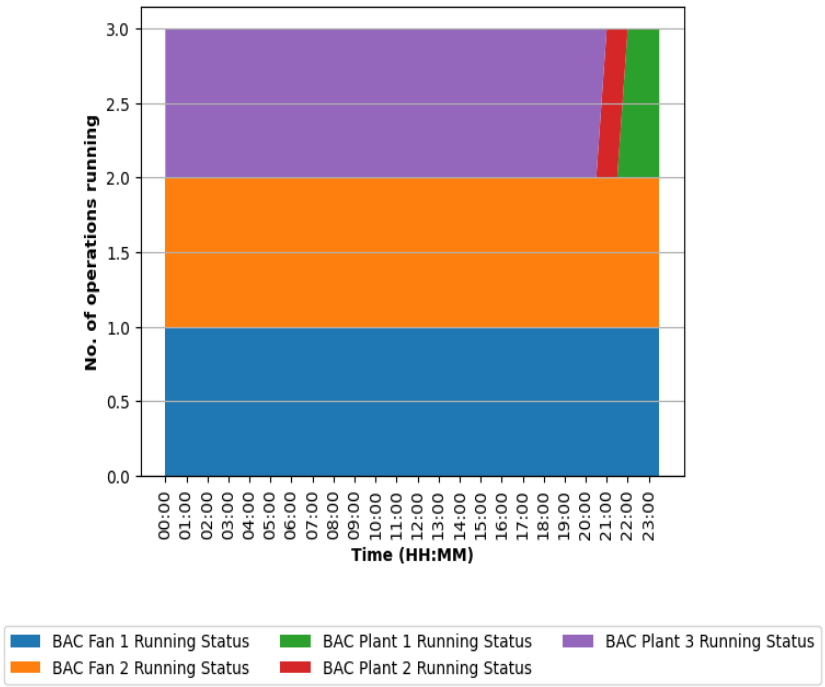

Figure 67: Summer BAC operations

Figure 67 shows the actual running statuses for the BAC operations (BAC fans and plants). The suggested operation based on the forecasted temperatures is observed in Figure 68.

Figure 68 shows the suggested operation based on the forecasted temperatures shown in Figure 65 and Figure 66. The operation suggestion strategy is proposed to be a real-time solution. These figures show the suggested strategy based on model E's forecasting model.

In a real-time scenario, the temperature is forecasted 30 minutes ahead of the actual time iteratively. The forecasted temperature will determine whether the BAC equipment should be switched off for that forecasted period.

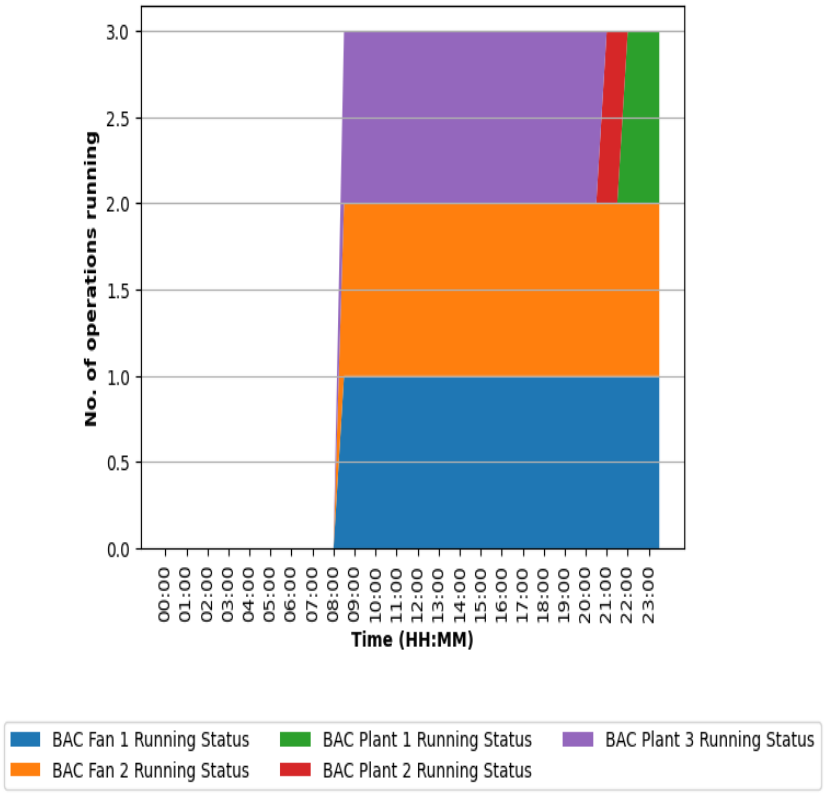

Figure 68: Suggested BAC operations strategy for summer

Model C achieved a MAPE of 10.42% and 1.92% for the surface air wet bulb temperatures and the 7 level air wet bulb temperatures. The model suggested the same summer operation as model E with an iterative two-hour forecast.

The same summer operation solution was observed for model D with MAPE values of 5.4% and 1.68% for the surface air wet bulb temperatures and the 7 level air wet bulb temperatures with iterative one-hour forecasts.

Winter operation suggestion

Figure 69 shows the real-time forecasted temperatures with the 7°C threshold based on a day in the winter months. The real-time forecasted temperatures achieved a MAPE of 6.82%.

The forecasted temperatures are slightly above the 7°C threshold for several periods during the day, with a maximum temperature of 7.11°C. Thus, the BAC fans and plants can be switched off all day.

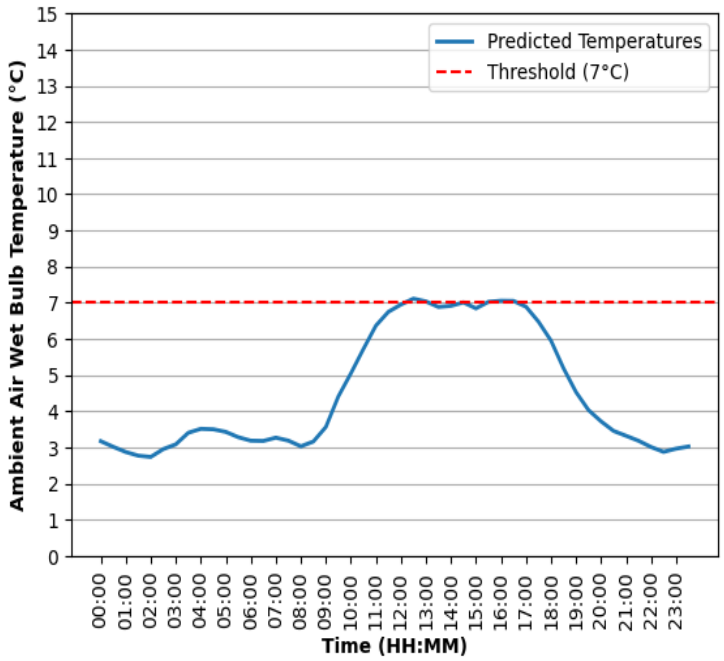

Figure 69: Forecasted winter surface air wet bulb temperatures using model E with the threshold

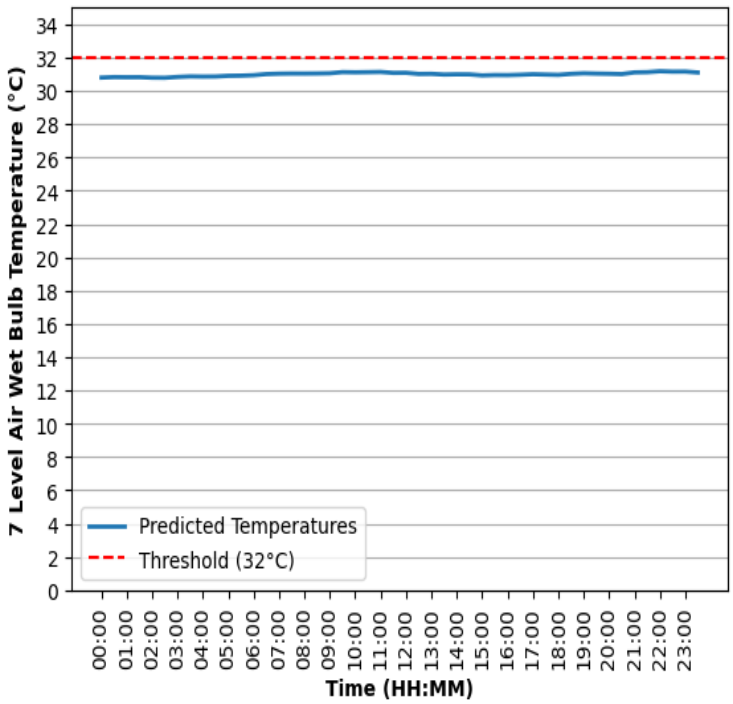

Figure 70: Forecasted winter 7 level air wet bulb temperatures using model E with the threshold

A MAPE of 2.31% was achieved, as shown in Figure 70. The forecasted temperatures are below 32°C. Thus, the temperatures indicate the possibility of switching off the BAC fans and plants based on the same assumption used in the summer months.

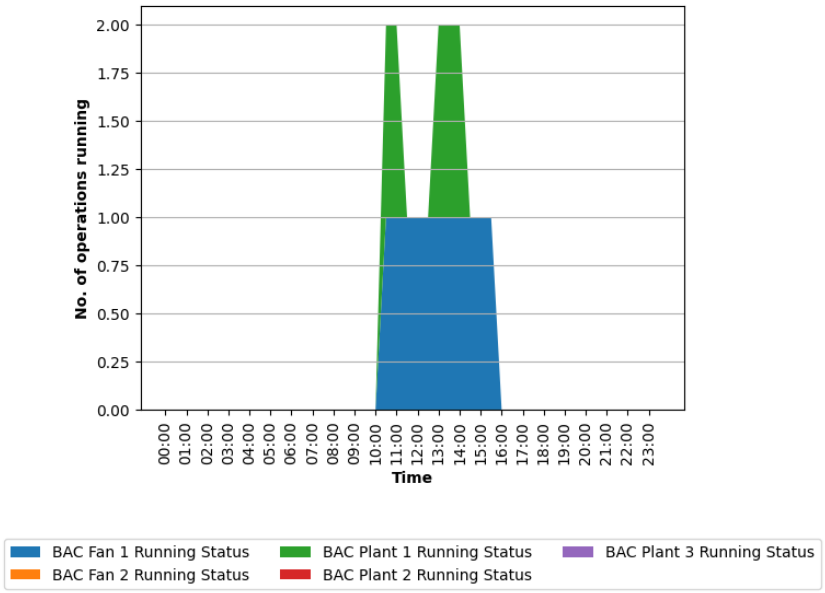

Figure 71: Winter BAC operations

Figure 71 shows the actual running statuses for the BAC operations during winter. A control strategy had already been implemented in the case study during the winter months by Lodewyk [41]. The strategy ensured that the surface BAC operations were on between 10:00 and 16:00. The suggested operation based on the forecasted temperatures is observed in Figure 72.

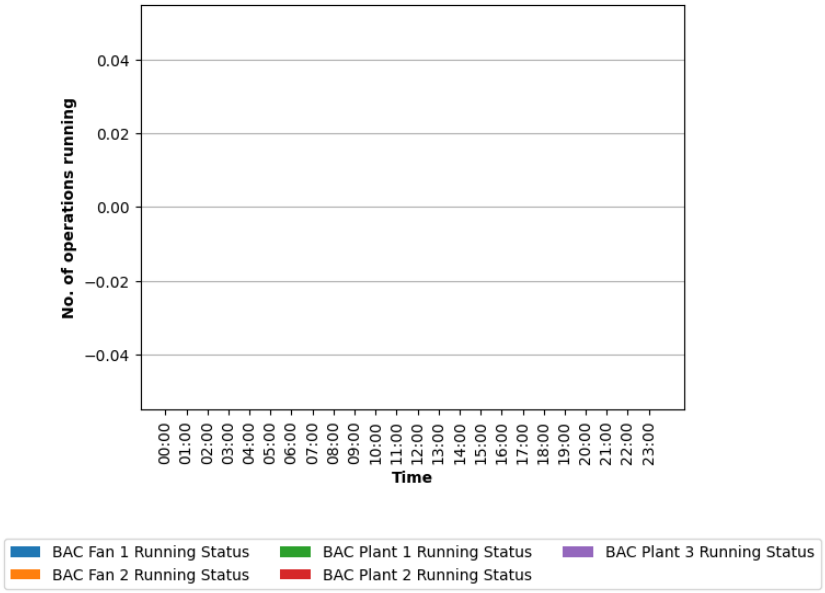

Figure 72: Suggested BAC operations strategy for winter

Figure 72 shows the suggested operation based on the forecasted temperatures shown in Figure 69 and Figure 70. As discussed for the summer operation suggestion,

the operation suggestion shown in Figure 72 is based on model E with iterative real-time 30-minute forecasts.

Model C achieved a MAPE of 13.81% and 2.80% for the surface air wet bulb temperatures and the 7 level air wet bulb temperatures. The model suggested the same winter operation as model E with an iterative two-hour forecast. The same winter operation solution was observed for model D with MAPE values of 8.26% and 2.68% for the surface air wet bulb temperatures and the 7 level air wet bulb temperatures with iterative one-hour forecasts.

Based on these results, model C is more likely to be inaccurate for the temperature forecasts, and model E provides the most accurate forecasts. Thus, model D (one-hour forecast) would be the most suitable model to implement on Mine A. This gives the mine enough lead time to prepare to switch on or off the BAC equipment with sufficient forecasting accuracy.

Mine A manually controls the BAC plants and fans via the instruction of the control room. Thus, the alarm system can indicate to the control room when the BAC plants and fans should be running. Using model D's solution, the control room will receive an alarm one-hour in advance indicating the operation of the BAC equipment. This allows sufficient time to send data from the control solution to the alarm system.

Based on the operation suggestion, electricity savings could have been achieved if the solution had been implemented for that day. The suggested solution depends on the day's temperature since the forecasted temperatures are dynamic. Therefore, Specification 3 was addressed based on the results.

All specifications were addressed in this section. Specification 1 was the daily acquisition procedure, 2 was the AI-based forecasting, and 3 was the daily operation suggestion for the BAC equipment. Therefore, research objective 3 was addressed.

3.4. Validation of the proposed solution on the case study

3.4.1. Preamble

This section shall address the final research objective.

Research objective 4: Validate the control solution which addresses the research problem.

Section 3.1 determined whether system parameters are closely related to the surface BAC equipment. This was important since developing an AI-based forecasting model relies on data availability from the system parameters, thus verifying research objective 1. Section 3.2 verified the feasibility of applying an LSTM-RNN model to forecast temperatures over various forecasting horizons, which addressed research objective 2. Section 3.3 indicated that a dynamic control solution can be developed using the temperature forecasting models developed in Section 3.2. Therefore, this section addressed research objective 3.

The first three research objectives address the feasibility of using AI-based forecasting to develop a dynamic control solution on a surface cooling system.

Research objective 4 consolidates the developed solution by detailing the possible electricity savings that could be realised during implementation and addresses the need for the study, as discussed in Section 1.6.

AI-inspired temperature forecasting is needed to develop a dynamic control solution for deep-level mine cooling systems.

3.4.2. Electricity cost savings

The electricity cost savings will be calculated to determine whether the developed dynamic control solution indicates a reduction in electricity usage. The electricity cost saving is determined for a day in the summer and a day in the winter. The summer day profile amounts to a reduction in electricity of 15 MWh, equivalent to ZAR 17 897 per day.

It is crucial to emphasise that the control solution is mainly applied during the transitional months between the summer and winter periods (May and September). This led to possible electricity cost savings of ZAR 0.5 million per annum using the 2022/2023 Eskom tariffs. Figure 73 illustrates the actual power usage in comparison to the possible power usage based on the dynamic control solution during summer.

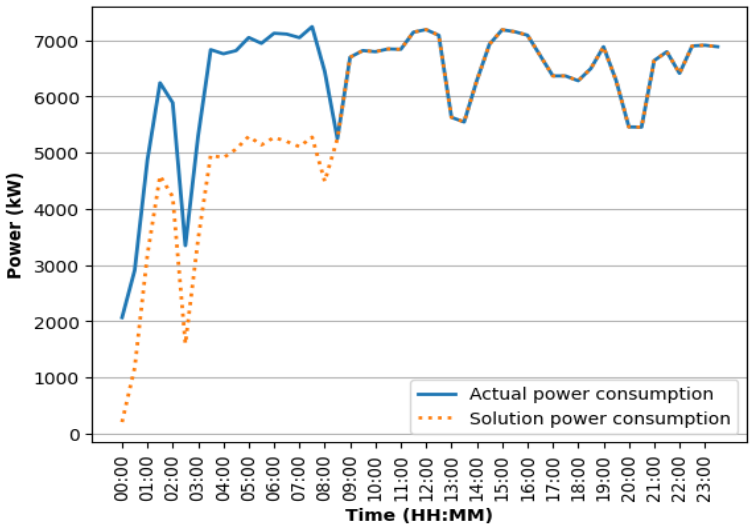

Figure 73: Summer actual and solution power usage comparison

The winter day profile amounts to a reduction of 5 MWh of electricity, amounting to ZAR 9 570 per day. As discussed in Section 3.3.4, a winter electricity savings strategy had already been implemented in Mine A. Thus, the electricity savings realised from the dynamic control solution supplement the existing electricity savings during winter. This led to a possible electricity cost savings of ZAR 0.8 million per annum. Due to the increased tariffs during the winter periods, higher electricity cost savings are realised.

Moreover, lower temperatures are realised during winter. Therefore, the BAC equipment does not need to be operational at greater frequencies during this period. Figure 74 indicates the actual power usage in comparison to the possible power usage based on the dynamic control solution during winter.

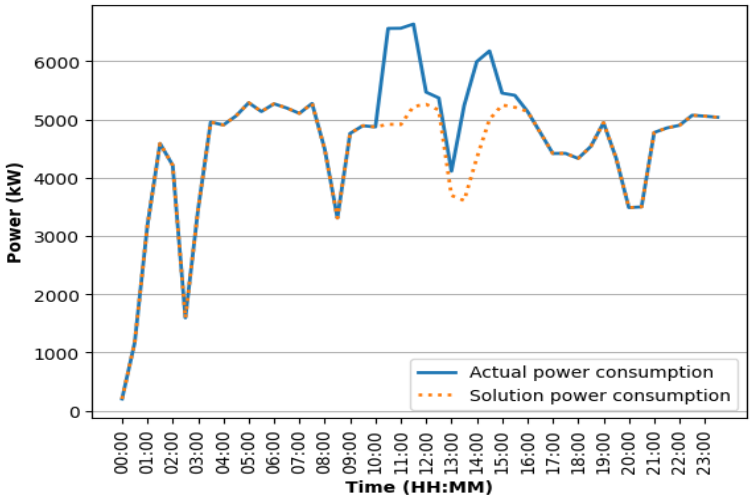

Figure 74: Winter actual and solution power usage comparison

This study aimed to develop an AI-based temperature forecasting model for a dynamic operation strategy on Mine A's cooling system, specifically the BAC APs and fans. Moreover, to determine whether possible electricity savings can be realised. The developed strategy yielded electricity cost savings of ZAR 0.5 million during summer and ZAR 0.8 million during winter. The total expected savings for the solution was ZAR 1.3 million per annum.

3.4.3. Discussion of findings

Section 3.4.2 compared the actual power consumption to the expected power consumption generated from the developed solution and showed that possible electricity savings could be realised if implemented. Although a possible electricity reduction is observed, the developed solution has some shortcomings.

The shortcomings are addressed from the following points:

- Section 3.2.6 discussed the development of five models with different forecasting horizons. It was found that models with forecasting horizons of 1 day and 12 hours were deemed inaccurate.
  The accuracy of the models can be improved by increasing the dataset while retraining the models. Moreover, alternative forecasting models should be investigated for longer forecasting horizons.
- Other models, such as CNN and GRU, should developed and compared to the LSTM-RNN for a more holistic approach to the feasibility of the model.

- The solution can be expanded to Mine A's cooling system, possibly yielding more electricity savings.
- Optimisation algorithms can be implemented during warmer temperatures, which are mainly observed during the summer periods. This leads to developing alternative energy savings strategies such as load shifting.
- Further validation can be achieved through an actual implementation using a test. Although a winter control strategy has been implemented, assessing the strategy during summer periods is important.

The potential of improving the control solution may be realised by addressing these shortcomings. However, a successful development of a solution was observed, thus indicating the viability of using AI temperature forecasting on a case study mine to achieve electricity cost savings.

As discussed in Section 1.2.2, energy reduction strategies are imperative to reduce gold mining industry costs. Therefore, the developed solution is an energy reduction strategy, indicating the potential to reduce gold mining costs. The literature summary in Section 1.5.1 shows a lack of AI-based forecasting techniques in the gold mining industry. The feasibility of applying such techniques was proved through this study. Harmse [8] used a mathematical model to characterise refrigeration plants and an AI optimisation algorithm to optimise the operations of said plants. The study suggested using ANNs for improved accuracy in characterising the plants and incorporating additional parameters with minimal effort.

This study indicated the feasibility of using an LSTM-RNN, a type of ANN, as part of the energy reduction strategy on a section of the refrigeration system in a deep-level mine. This indicates the relevance of this study to deep-level mine cooling systems.

3.5. Conclusion

The results of the methodology from Chapter 2 were explored in this chapter. The chosen case study mine was a deep-level gold mine with a complex and integrated cooling system. The study only focused on a section of the cooling system: the surface BAC plants and fans.

The background of the case study cooling system and parameter identification was discussed in Section 3.1. The parameters were identified using the mine's SCADA system and compared to the parameter requirements used for a traditional simulation method, which addressed research objective 1.

After identifying the parameters, the next step was to develop LSTM-RNN temperature forecasting models. The models were developed to forecast the surface and underground wet bulb and dry bulb temperatures. This was done using the steps detailed in Section 0. The data for each parameter was extracted from the case study mine's historian database. The was cleaned by removing outliers and applying the KNN imputation technique to replace missing data points. Only seven of the parameters were selected for further processing for the models. The additional parameters were not required to improve the accuracy of the models; thus, they were discarded. The data was further processed using the sliding window implementation, data partitioning and scaling methods as discussed in Section 3.2.5.

Hyperparameters were determined based on literature and altered using a random search algorithm. The concluding hyperparameters were detailed in Section 3.2.6. Once the model's architecture was determined, and the training commenced, the model's performance was monitored iteratively, indicating improvement in the MSE error after each epoch. The model performance on the training set and set were then evaluated using the CV(RMSE), RMSE, and MAPE metrics. The models yielded lower values for the validation sets when compared to the training sets. This indicated that the models tended to perform well on unseen data. The performance of the model was validated using the test sets. These sets were not involved in the training phase of the model.

Models D and E achieved CV(RMSE) values below the 5% threshold, and models C, D and E achieved MAPE values below the 10% threshold for all forecasted temperatures. Thus, models C, D and E were deemed accurate. Model A (1-day forecasts) yielded the worst metrics performance. Table 9 indicates the CV(RMSE) values, and Table 10 shows the MAPE values.

Table 9: CV(RMSE) values for model A

Parameter	CV(RMSE) (%)
Surface air wet bulb temperature	8.15
Surface air dry bulb temperature	11.06
7 level air wet bulb temperature	3.79
7 level air dry bulb temperature	5.78

Table 10: MAPE values for model A

Parameter	MAPE (%)
Surface air wet bulb temperature	13.28
Surface air dry bulb temperature	11.43
7 level air wet bulb temperature	2.33
7 level air dry bulb temperature	3.37

Model E yielded the best performance for all performance metrics. The CV(RMSE) and the MAPE values are detailed in Table 11 and Table 12.

Table 11: CV(RMSE) values for model E

Parameter	CV(RMSE) (%)
Surface air wet bulb temperature	1.66
Surface air dry bulb temperature	2.78
7 level air wet bulb temperature	1.55
7 level air dry bulb temperature	1.68

Table 12: MAPE values for model E

Parameter	MAPE (%)
Surface air wet bulb temperature	2.29
Surface air dry bulb temperature	2.46
7 level air wet bulb temperature	1.01
7 level air dry bulb temperature	0.95

These results indicate the feasibility of using LSTM-RNN models for air temperature forecasting in the deep-level mining industry, thus verifying research objective 2.

After determining the verified accurate models, these models were applied to develop a dynamic control solution. The developed solution consisted of three specifications: daily data acquisition, real-time AI-based temperature forecasting, and the suggested

dynamic control strategy discussed in Section 3.3. Control solutions were developed for models C, D, and E.

Specification 1 was addressed in Section 3.3.2, which involved the data acquisition procedure. Section 3.3.3 details the real-time AI-based temperature forecasting models for each accurate model. The models that achieved MAPE values are observed in Table 13

Table 13: MAPE values for real-time forecasting

Model	**Parameter**	**MAPE (%)**
C	Surface air wet bulb temperature	7.72
	7 level air wet bulb temperature	2.32
D	Surface air wet bulb temperature	6.11
	7 level air wet bulb temperature	2.48
E	Surface air wet bulb temperature	4.90
	7 level air wet bulb temperature	2.14

The dynamic control strategy was developed using the real-time forecasting models from Specification 2 to determine when the surface BAC plants and fans are operational. The summer operating strategy led to a potential electricity cost savings of ZAR 0.5 million per annum, and the winter operating strategy led to a potential savings of ZAR 0.8 million per annum. This equated to a total savings of ZAR 1.3 million per annum. The developed strategies and the potential electricity cost savings verified that research objectives 3 and 4 were addressed.

This chapter confirmed the achievement of all research objectives. Moreover, the discussion of results indicates that the need for the study was addressed. Furthermore, the shortcomings indicating possible improvements were indicated.

Chapter 4: Conclusion

“Though the road's been rocky, it sure feels good to me.”

— Bob Marley

4. CONCLUSION

4.1. Summary

Electricity costs in South African deep-level mines are one of the challenges to overcome to remain profitable. As discussed in Chapter 1, mining cooling systems account for approximately 28% of a deep-level mine's energy consumption due to their complexity.

Literature has shown that control strategies have been developed to enhance the efficiency of these systems, leading to electricity cost savings. However, additional electricity cost savings are missed since the proposed strategies are often static, and the parameters used are dynamic. The use of AI allows the opportunity to control these systems dynamically.

Against this backdrop, a need for the study was identified.

AI-inspired temperature forecasting is needed to develop a dynamic control solution for deep-level mine cooling systems.

The following objectives were developed to address the problem and address limitations:

- **Research objective 1**: Identify the parameters of the system that are closely related to the surface BACs.
- **Research objective 2:** Determine, develop, and evaluate an appropriate temperature forecasting model.
- **Research objective 3:** Develop a dynamic control solution for the surface BAC cooling plants and the BAC.
- **Research objective 4:** Validate the control solution which addresses the research problem.

This study followed the case study research methodology to fulfil objectives. The methodology starts with the problem identification and a literature review, which was discussed in Chapter 1.

This chapter observed the energy reduction strategies implemented in the mining industry. Moreover, a review of relevant AI-inspired temperature forecasting technologies was provided. This formed the basis for the need for the study.

A method was developed to address the research objectives discussed in the case study methodology. This method included identifying system parameters, model development, and developing a dynamic control solution.

According to the existing literature, the LSTM-RNN model is the most popular algorithm. Thus, this model was selected to forecast the case study mine's temperatures. However, some literature indicates that the CNN and GRU models can be used for temperature forecasting.

The model development procedure included data cleaning, feature selection, further data pre-processing, and hyperparameter selection, which formed the basis of the procedure. Five models were developed with different forecasting horizons; model A had the largest forecasting horizon with 1 day, and model E had the smallest horizon with 30 minutes. The models were then evaluated with the test dataset, which was not involved during the training phase, to identify which models were accurate for the dynamic control solution. Model C (two-hour forecasts), model D (one-hour forecasts), and model E (30-minute forecasts) were deemed as accurate, yielding CV(RMSE) values below the 5% threshold and MAPE values below the 10% threshold.

The dynamic control solution was developed using accurate models. The models were forecasted in real-time, yielding MAPE values of 4.90% for the surface air wet bulb temperatures and 2.14% for the underground wet bulb temperatures. The real-time forecasts were used to identify the control suggestion for the surface BAC plants and fans. The control suggestions yielded different solutions for the summer and winter periods—a potential annual electricity cost reduction of ZAR 1.5 million.

4.2. Recommendations for future work

The following remarks and recommendations were made based on the results observed for the case study. These recommendations were based on the shortcomings observed in Section 3.4.3:

- This study involved underground air temperatures as model parameters for one level of the case study mine. Additional weather stations are recommended to be installed on all working levels. Moreover, the stations should be installed where the surface BAC plants and fans impact the underground areas most. This isolates the underground conditions' dependency on the surface BAC plants and fans.
- A more sophisticated approach to removing outliers should be applied in a data cleaning procedure, such as implementing clustering algorithms to detect outliers.
- A comparison of different imputation techniques can be implemented and assessed to determine the most appropriate imputation technique for the data cleaning procedure.
- Alternative models should be implemented to improve the performance of models with longer forecasting horizons.
- A feasibility study is recommended to compare GRU and CNN to the LSTM-RNN model to determine the holistic feasibility of using AI-based temperature forecasting in the mining industry.
- It is recommended that the forecasting horizon should be decreased to implement a real-time control strategy of the surface BAC plants and fans. This will be suitable if the case study mine implements automated control strategies using VSDs and automated valves.
- The proposed can be implemented as part of a holistic control strategy for the entire cooling system.

5. LIST OF REFERENCES

[1] United States Bureau of Mines: A Dictionary of Mining, Mineral, and Related Terms, Illinois: U.S. Bureau of Mines, 1968.

[2] D. S. Brose and M. H. Wolpoff, “Early upper Paleolithic man and late middle Paleolithic tools,” *American Anthropologist ,* vol. 73.5, pp. 1156-1194, 1971.

[3] R. Pickering, “Deep level mining and role of R & D,” *The Journal of The South African Institute of Mining and Metallurgy,* pp. 173-176, 1996.

[4] T. S. Moropa, “Cost and energy savings on mine surface cooling systems,” M.Eng Dissertation, North West University, Potchefstroom, 2016.

[5] J. Buys , “Optimising Refrigeration and Cooling Systems of a Platinum Mine,” M.Eng Dissertation, North-West University, Potchefstroom, 2014.

[6] H. J. van Staden, J. F. van Rensburg and H. J. Groenwald, “Optimal use of mobile cooling units in a deep-level gold mine,” *International Journal of Mining Science and Technology,* no. 4, pp. 547-553, 2020.

[7] “Department of Mineral Resources and Energy: South African Energy Price Report,” 2021.

[8] M. D. Harmse, “Optimising mining refrigeration systems through artificial intelligence,” M.Eng Dissertation, North-West University, Potchefstroom, 2021.

[9] S. Cabaneros, J. Calautit and B. Hughes, “A review of artificial neural network models for ambient air pollution prediction,” *Environmental Modelling & Software,* vol. 119, pp. 285-304, 2019.

[10] K. B. Sesele, “Women and Mining Decline in the Free State Goldfields,” PhD Thesis, University of the Free State, Bloemfontein, 2020.

[11] “Statistics South Africa: Mining; Production and sales, May 2023,” 13 July 2023. [Online]. Available: https://www.statssa.gov.za/?page_id=1854&PPN=P2041. [Accessed 19 July 2023].

[12] “Department of Mineral Resources and Energy: Exploration Strategy of South Africa: Exploration Strategy for the Mining Industry of South Africa,” 14 April 2022. [Online]. Available: https://www.gov.za/sites/default/files/gcis_document/202204/46246gon2026.pdf. [Accessed 5 June 2022].

[13] T. Khubana, C. Rootman and E. E. Smith, “Antecedents of Shared Value: Perceptions within the South African mining industry,” *Journal of Contemporary Management,* vol. 19, no. 1, pp. 132-167, 2022.

[14] “Department of Mineral Resources and Energy: New Technological Applications in Deep-level Gold Mining,” 2013. [Online]. Available: https://www.dmr.gov.za/LinkClick.aspx?fileticket=CIEuCiHYXIA%3D&portalid=0. [Accessed 11 November 2023].

[15] P. Mare, “Novel simulations for energy management of mine cooling systems,” PhD Thesis, North-West University, Potchefstroom, 2017.

[16] Eskom, “Tarriff History,” 2023. [Online]. Available: https://www.eskom.co.za/distribution/tariffs-and-charges/tariff-history/. [Accessed 24 July 2023].

[17] B. B. Ateba, J. J. Prinsloo and R. Gawlik, “The significance of electrical supply sustainability to industrial growth in South Africa,” *Energy Reports,* vol. 5, pp. 1324-1338, 2019.

[18] W. G. Shaw and M. M. J. Mathew, “Holistic analysis of the effect on electricity cost in South Africa's platinum mines when varying shift schedules according to time-of-use shifts,” *Journal of Energy in Southern Africa,* vol. 30, no. 4, pp. 26-40, 2019.

[19] R. P. Mulder, “Improving air distribution in deep-level mine ventilation systems,” M.Eng Dissertation, North-West University, Potchefstroom, 2020.

[20] J. A. Crawford, H. P. R. Joubert, M. J. Mathews and M. Kleingeld, “Optimised dynamic control philosophy for improved performance of mine cooling systems,” *Applied Thermal Engineering,* vol. 150, pp. 50-60, 2019.

[21] “ MHSA of South Africa: Mine Health and Safety Act 29 of 1996 and Regulations,” 2018.

[22] T. Matepa and S. M. Rupprecht, “Study of ventilation and cooling in gold mines in South Africa as a means to improve safety and productivity,” in *IMCET 2019–Proceedings of the 26th International Mining Congress and Exhibition of Turkey*, 2019.

[23] S. M. Sithole, “Optimal mine water management to improve ambient conditions,” M.Eng Dissertation, North-West University, Potchefstroom , 2021.

[24] A. Martinez, D. Astrain, P. Rodriguez and P. Aranguren, “Advanced computational model for Peltier effect based refrigerators,” *Applied Thermal Engineering,* vol. 95, pp. 339-347, 2016.

[25] A. Aliane, S. Abboudi, S. C and G. B, “An illustrated review on solar absorption cooling experimental studies,” *Renewable and Sustainable Energy Reviews,* vol. 65, pp. 443-458, 2016.

[26] S. S. Alrwashdeh and H. Ammari, “Life cycle cost analysis of two different refrigeration systems powered by solar energy,” *Case Studies in Thermal Engineering,* vol. 16, pp. 1-11, 2019.

[27] L. Zietsman, “Identification model for cost-effective electricity savings on a mine cooling system,” M.Eng disseration, North-West University, Potchefstroom, 2018.

[28] B. Pascoe, “Improved control processes to sustain electricity cost savings on a mine water reticulation system,” PhD Thesis, North-West University, Potchefstroom, 2018.

[29] J. Vermuelen, “Cost effective management strategies for platinum mine cooling systems,” M.Eng Dissertation, North-West University, Potchefstroom , 2015.

[30] J. Badenhorst, “Utilising mine-cooling auxiliaries for optimal performance during seasonal changes,” M.Eng Dissertation, North-West University, Potchefstroom , 2022.

[31] A. J. Schutte, “An integrated energy efficiency strategy for deep mine ventilation and refrigeration,” PhD Thesis, North-West University, Potchefstroom , 2014.

[32] D. Upadhyay and S. Sampali, “SCADA (Supervisory Control and Data Acquisition) systems: Vulneralbility assessment and security recommendations,” *Computers and Security,* vol. 89, p. 101666, 2019.

[33] D. Pliatsios, P. Sarigiannidis, T. Lagkas and A. G. Sarigiannidis, “A survey on SCADA systems: secure protocols, incidents, threats and tactics,” *IEEE Communications Surveys & Tutorials,* vol. 22, no. 3, pp. 1942-1976, 2020.

[34] G. J. Mathee, “Improved control of compressed air networks using machine learning,” M.Eng Dissertation, North-West University, Potchefstroom , 2021.

[35] P. F. H. Peach, J. I. G. Bredenkamp and v. R, “Dynamic Optimisation of Deep-level Mine Refrigeration Control,” *South African Journal of Industrial Engineering,* vol. 29, no. 3, pp. 202-216, 2019.

[36] Y. Kim, J. Lee and S. Jeon, “12 - Hybrid ground-source heat pump systems,” *Advances in Ground-Source Heat Pump Systems,* pp. 331-357, 2016.

[37] Woolf, Chemical Process Dynamics and Controls, Michigan: University of Michigan Engineering Controls Group, 2009.

[38] J. Hahn and T. Edgar, Process Control: Kirk-Othmer Encyclopedia of Chemical Technology, Austin , 2003.

[39] R. C. Ilambirai, P. Sivasankari, S. Padmini and H. Chowdary, “Efficient Self-Learning Artificial Neural Network Controller for Critical Heating, Ventilation and Air Conditioning Systems,” in *AIP Conference Proceedings*, 2019.

[40] P. Albertos and A. O. M. Sala, “Fuzzy Logic Controllers. Methodology, Advantages and Drawbacks,” in *VIII international congress of automatic control*, Laxenburg, 1998.

[41] J. Lodewyk, “Holistic evaluation of surface cooling plant configurations for different seasons at deep mines,” M.Eng Dissertation, North-West University, Potchefstroom, 2022.

[42] Eskom, “Tariffs and charges,” 2023. [Online]. Available: https://www.eskom.co.za/distribution/tariffs-and-charges/. [Accessed 2 August 2023].

[43] W. Wang and K. Siau, “ Artificial intelligence, machine learning, automation, robotics, future of work and future of humanity: A review and research agenda,” *Journal of Database Management (JDM),* vol. 30, no. 1, pp. 61-79, 2019.

[44] P. M. Kraft, M. Young, M. Katell and B. G. Huang, “Defining AI in Policy versus Practice,” in *AIES '20: Proceedings of the AAAI/ACM Conference on AI, Ethics, and Society*, 2020.

[45] J. Bughin, E. Hazan, S. Ramaswamy, M. Chui, T. Allas, P. Dahlstrom, N. Henke and M. Trench, “Artificial intelligence: the next digital frontier?,” McKinsey Global Institute, 2017.

[46] K. K. Ng, C.-H. Chen, C. K. M. Lee, J. Jiao and Z.-X. Yang, “A systematic literature review on intelligent automation: Aligning concepts from theory, practice, and future perspectives,” *Advanced Engineering Informatics,* vol. 47, p. 101246, 2021.

[47] S. Robertson, H. Azizpour, K. Smith and J. Hartman, “Digital image analysis in breast pathology - from image processing techniques to artificial intelligence,” *The Journal of Laboratory and Clinical Medicine,* vol. 194, pp. 19-35, 2018.

[48] K. P. Smith and J. E. Kirby, “Image analysis and artificial intelligence in infectious disease diagnostics,” *Clinical Microbiology and Infection,* vol. 26, no. 10, pp. 1318-1323, 2020.

[49] I. Schuin, “Evaluating different statistical regression models for industrial energy measurement and verification,” M.Eng Dissertation, North-West University, Potchefstroom , 2019.

[50] H. Ouanan, “Image processing and machine learning applications in mining industry: Mine 4.0,” in *In 2019 International Conference on Intelligent Systems and Advanced Computing Sciences (ISACS)*, 2019.

[51] H. Nguyen, “Application of the k - nearest neighbors algorithm for predicting blast - induced ground vibration in open - pit coal mines: a case study,” *Journal of Mining and Earth Sciences,* vol. 61, no. 6, pp. 22-29, 2020.

[52] Z. Hyder, K. Siau and F. Nah, “Artificial intelligence, machine learning, and autonomous technologies in mining industry,” *Journal of Database Management (JDM),* vol. 30, no. 2, pp. 67-79, 2019.

[53] C. Ntakolia, A. Anagnostis, S. Moustakidis and N. Karcanias, “Machine learning applied on the district heating and cooling sector: a review,” *Energy Systems,* pp. 1-30, 2021.

[54] T. Mitchell, Machine learning, McGraw Hill , 1997.

[55] A. Géron, Hands-on Machine Learning with Scikit-Learn, Keras, and TensorFlow, Sebastopol: O’Reilly Media, 2019.

[56] I. H. Sarker, “Machine Learning: Algorithms, Real-World Applications and Research Directions,” *SN Computer Science ,* vol. 160, pp. 2-21, 2021.

[57] M. A. Alsheikh, L. Shaowei, D. Niyato and H.-P. Tan, “Machine learning in Wireless Sensor Networks: Algorithms, Strategies, and Applications,” *IEEE Communications Surveys & Tutorials,* vol. 16, no. 4, pp. 1996-2018, 2014.

[58] J. Moolayi, Learn Keras for Deep Neural Networks, Vancouver: Apress, 2019.

[59] J. Li, A. S. Sun, J. Han and C. Li, “A Survey on Deep Learning for Named Entity Recognition,” *IEEE Transactions on Knowledge and Data Engineering,* vol. 34, no. 1, pp. 50-70, 2020.

[60] K. Yetilmezsoy, B. Ozkaya and M. Cakmakci, “Artificial intelligence-based prediction models for environmental engineering,” *Neural Network World,* vol. 21, no. 3, pp. 193-218, 2011.

[61] X. Godinho, H. Bernardo, F. T. Oliveira and J. C. Sousa, “Forecasting Heating and Cooling Energy Demand in an Office Building using Machine Learning

Methods," in *2020 International Young Engineers Forum (YEF-ECE). IEEE*, 2020.

[62] T. T, S. Bateni, S. Ki and H. Vosoughifar, "A Review of Neural Networks for Air Temperature Forecasting," *Water 2021,* vol. 13, no. 9, pp. 1294-1309, 2021.

[63] A. D. Jagtap, Y. Shin, K. Kawaguchi and E. Karniadakis, "Deep Kronecker neural networks: A general framework for neural networks with adaptive activation functions," *Neurocomputing ,* vol. 468, pp. 165-180, 2022.

[64] R. Saleem, B. Yuan, F. Kurugollu, A. Anjum and L. Liu, "Explaining deep neural networks: A survey on the global interpretation methods," *Neurocomputing,* vol. 513, pp. 165-180, 2022.

[65] P. Chen, N. Aichen, L. Duanyang, W. Jiang and B. Ma, "Time Series Forecasting of Temperatures using SARIMA: An Example from Nanjing," *IOP Conference Series: Materials Science and Engineering,* vol. 394, no. 5, p. 052024, 2018.

[66] P. Yamak, L. Yujian and P. K. Gadosey, "A Comparison between ARIMA, LSTM, and GRU for Time Series Forecasting," in *Proceedings of the 2019 2nd International Conference on Algorithms, Computing and Artificial Intelligence*, Sanya, 2019.

[67] R. Shumway and D. Stoffer, Time Series Analysis and Its Application with R Examples, New York: Springer, 2011.

[68] E. Isufi, A. Loukas, N. Perraudin and G. Leus, "Forecasting time series with varma recursions on graphs," *IEEE Transactions on Signal Processing,* vol. 67, no. 18, pp. 4870-4885, 2019.

[69] B. Lim and Z. S. Zohren, “Time Series Forecasting With Deep Learning: A Survey,” *Philosophical Transactions of the Royal Society ,* vol. 379, no. 2194, p. 20200209, 2021.

[70] G. E. P. Box, G. M. Jenkins, G. C. Reinsel and G. M. Ljung, Time Series Analysis: Forecasting and Control, Wiley, 2015.

[71] A. Alsharef, K. Aggarwal, M. Kumar and A. Mishra, “Review of ML and AutoML Solutions to Forecast Time-Series Data,” *Archives of Computational Methods in Engineering,* pp. 1-15, 2022.

[72] R. J. Hyndman, International Encyclopedia of Statistical Science: Moving Averages, Springer, 2010.

[73] Z. Zhang and J. C. Moore, “Chpater 8 - Autoregressive Moving Average Models,” in *Mathematical and Physical Fundamentals of Climate Change*, Beijing, Elsevier, 2015, pp. 239-290.

[74] C. S. Fiskin, O. Turgut, S. Westgaard and A. Cerit, “Time series forecasting of domestic shipping market: comparison of SARIMAX, ANN-based models and SARIMAX-ANN hybrid model,” *International Journal of Shipping and Transport Logistics,* vol. 14, no. 3, pp. 193-221, 2022.

[75] I. Aijaz and P. Agarwal, “A study on time series forecasting using hybridization of time series models and neural networks,” *Recent Advances in Computer Science and Communications (Formerly: Recent Patents on Computer Science),* vol. 13, no. 5, pp. 827-832, 2020.

[76] R. Madan and P. S. Mangipudi, “Predicting computer network traffic: a time series forecasting approach using DWT, ARIMA and RNN,” in *2018 Eleventh International Conference on Contemporary Computing*, 2018.

[77] X. Zhang, Y. Liu, M. Yang, T. Zhang, A. A. Young and L. Xiaosong, “Comparative Study of Four Time Series Methods in Forecasting Typhoid Fever Incidence in China,” *Plos one (Public Library of Science),* vol. 8, no. 5, 2013.

[78] J. Brownlee, Deep learning for time series forecasting: predict the future with MLPs, CNNs and LSTMs in Python. Machine Learning Mastery, 2018.

[79] B. Beebe, J. Jaffe, B. Karen, H. Chen, P. Cohen, S. Blatt, T. Kaminer and S. Feldstien, “Six-Week Postpartum Maternal Self-Criticism and Dependency and 4-Month Mother–Infant Self- and Interactive Contingencies,” *Developmental Psychology,* vol. 43, no. 6, pp. 1360-1376, 2007.

[80] X. Ying, “An Overview of Overfitting and its Solutions,” *Journal of physics: Conference series,* vol. 1168, no. 2, 2019.

[81] Z. Che, S. Purushotham, K. Cho, D. Sontag and Y. Liu, “Recurrent Neural Networks for Multivariate Time Series with Missing Values,” in *International conference on machine learning and data mining*, Berlin, 2017.

[82] D. Faustryjak, L. Jackowska-Strumiłło and M. Majchrowicz, “Forward forecast of stock prices using LSTM neural networks with statistical analysis of published messages,” in *2018 International Interdisciplinary PhD Workshop (IIPhDW)*, Świnoujście, 2018.

[83] R. J. Hyndman and G. Athanasopoulos, Forecasting: principles and practice, OTexts, 2018.

[84] M. Afzali, A. Afzali and G. Zahdei, “Ambient Air Temperature Forecasting Using Artificial Neural Network Approach,” in *International Conference on Environmental and Computer Science*, Singapore, 2011.

[85] P. Hietaharju, M. Ruusunen and K. Leiviskä, “A Dynamic Model for Indoor Temperature Prediction in Buildings,” *Energies,* vol. 13, no. 12, 2018.

[86] A. Aliberti, L. Bottaccioli, E. Macci, S. Di Cataldo, A. Acquaviva and E. Patti, “A Non-Linear Autoregressive Model for Indoor Air-Temperature Predictions in Smart Buildings,” *Electronics,* vol. 8, no. 9, pp. 979-996, 2019.

[87] F. Elmaz, R. Eyckerman, W. Casteels, S. Latré and P. Hellinckx, “CNN-LSTM architecture for predictive indoor temperature modeling,” *The International Journal of Building Science and its Applications,* vol. 206, 2021.

[88] F. Mtibaa, K.-K. Nguyen, M. Azam, A. Papachristou, J.-S. Venne and M. Cheriet, “LSTM-based indoor air temperature prediction framework for HVAC systems in smart buildings,” *Neural Computing and Applications,* vol. 32, pp. 17569-17585, 2020.

[89] A. Bellagarda, S. Cesari, A. Aliberti, F. Ugliotti, L. Bottaccioli, E. Macii and E. Patti, “Effectiveness of neural networks and transfer learning for indoor air-temperature forecasting,” *Automation in Construction,* vol. 140, 2022.

[90] S. Teegavarapu and J. D. Summers, “Case Study for Research Design,” in *ASME 2008 International Design Engineering Technical Conferences and Computers and Information in Engineering Conference and Computers and Information in Engineering Conference*, New York , 2008.

[91] A. M. Holman, G. P. Heyns and R. Pelzer, “Benefits of improved performance monitoring of mine cooling systems,” in *2014 International Conference on the Eleventh industrial and Commercial Use of Energy*, 2014.

[92] D. Nell, “Optimising production through improving the efficiency of mine compressed air networks with limited infrastructure,” M.Eng dissertation, North-West University, Potchefstroom , 2017.

[93] D. Adhikari, W. Jiang, J. Zhan and Z. He, “A Comprehensive Survey on Imputation of Missing Data in Internet of Things,” *ACM Computing Surveys,* vol. 55, no. 7, pp. 1-38, 2022.

[94] C. Velasco-Gallego and I. Lazakis, “Real-time data-driven missing data imputation for short-term sensor data of marine systems. A comparative study.,” *Ocean Engineering,* vol. 218, pp. 108261-108308, 2020.

[95] T. Emmanuel, T. Maupong, D. Mpoeleng, T. Semong, B. Mphago and O. Tabona, “A survey on missing data in machine learning,” *Journal of Big Data,* vol. 8, no. 1, pp. 1-37, 2021.

[96] P. D. Allison, “Multiple imputation for missing data: A cautionary tale,” *Sociological methods & research,* vol. 28, no. 3, pp. 301-309, 2000.

[97] A. Chong, K. P. Lam and W. K. O. T. M. Y. Xu, “Imputation of missing values in building sensor data,” *ASHRAE and IBPSA-USA SimBuild 6,* pp. 407-414, 2016.

[98] B. VanBerlo, D. Wu, B. Li, M. A. Rahman, G. Hogg, B. VanBerlo, J. Tschirhart, A. Ford, J. Ho, J. McCauley, B. Wu, J. Deglint, J. Hargun, R. Chaudhary, C. Dave and R. Arntinfield, “Accurate assessment of the lung sliding artefact on lung ultrasonography using a deep learning approach,” *Computers in Biology and Medicine,* vol. 148, p. 105953, 2022.

[99] A. Zheng and A. Casari, Feature Engineering for Machine Learning: Principles and Techniques for Data Scientists, Sebastopol: O'Reilly, 2018.

[100] M. Amirabadi, M. Kahaei and S. Nezamalhosseini, “Novel suboptimal approaches for hyperparameter tuning of deep neural network [under the shelf of optical communication],” *Physical Communication,* vol. 41, 2020.

[101] S. Boutkif, A. Fiaz, A. Ouni and M. A. Serhani, “Optimal Deep Learning LSTM Model for Electric Load Forecasting using Feature Selection and Genetic Algorithm: Comparison Learning Approaches,” *Energies,* vol. 11, no. 7, p. 1636, 2018.

[102] S.-A. N. Alexandropoulos, S. B. Kotsiantis and M. B. Vrahatis, “Data preprocessing in predictive data mining,” *The Knowledge Engineering Review,* vol. 34, pp. 1-33, 2019.

[103] J. Wang, W. Jiang, Z. Li and W. Lu, “A new multi-scale sliding window LSTM framework (MSSW-LSTM): a case study for GNSS time-series prediction,” *Remote Sensing,* vol. 13, pp. 3328-3343, 2021.

[104] T. G. Dietterich, “Machine learning for sequential data: A review,” in *Structural, Syntactic, and Statistical Pattern Recognition: Joint IAPR International Workshops SSPR 2002 and SPR 2002 Windsor, Ontario, Canada, August 6–9, 2002 Proceedings*, Ontario, 2002.

[105] V. R. Joseph, “Optimal ratio for data splitting,” *Statistical Analysis and Data Mining: The ASA Data Science Journal,* vol. 15, no. 4, pp. 531-538, 2022.

[106] T. Hastie and R. F. J. Tibshirani, The Elements of Statistical Learning, Springer, 2009.

[107] “ASHRAE Guideline: Measurement of energy, demand, and water savings: ASHRAE Guideline 14,” 2014.

6. APPENDICES

Appendix A: Additional Results

A1: Training and Validation Loss During Model Training

Model training was done in five models, respectively, as discussed in Section 3.2.6. The training loss for model A was observed. The training loss for the other four models is in Figure 75.

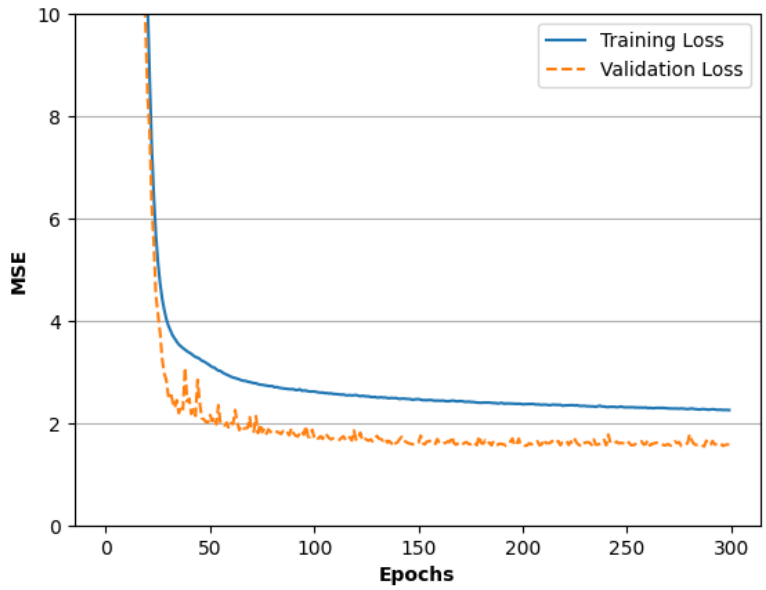

Figure 75: Model B mean square error during the training phase.

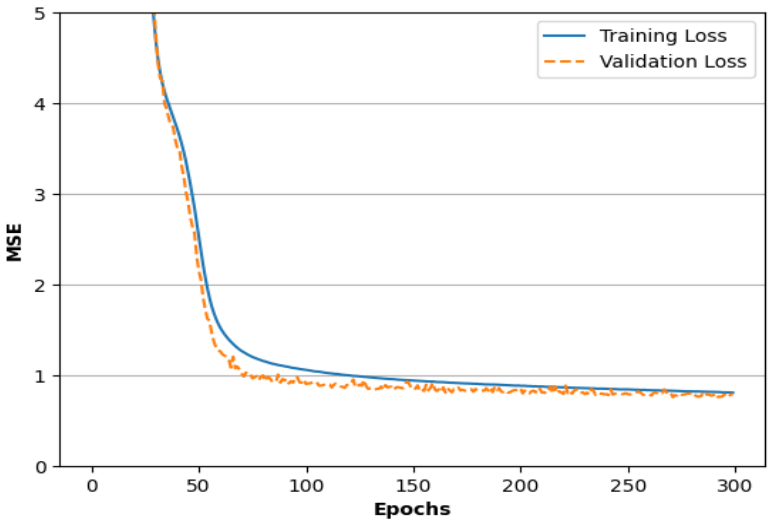

Figure 76: Model C mean square error during the training phase.

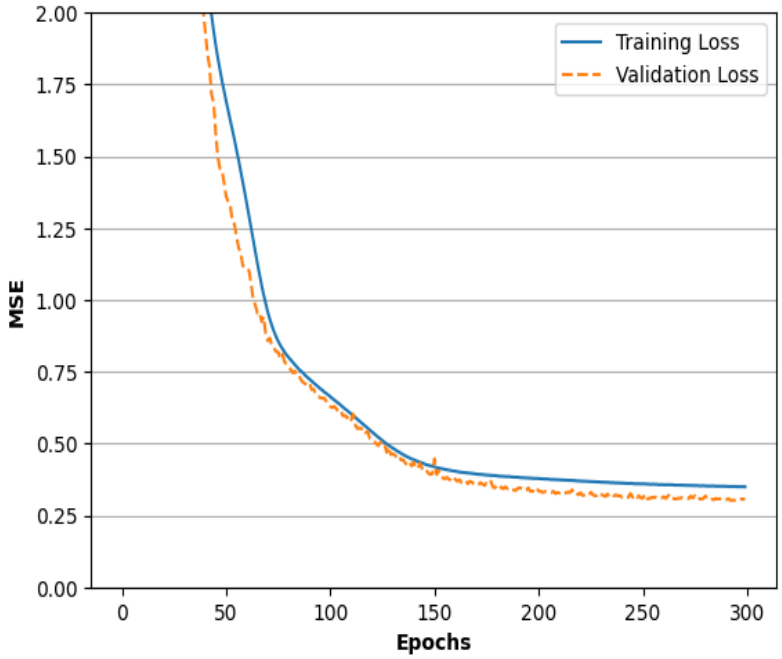

Figure 77: Model D mean square error during the training phase.

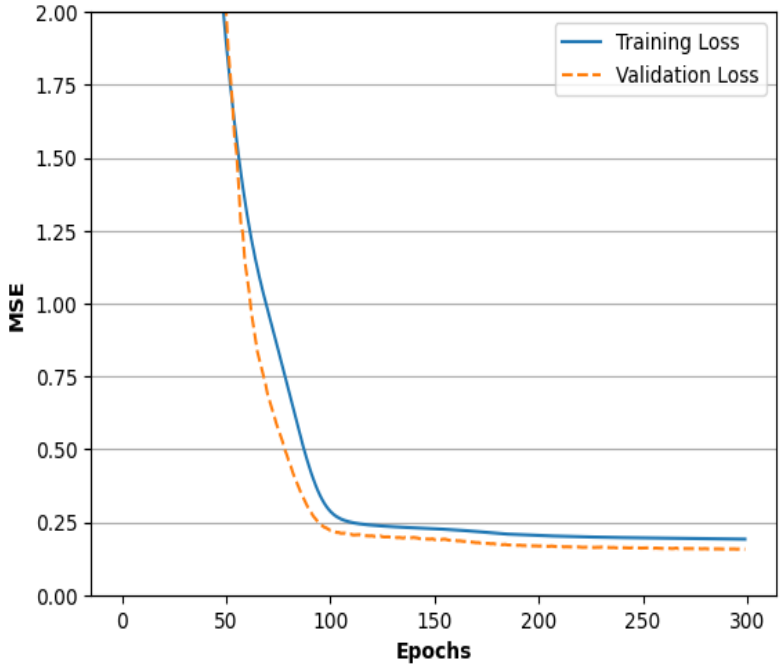

Figure 78: Model E mean square error during the training phase.

A2: Actual vs Forecasted Temperatures

This section shows the additional comparisons of the temperatures based on the evaluation metrics detailed in Figure 54 and Figure 55.

Surface air dry bulb temperatures

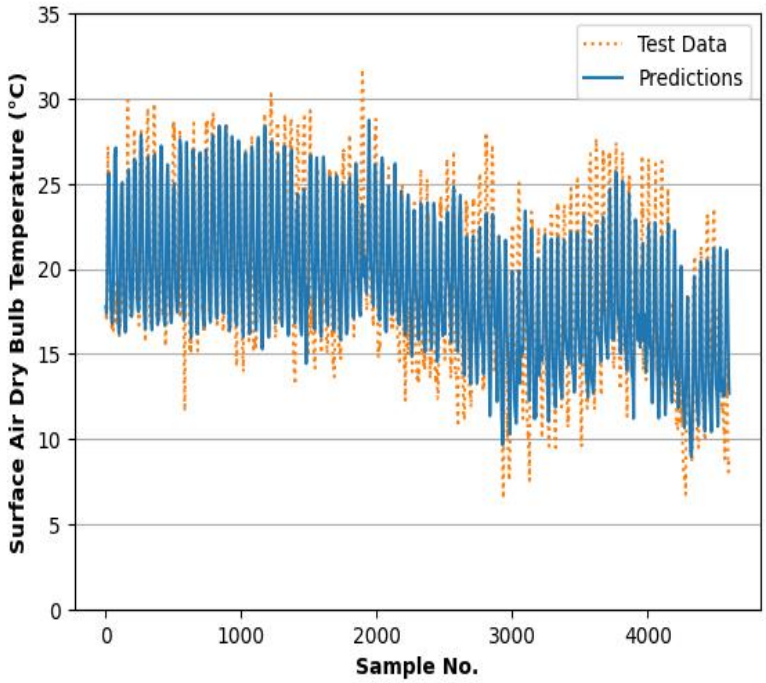

Figure 79: Model A surface air dry bulb temperature predictions on test set.

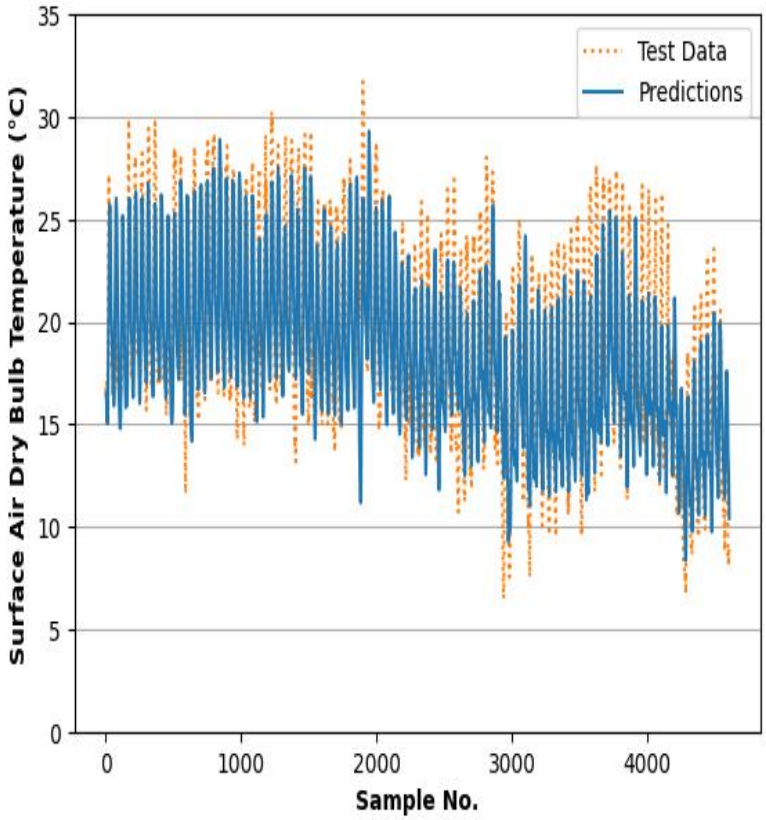

Figure 80:Model B surface air dry bulb temperature predictions on test set.

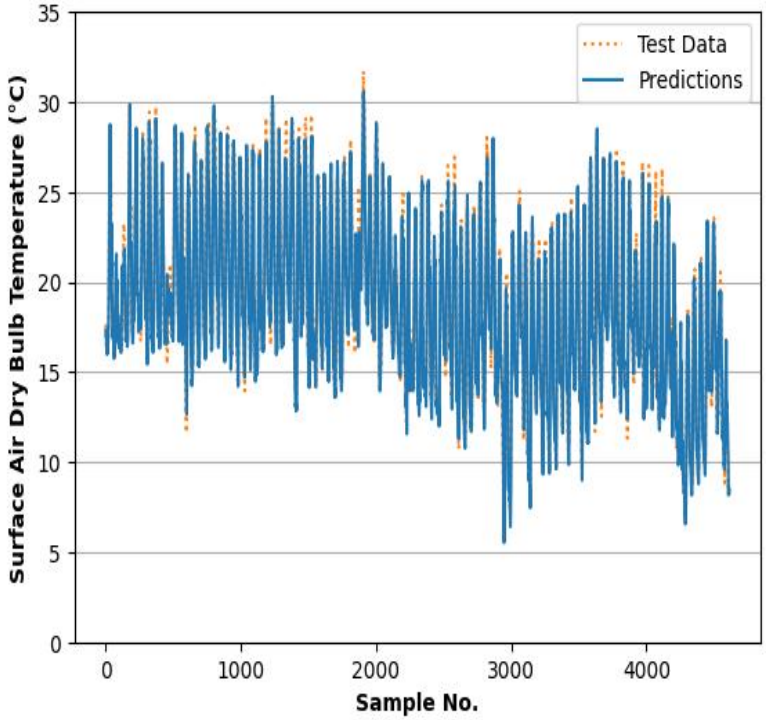

Figure 81: Model C surface air dry bulb temperature predictions on test set.

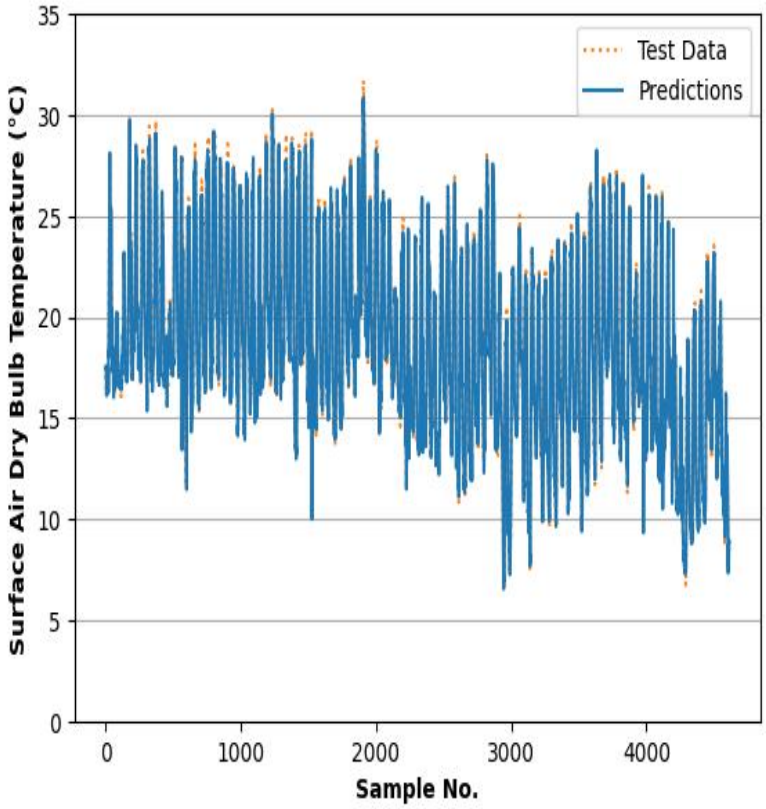

Figure 82: Model D surface air dry bulb temperature predictions on test set.

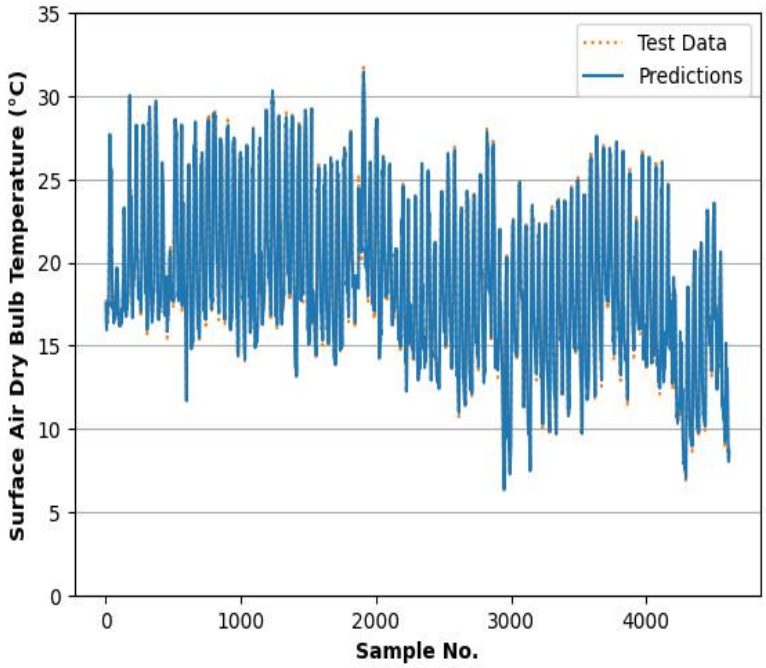

Figure 83: Model E surface air dry bulb temperature predictions on test set.

Surface air wet bulb temperatures

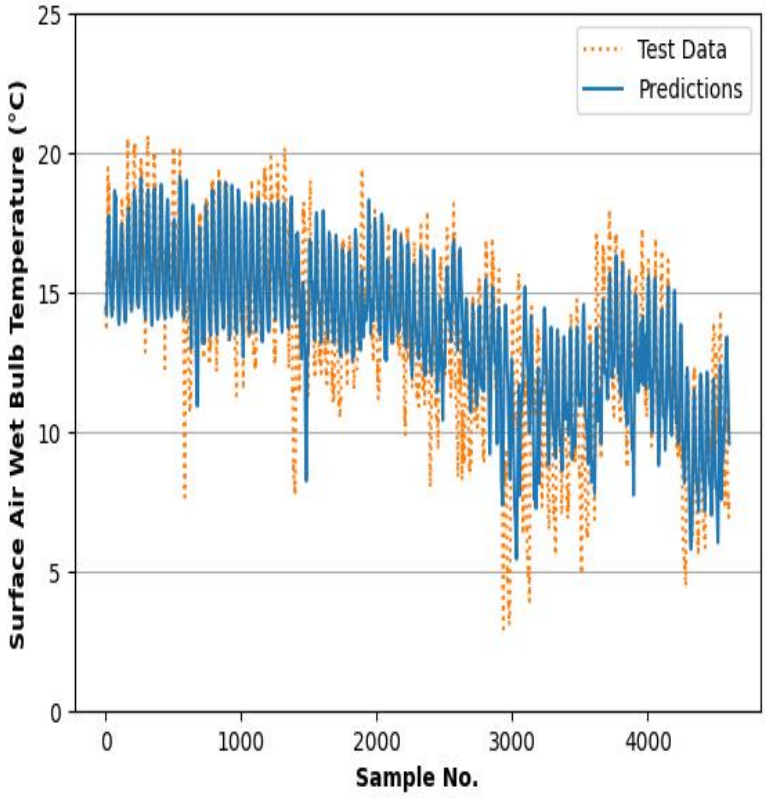

Figure 84: Model A surface air wet bulb temperature predictions on test set.

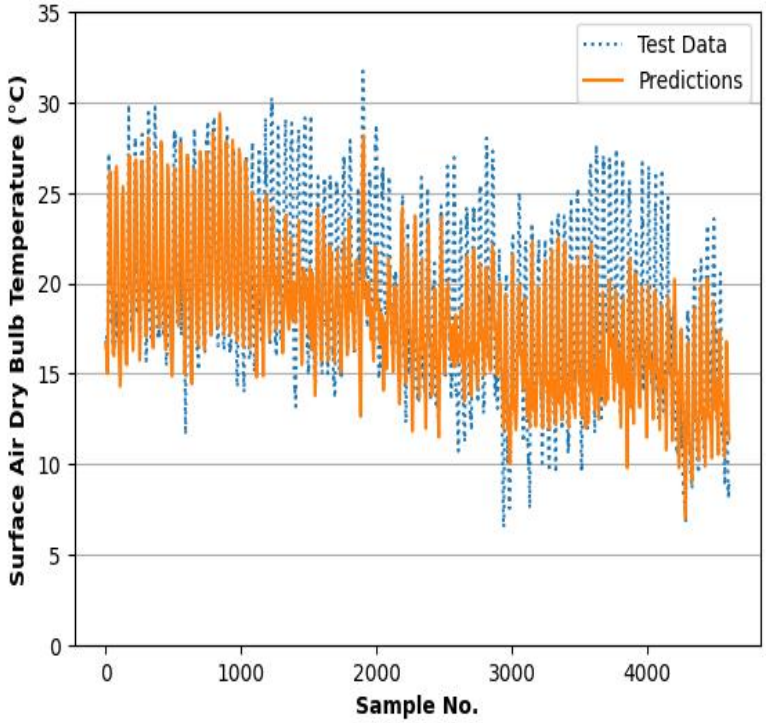

Figure 85: Model B surface air wet bulb temperature predictions on test set.

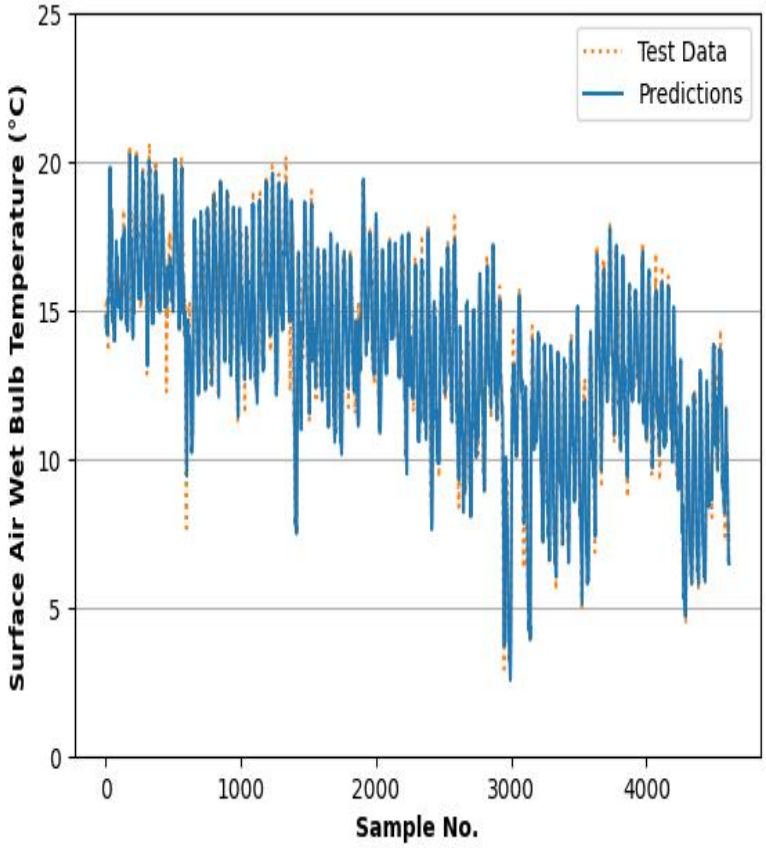

Figure 86: Model C surface air wet bulb temperature predictions on test set.

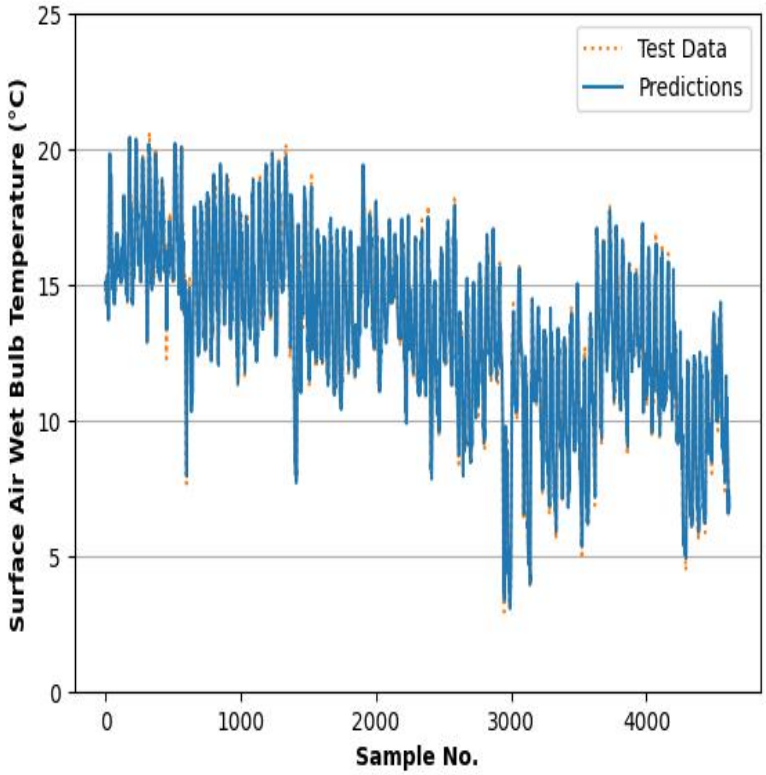

Figure 87: Model D surface air wet bulb temperature predictions on test set.

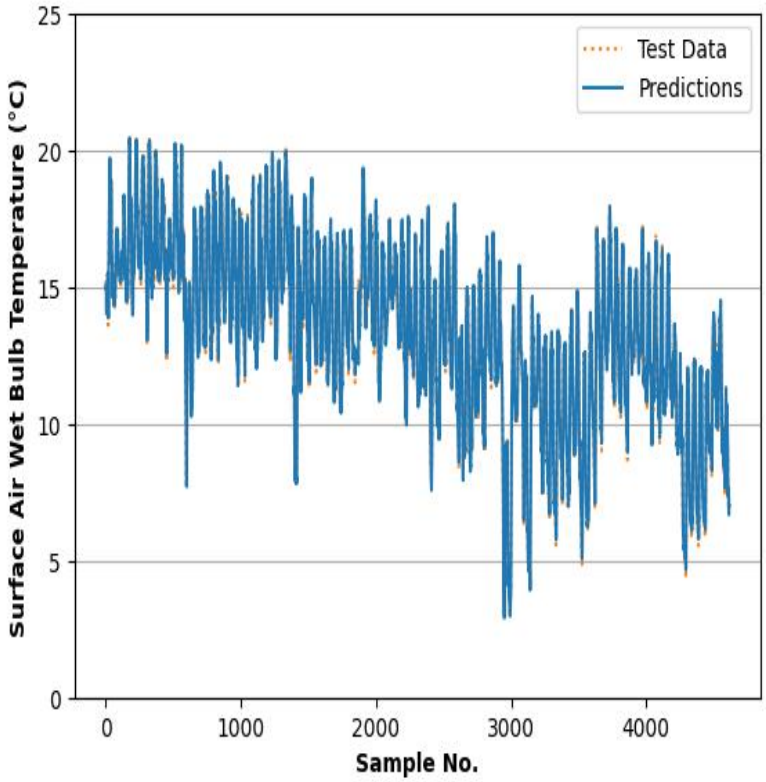

Figure 88: Model E surface air wet bulb temperature predictions on test set.

7 level air dry bulb temperature

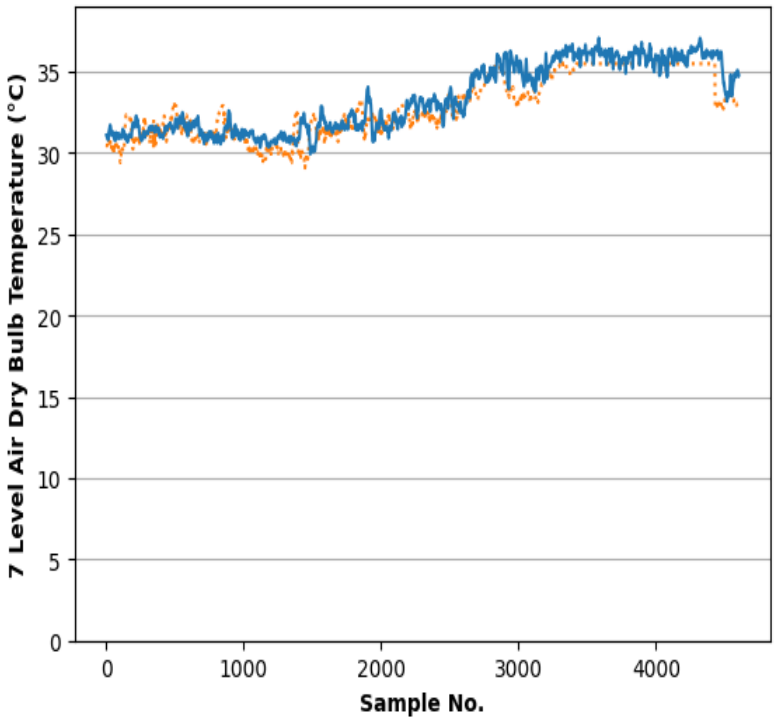

Figure 89: Model A 7 level air dry bulb temperature predictions on test set.

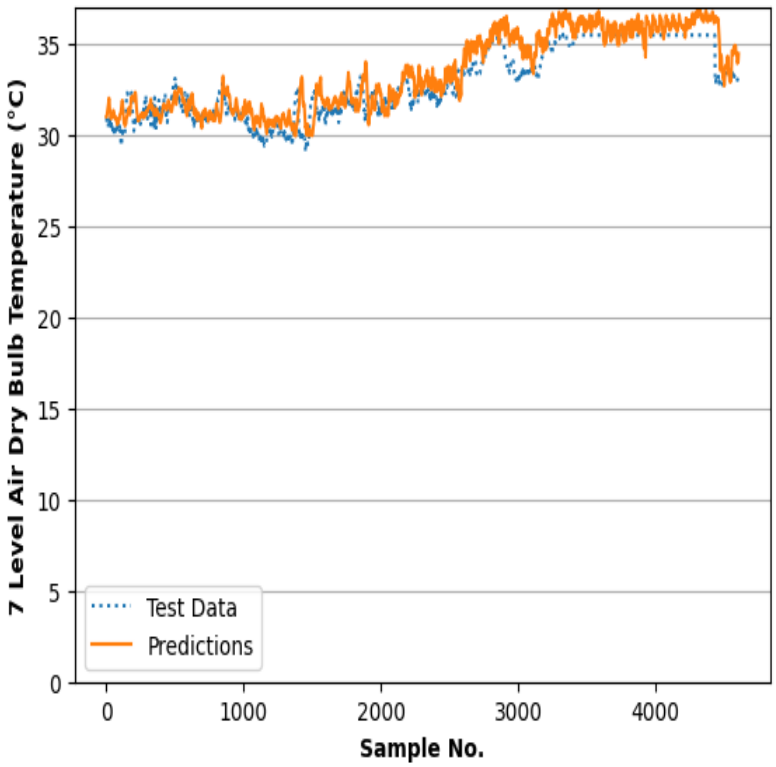

Figure 90: Model B 7 level air dry bulb temperature predictions on test set.

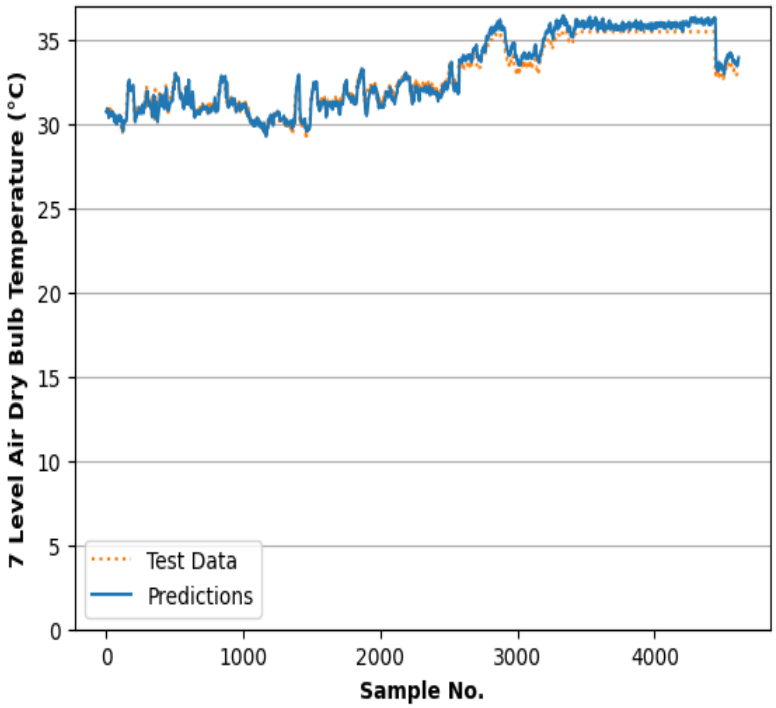

Figure 91: Model C 7 level air dry bulb temperature predictions on test set.

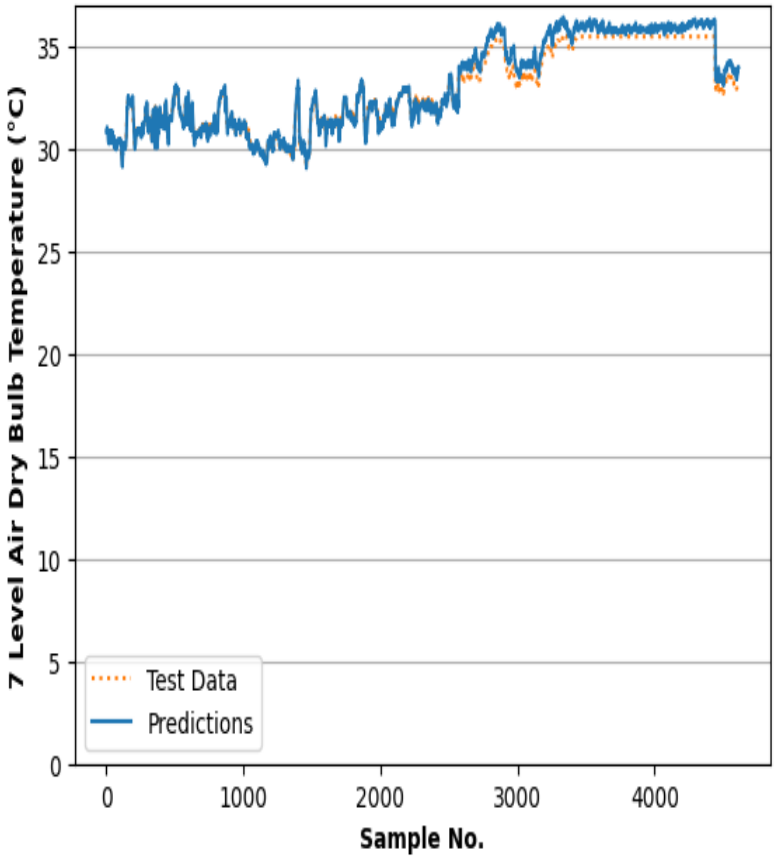

Figure 92: Model D 7 level air dry bulb temperature predictions on test set.

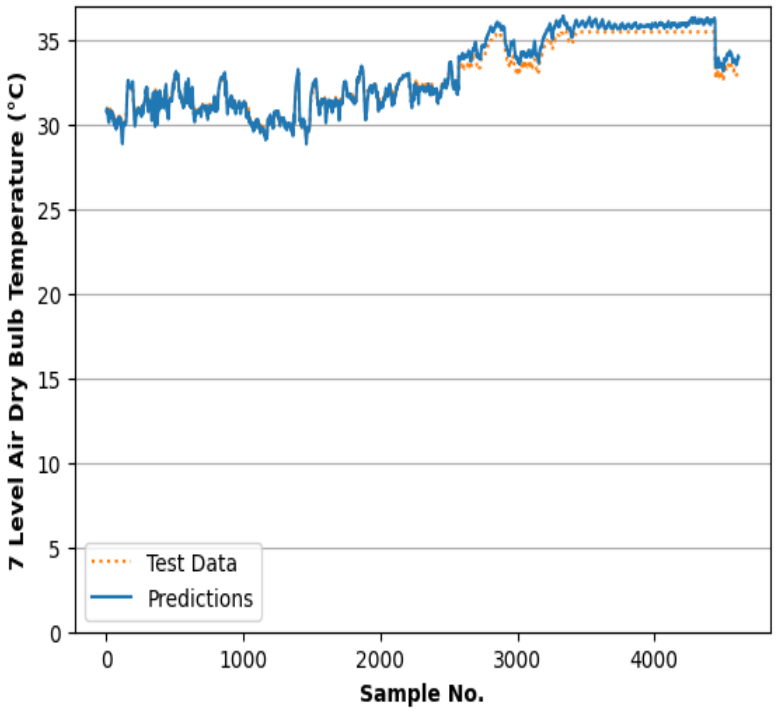

Figure 93: Model E 7 level air dry bulb temperature predictions on test set.

7 level air wet bulb temperatures

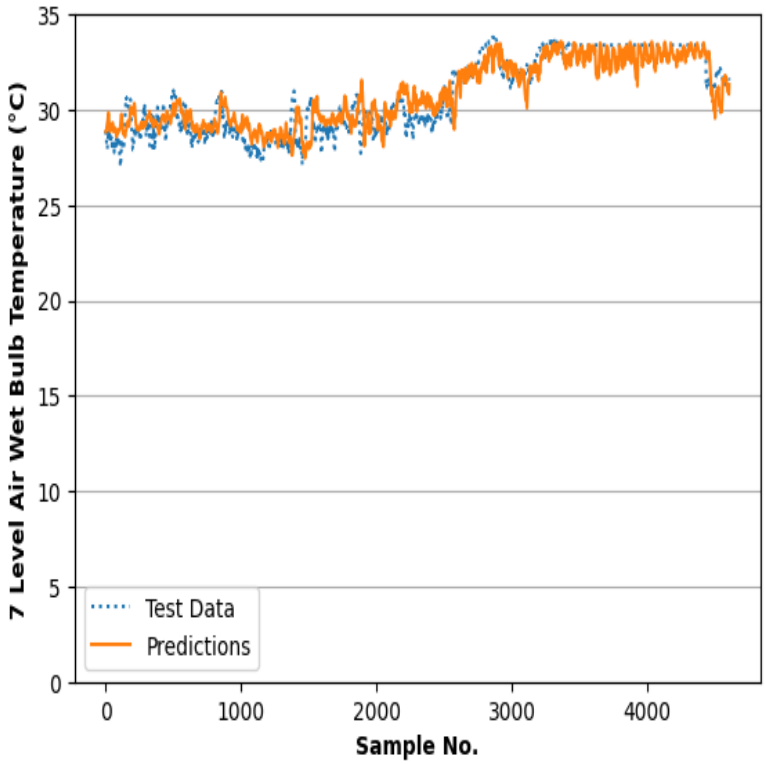

Figure 94: Model B 7 level air wet bulb temperature predictions on test set.

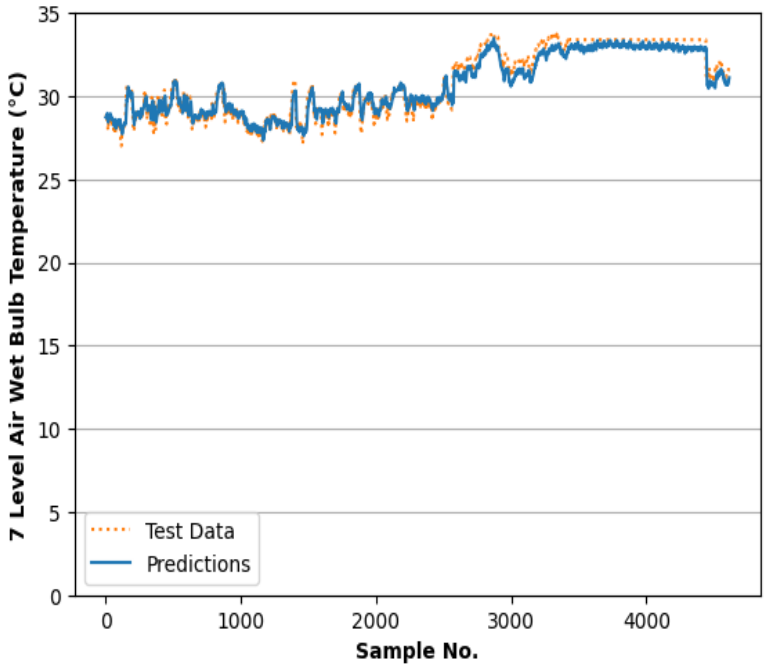

Figure 95: Model C 7 level air wet bulb temperature predictions on test set.

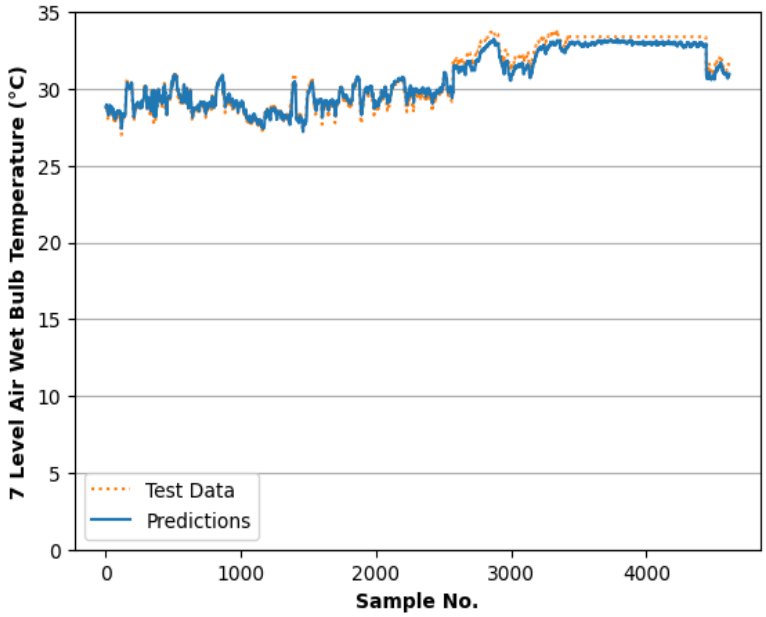

Figure 96: Model D 7 level air wet bulb temperature predictions on test set.